*minerals*

MDPI

*Article*

# Clay Mineralogy and Major and Trace Element Geochemistry of Recent Sediments in Rivers Along the West Coast of India: Implications for Provenance and Chemical Weathering

**Shaik Sai Babu [1], Venigalla Purnachandra Rao [1,*] and Mekala Ram Mohan [2]**

[1] Vignan's Foundation for Science, Technology and Research (VFSTR), Deemed to be Vignan's University, Vadlamudi, Guntur 522 213, Andhra Pradesh, India; sksaibabu19932@gmail.com
[2] Council of Scientific and Industrial Research, CSIR-National Geophysical Research Institute, Uppal Road, Hyderabad 500 007, Telangana, India; rammohan@ngri.res.in
* Correspondence: vprao55@gmail.com

**Abstract:** The clay mineralogy and major and trace element geochemistry of the sediments deposited at the lower reaches of 90 medium and minor rivers from five states along the west coast of India indicate distinct clay mineral assemblages in the Archean–Proterozoic (A-P) terrain and Deccan Trap (DT) terrain. The sediments from A-P terrain are dominated by kaolinite, with minor illite and gibbsite and traces of goethite, and those from DT terrain are dominated by smectite with minor illite, kaolinite and chlorite. The sediments are depleted of Si, Ca, Mg, Na and K relative to those of Post-Archean average Australian Shale. The $SiO_2/Al_2O_3$ ratio of the sediments suggests lateritic soils in the A-P terrain and non-lateritic, chemically weathered soils in the DT terrain. Weathering indices indicate strong weathering in the clay fractions of all sediments. The silt fractions of sediments from Goa, Maharashtra and Gujarat exhibit intermediate to weak weathering and influence by hydraulic sorting processes and source rock characteristics. The total trace element content (∑TE) was higher in the silt fractions than in clay fractions of all sediments, and peaks of high ∑TE occur in the silt fractions of Kerala and Maharashtra. The silt fractions exhibit relatively high Th, U, La, Zr and Hf from A-P terrain, and high Sc, Cr, Co, Ni, V and Ga from DT terrain. The Th/U and Rb/Sr ratios are controlled by the intensity of weathering and lithology of source rocks. The standard plots using trace elements reveal that the clay fractions of sediments are more mafic from both the terrains, while silt fractions exhibit intermediate provenance between felsic and mafic sources. Since mafic component-dominated clays are transported to the adjacent seas and oceans, it would be a challenge to identify the provenance of clays from granitic terrain in the oceans using trace element chemistry.

**Keywords:** fluvial sediments; trace elements; Western Ghats; Deccan Trap terrain; Archean–Proterozoic terrain; chemical weathering; provenance



Academic Editors: Manuel Pozo Rodríguez, Diego De Souza Sardinha, Vania Rosolen and Leticia Hirata Godoy

Received: 9 October 2024
Revised: 16 December 2024
Accepted: 27 December 2024
Published: 31 December 2024

**Citation:** Babu, S.S.; Purnachandra Rao, V.; Mohan, M.R. Clay Mineralogy and Major and Trace Element Geochemistry of Recent Sediments in Rivers Along the West Coast of India: Implications for Provenance and Chemical Weathering. *Minerals* **2025**, *15*, 43. https://doi.org/10.3390/min15010043



## 1. Introduction

Rivers are the most significant dynamic systems which erode the earth's surface and transport weathered continental material to the oceans. The composition of river sediment can be influenced by factors such as the type of source rocks, climate, low and high relief, the degree of chemical weathering, transport and post-depositional diagenetic effects [1–12]. The river sediments thus provide cumulative information on the composition of the continental crust, impact of weathering, tectonic setting of the source terrain and

sedimentary processes associated with transportation and deposition [13–24]. It is, however, possible to point out the influence of these parameters from the mineral and chemical characteristics of sediments. For example, tropical climatic conditions are associated with high precipitation and intense chemical weathering [25]. Chemical weathering causes chemical degradation of rocks, resulting in high dissolved load of mobile elements and enrichment of immobile elements in the sediments, and high sediment yield into the rivers. The erosional products of chemical weathering are finer than those derived from physical or mechanical weathering. The geomorphology of the terrain influences the sediment characteristics. For instance, steep slopes promote more physical weathering and produce relatively coarser sediment. Sediment texture, mineralogy and chemistry are modified by hydraulic sorting processes during transport [20]. Post-depositional processes such as diagenesis modify the sediment composition, depending on oxic, sub-oxic and anoxic conditions in the sediments. However, recent sediments exhibit little or no diagenetic effect on sediment composition [25].

Numerous studies have investigated the mineralogy and geochemistry of the sediments from large as well as small rivers to better understand the provenance and impact of chemical weathering on source rocks [7,20,22,26–40]. The sediments from large rivers provide cumulative information on weathering and provenance, as they usually drain through different rock types and experience different climatic conditions during transport. On the other hand, the sediments deposited by small rivers are more helpful to provide information on the weathering and nature of source rocks, because their catchment areas experience relatively homogeneous climatic and lithological settings [20,41]. The sediment mineralogy and major element chemistry (mobile and easily leachable elements) have been used to deduce the weathering history [18,42], while immobile trace elements, such as La, Zr, Sc, Cr, V, Th, Hf and Yb have been used for provenance [17,42–44]. A variety of weathering indices based on geochemical analysis have been used to understand the intensity and type of weathering. Recent studies, however, suggest that the weathering indices are affected by source area lithology, hydraulic sorting processes during transport and deposition and enhanced sedimentary recycling [18,21]. However, clay fractions more likely reflect weathering processes coeval with deposition [20]. In this study, we have investigated clay mineralogy and major and trace element characteristics of the clay and silt fractions of sediments deposited at the lower reaches of the medium and minor rivers along the west coast of India. These rivers drain the Western Ghats (WG) that comprise two distinct geological formations along their length and experience humid, tropical climate. The western slope of the WG is much steeper in the northern and southern parts than in the central part [45]. The basement rocks of the WG are covered by laterites, whose thickness decreases considerably from south to north. Several investigators reported the clay mineralogy and geochemistry of the suspended and/or bed sediments of the rivers and estuaries [27,34–36,40,46–60], or the clay minerals and Sr-Nd isotopic composition of the sediments in the adjacent continental shelf [56,61]. The purpose of this study is to report clay minerals and major and trace element characteristics of the sediments in rivers along the west coast of India, to better understand the impact of weathering on the composition and provenance of sediments.

## 2. Geological Setting

**Geomorphology:** The present study is on the clay mineralogy and major and trace element geochemistry of sediments in 90 medium and minor rivers along the west coast of India (Figure 1). Rao [62] classified the rivers of Peninsular India into the major, medium and minor rivers based on the size of catchment area. Major rivers are those with catchment area > 20,000 sq. km, medium rivers with catchment area < 20,000 to 2000 sq. km and minor

rivers with <2000 sq. km area. We followed his terminology for classifying the rivers. The rivers receive sediment load and waters from the Western Ghats (WG; mountain range), a linear geomorphic feature that runs parallel to the west coast of India (Figure 1; [63]. The Western Ghats start near the border of Gujarat and Maharashtra, south of the Tapti River and run ~1600 km through the states of Maharashtra, Goa, Karnataka, Kerala and Tamil Nadu and ends at Kanyakumari. The northern Western Ghats (Gujarat through Maharashtra up to Goa) exhibit steep gradient and are remarkably straight and lie at the edge of the Arabian Sea, also known as the Great Escarpment of India [64]. Rugged topography, steep cliffs, deep valleys and dense forests are also characteristic of the Ghats in this region [45]. The Western Ghats are further inland, 50 to 80 km away from the seashore between Bhatkal and Cochin in the central and southern part and, again located on the coast in south Kerala and around Tiruvunanthapuram. The height of the Western Ghats is up to 2600 m, with an average elevation of ~1200 m, and their width varies between 50 and 80 km.

**Geology:** The Western Ghats comprise the continental flood basalts (Deccan Traps) in the north and Archean–Proterozoic formations in the south (Figure 1; [63]). The basalts cover >500,000 $km^2$ for the Deccan Traps and represent the extrusion of phenomenal volumes of lava. The thickness of the Deccan Traps varies from 2 km to 200 m, with its maximum in the plateau region. The thickness and number of discrete lava flows is greatest in the western parts and decrease gradually towards east and south. The Deccan Trap basalts can be divided into four stratigraphic subdivisions. The lower basalts (the Bushe and Poladpur formations) are largest and show evidence of contamination with upper crustal material. The upper basalts (the Ambenali and Mahabaleshwar formations) show low contamination and/or mobilisation of material from the mantle lithosphere [65]. The lateral transition from the Deccan basalts to Archean–Proterozoic formations (APF) occurs close to the border of Maharashtra and Goa (Figure 1). The APF can further be divided into granites and gneisses in the north and, and high-grade charnockites and khondalites in the south ([66]; Figure 1). The rocks of Goa and Karnataka belong to the Dharwar Super Group [67] with green schists and gneisses. The iron and manganese ore deposits occur in Goa and are being mined by the open cast method [67,68]. The Mandovi and Zuari Rivers drain through these ore deposits and carry ore particulates in their suspended and bed loads [52,53]. Supergene Mn ore deposits formed on Late Archean rocks also occur in the northern Karnataka [69]. Limestones, dolomites, ultramafic rocks, orthoquartzites, argillite and banded magnetite/hematite quartzites are minor rock types of Karnataka. The Precambrian rocks occur abundantly in Kerala and consist of Khondalite Group, Charnockite Group, Sargur Group and Dharwar Group [70]. The rocks are intruded by basic and ultrabasic rocks. Khondalites are interlayered with garnetiferous-biotite gneiss, leptynite and narrow bands of charnockites, often intruded by pegmatites. Biotite–hornblende gneiss and cordierite gneiss are seen associated with charnockites and khondalites [71]. Laterites cover extensively the basement rocks of the Western Ghats at different topographic levels between Kerala and Maharashtra. The thickness of the laterites is up to 30 m in Kerala, Karnataka and Goa and decreases to <10 m in Maharashtra region [72].

**Climate:** Humid, tropical climate prevails all along the Western Ghats. Semi-arid climate is prevalent in the north of the Narmada and Tapti Rivers and Gujarat [63,73]. The mountain ranges intercept the rain-bearing westerly winds during the southwest monsoon (June–September). Consequently, the western slopes of the Western Ghats receive far more rainfall (av. 250 cm/yr) than their eastern slopes (100 cm/yr). Precipitation is much heavier, with a higher average rainfall (300–400 cm/yr) in the states of Maharashtra, Goa and northern Karnataka than in the southern Karnataka and Kerala. Numerous rivers

draining the western slope of the Western Ghats (Figure 1) bring suspended and bed load of sediment into the Arabian Sea.

| # | River Name (Length (km)) | # | River Name (Length (km)) |
|---|---|---|---|
| 1 | Neyyar (56) | 46 | Mandovi (81) |
| 2 | Vamanpuram (88) | 47 | Mapusa (20) |
| 3 | Ithikkara (56) | 48 | Nerul (17) |
| 4 | Kallada (120) | 49 | Baga (15) |
| 5 | Achankovil (128) | 50 | Anjuna (19) |
| 6 | Pamba (176) | 51 | Chapora (21) |
| 7 | Manimalayar (90) | 52 | Terikhol (28) |
| 8 | Meenachil (78) | 53 | Mochemaad (27) |
| 9 | Muvattupuzha (121) | 54 | Mandavi (12) |
| 10 | Periyar (244) | 55 | Karli (14) |
| 11 | Chalakudi (145) | 56 | Gad (66) |
| 12 | Karuvannur (45) | 57 | Naringre (27) |
| 13 | Bharathapuzha (209) | 58 | Vaghotan (40) |
| 14 | Kadalundy (130) | 59 | Arjuna (37) |
| 15 | Chaliyar (169) | 60 | Muchkundi (59) |
| 16 | Kuttyadi (74) | 61 | Gautami (29) |
| 17 | Mahe (54) | 62 | Kajali (37) |
| 18 | Valapatanam (110) | 63 | Jaigad (42) |
| 19 | Kuppam (88) | 64 | Vashisti (35) |
| 20 | Thejaswini (64) | 65 | Bharja (27) |
| 21 | Chandragiri (105) | 66 | Savitri (110) |
| 22 | Netravati (103) | 67 | Kundalika (74) |
| 23 | Gurupura (30) | 68 | Amba (63) |
| 24 | Nandini (103) | 69 | Bhogavati (52) |
| 25 | Shambavi (60) | 70 | Patalganga (16) |
| 26 | Pangala (37) | 71 | Tansa (16) |
| 27 | Udyavara (27) | 72 | Vaitarna (154) |
| 28 | Suvarna (88) | 73 | Surya (21) |
| 29 | Sita (50) | 74 | Bananga (17) |
| 30 | Haladi (70) | 75 | Darotha (27) |
| 31 | Kolluru (38) | 76 | Daman Ganga (131) |
| 32 | Yadamavu (32) | 77 | Par (51) |
| 33 | Uppunda (27) | 78 | Wanki (17) |
| 34 | Venkatapur (50) | 79 | Auranga (97) |
| 35 | Pallinadu (42) | 80 | Kharera (40) |
| 36 | Alvekodi (27) | 81 | Ambika (136) |
| 37 | Sharavati (128) | 82 | Purna (180) |
| 38 | Badagani (21) | 83 | Mindhola (105) |
| 39 | Agnashini (117) | 84 | Tapi (724) |
| 40 | Gangavali (152) | 85 | Kim (107) |
| 41 | Kali (184) | 86 | Narmada (1312) |
| 42 | Galgibaga (15) | 87 | Viswamitri (142) |
| 43 | Talpona (31) | 88 | Mahi (583) |
| 44 | Sal (35) | 89 | Sabarmati (371) |
| 45 | Zuari (34) | 90 | Bhogawo (120) |

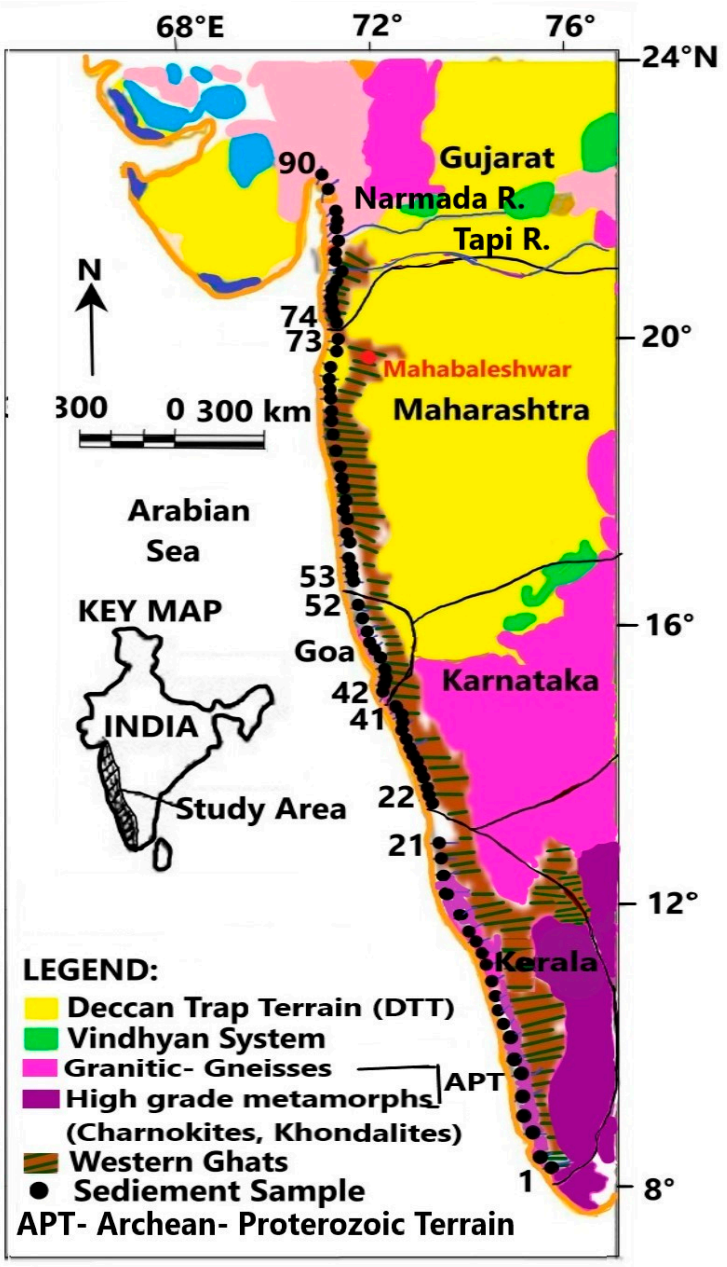


**Figure 1.** Map of the West Coast of India. Rivers investigated in this study are numbered. A dot marks the sample location in each river. Location of the Western Ghats along the coast and basic geology of western India are also shown in the map. States and state boundaries are marked. Major rivers (Narmada and Tapi) are also shown.

## 3. Materials and Methods

For the present study, sediments were collected at the lower reaches of 90 rivers from five states, between the Neyyar River of Kerala and the Bhogawa River of Gujarat (Figure 1), using Van Veen Grab. The sediments recovered were dried. The sediments from the rivers of Kerala, Karnataka and Goa are derived largely from the Archean–Proterozoic (A-P) terrain, while those from Maharashtra and Gujarat are from the Deccan Trap (DT) terrain. The sand, silt and clay fractions of sediments were separated in the laboratory, following Folk [74]. The <62 μm fraction of the sediment was separated from the total

sediment by wet sieving, using a 230 (ASTM) mesh sieve. This fraction was collected in a measuring glass cylinder, made up to 1000 mL volume with distilled water and stirred vigorously for homogeneity. Three size fractions were separated from a <62 μm fraction of the sediment in the cylinder. The <2 μm fraction was separated based on Stoke's settling velocity, and 250 mL of this fraction was collected in a beaker and used for clay mineralogy (see procedure below). Again, distilled water was added to the cylinder and the volume was made up to 1000 mL and stirred vigorously. The <4 μm fraction (clay) was separated and collected in a beaker, dried in an oven at 60 °C and then powdered. This procedure was repeated several times to ensure that the clay fraction was removed completely from the <62 μm fraction of sediment in the cylinder. Then the remaining fraction was dried and powdered, as it represents silt fraction (>4 to 62 μm). We are aware that this procedure may not completely separate silts from the clay fraction. Since we used a low amount of initial sediment and repeated the experiment and decanted the clay fraction several times, the silt fraction was successfully separated. The powdered sediment size fractions were used for geochemical analyses.

The <2 μm fraction of the sediment solution was used for clay mineralogy. The sample solutions in a beaker were made free of organic matter and carbonate by treating it with 5% $H_2O_2$ and 0.2 M HCl, respectively. Then these solutions were made free of acid by repeated washing. One ml of sample solution was pipetted on a glass slide and allowed to dry in air. Then the dried sample on the slides was exposed to ethylene glycol vapours in a desiccator that heated to 100 °C for one hr, and then slides were scanned from 4° to 30° at 2° 2θ/min on a PAN-analytical, Empyrean X-ray powder diffractometer using Ni-filtered, Cu Ka radiation at SRM University, Amaravati, Andhra Pradesh. Clay minerals were identified. Of the 90 samples, only 20 clay slides were analysed for clay mineralogy, and the procedure mentioned in Rao and Rao [61] was followed for quantitative clay mineralogy. Representative X-ray diffractograms are shown in Figure 2.

The major elements were determined on clay and silt fractions of sample powders by using an X-ray fluorescence spectrometer, 'WD XRF' Model Axios mAX4, P-Analytical, at the CSIR-National Geophysical Research Institute (CSIR-NGRI), Hyderabad. A detailed procedure was given by Sai Babu et al. [34]. For trace and rare earth element analysis, the detailed procedure mentioned in Sai Babu et al. [36] was used, and is repeated below: Powder samples of 50 mg were taken in Savillex vessels, to which 10 mL of acid mixture containing hydrofluoric acid (HF) and nitric acid ($HNO_3$) was added in a 7:3 ratio. These vials were tightly closed and were heated at 150 °C for 48 h. Following this step, these vials were opened and heated at 100 °C to near dryness. The sample residue was further mixed with 10 mL of acid mixture containing nitric acid ($HNO_3$) and Millipore water in a 1:1 ratio and was heated at 80 °C for 1 h. To obtain the necessary TDS level, and to minimise the matrix effects, the obtained sample solution was diluted 50,000 times. Trace elements were determined by High-Resolution Inductively Coupled Plasma Mass Spectrometer (HR-ICP-MS, Attom, Hyderabad, Telangana, India), Nu Instruments at CSIR-NGRI, Hyderabad. The instrument drift was monitored and corrected using $^{103}$Rh as the internal standard. The within-run RSDs for all the analysed elements were under 3%. Certified reference material JSD-3 μg/g was repeatedly analysed as an unknown to monitor the accuracy and reproducibility of the obtained trace element data.

Table 1 shows the major element data of the clay and silt fractions of sediments. Weathering indices, such as chemical index of alteration (CIA; [2], plagioclase index of alteration [6], index of chemical variability [16] and mafic index of alteration (MIA: [58]) were calculated using molecular proportions of major element oxides. CaO represents the amount of CaO in silicate fractions. We do not have $CO_2$ data for our analyses and are thus unable to correct Ca in carbonates to obtain CaO. Bock et al. [75] recommended to accept the

value of CaO, if CaO ≤ $Na_2O$. If, however, CaO > $Na_2O$, then we assumed that the moles of CaO = $Na_2O$ [5]. The values of weathering indices are given in Table 1. Trace element data for the clay and silt fractions of sediments are given in Tables 2 and 3, respectively. Table 4 shows the correlation matrix for the clay fraction of sediments, separately for Archean–Proterozoic terrain (APT) and Deccan Trap terrain (DTT).

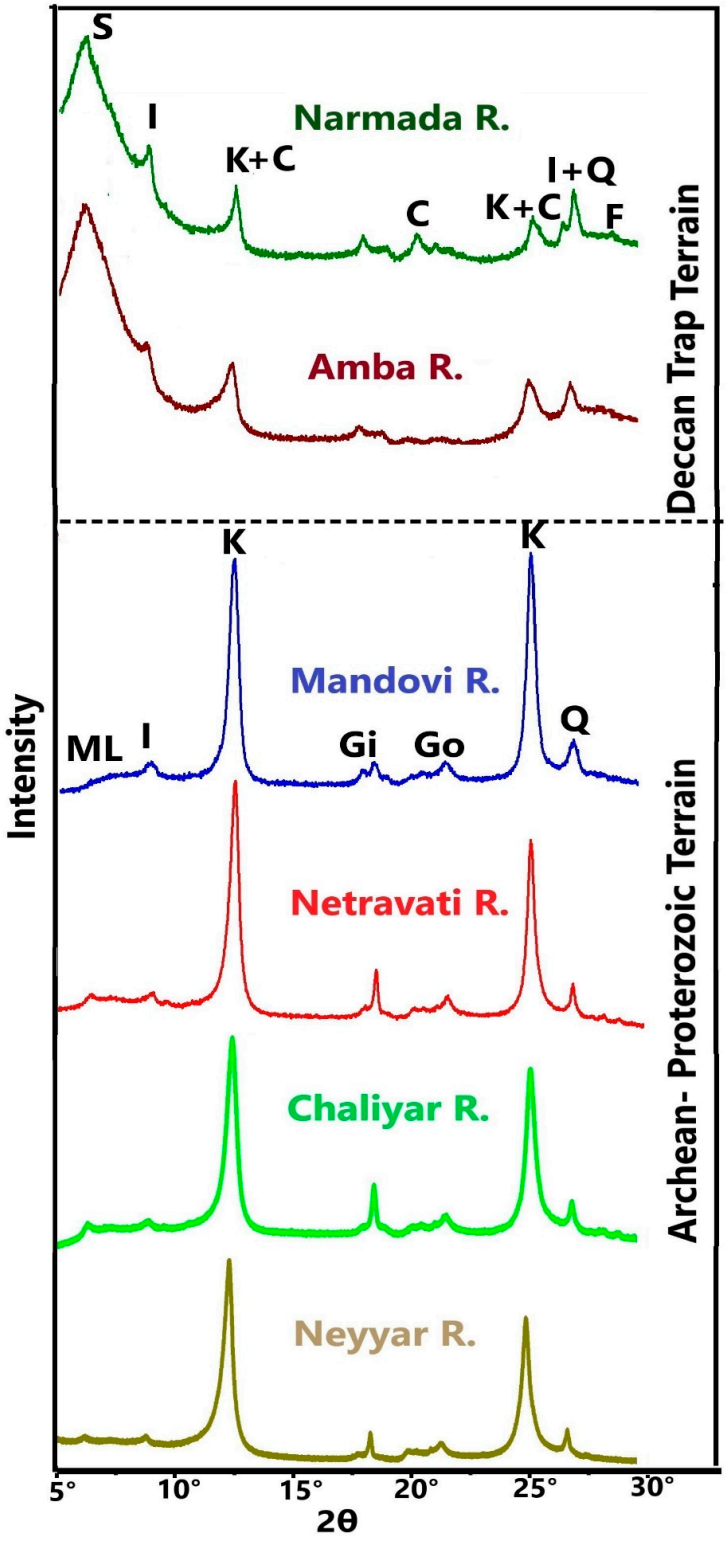


**Figure 2.** Selected X-ray diffractograms of the clay fraction of sediments. S—smectite, K—kaolinite, I—illite, C—chlorite, Gi—gibbsite, Go—goethite, Q—quartz and F—feldspar.

**Table 1.** Major element content (%) of the clay (<4 μm) and silt (>4 to 63 μm) fraction of sediments in the rivers of the west coast of India.

| **Clay fraction** | | | | | | | | | | | | | | | | | | |
|---|---|---|---|---|---|---|---|---|---|---|---|---|---|---|---|---|---|---|
| **State (No. of Rivers)** | | **$SiO_2$** | **$Al_2O_3$** | **$Fe_2O_3$** | **MnO** | **MgO** | **CaO** | **$Na_2O$** | **$K_2O$** | **$TiO_2$** | **$P_2O_5$** | **$SiO_2/Al_2O_3$** | **$Fe_2O_3/Al_2O_3$** | **$Al_2O_3/TiO_2$** | **CIA** | **PIA** | **ICV** | **$MIA_{(O)}$** | **$MIA_{(R)}$** |
| Kerala (21) | Range | 29.01–40.66 | 11.37–32.01 | 7.39–15.27 | 0.05–0.22 | 0.65–3.70 | 0.25–2.96 | 0.16–25.28 | 0.68–2.88 | 0.71–1.44 | 0.15–0.83 | 1.05–2.91 | 0.35–0.82 | 11.42–37.04 | 26.95–96.35 | 20.82–93.92 | 0.44–3.76 | 38.75–95.87 | 21.72–72.67 |
| | Avg., | 34.24 | 23.59 | 11.84 | 0.12 | 1.69 | 0.68 | 2.82 | 1.18 | 1.11 | 0.45 | 1.45 | 0.50 | 21.22 | 86.10 | 79.69 | 0.97 | 85.84 | 58.07 |
| | STD (±) | 2.94 | 4.48 | 2.12 | 0.05 | 0.81 | 0.59 | 7.22 | 0.57 | 0.22 | 0.16 | 0.48 | 0.11 | 6.72 | 19.04 | 20.61 | 0.78 | 15.74 | 12.61 |
| Karnataka (20) | Range | 37.88–52.33 | 18.09–21.88 | 6.32–17.33 | 0.02–0.34 | 0.29–2.76 | 0.11–0.85 | 0.06–1.04 | 0.51–1.64 | 0.89–1.80 | 0.10–0.40 | 1.91–2.54 | 0.31–0.95 | 11.73–20.38 | 84.49–96.60 | 76.90–94.35 | 0.51–1.24 | 83.14–97.07 | 48.16–71.78 |
| | Avg., | 43.12 | 19.43 | 12.39 | 0.08 | 1.18 | 0.42 | 0.44 | 1.09 | 1.23 | 0.26 | 2.22 | 0.64 | 16.35 | 90.87 | 85.76 | 0.87 | 91.08 | 58.00 |
| | STD (±) | 3.86 | 1.03 | 2.86 | 0.07 | 0.61 | 0.20 | 0.35 | 0.33 | 0.26 | 0.08 | 0.14 | 0.17 | 2.79 | 2.86 | 4.22 | 0.19 | 3.27 | 6.13 |
| Goa (11) | Range | 36.14–43.11 | 15.61–21.66 | 9.67–17.71 | 0.04–0.58 | 1.21–3.87 | 0.29–1.33 | 0.56–8.40 | 1.28–1.63 | 1.01–1.97 | 0.17–0.49 | 1.82–2.57 | 0.50–1.13 | 9.23–15.94 | 61.49–88.35 | 55.96–81.79 | 0.83–1.61 | 70.30–90.49 | 41.30–59.13 |
| | Avg., | 40.06 | 18.05 | 13.20 | 0.16 | 2.45 | 0.72 | 2.33 | 1.49 | 1.36 | 0.32 | 2.24 | 0.74 | 13.71 | 80.97 | 74.25 | 1.21 | 82.19 | 49.21 |
| | STD (±) | 2.27 | 1.95 | 2.01 | 0.17 | 0.73 | 0.33 | 2.57 | 0.12 | 0.32 | 0.09 | 0.22 | 0.16 | 2.03 | 8.52 | 7.99 | 0.24 | 6.06 | 5.43 |
| Archean–Proterozoic Terrain (APT) | Range | 29.01–52.33 | 11.37–32.01 | 6.32–17.71 | 0.04–0.58 | 0.65–3.87 | 0.11–2.96 | 0.06–25.28 | 0.51–2.88 | 0.71–1.97 | 0.10–0.83 | 1.05–2.91 | 0.31–1.13 | 9.23–37.04 | 26.95–96.60 | 20.82–94.35 | 0.44–3.76 | 38.75–97.07 | 21.72–72.67 |
| | Avg., | 38.89 | 20.82 | 12.34 | 0.11 | 1.65 | 0.59 | 1.80 | 1.21 | 1.21 | 0.35 | 1.95 | 0.61 | 18.10 | 85.98 | 79.90 | 1.01 | 86.37 | 55.09 |
| | STD (±) | 5.11 | 3.82 | 2.42 | 0.10 | 0.85 | 0.44 | 4.79 | 0.44 | 0.27 | 0.15 | 0.47 | 0.17 | 5.77 | 10.14 | 10.94 | 0.40 | 8.35 | 7.10 |
| Maharashtra (21) | Range | 28.32–51.21 | 13.71–21.65 | 3.13–14.67 | 0.07–0.44 | 0.79–5.72 | 0.26–2.10 | 0.12–13.22 | 0.55–1.34 | 0.63–2.98 | 0.06–0.54 | 1.87–3.32 | 0.14–0.88 | 7.27–29.27 | 48.67–94.06 | 45.86–91.36 | 0.42–2.13 | 61.96–93.91 | 34.01–79.08 |
| | Avg., | 42.28 | 16.90 | 10.75 | 0.18 | 2.23 | 1.07 | 1.09 | 0.91 | 1.51 | 0.25 | 2.54 | 0.65 | 11.98 | 85.19 | 80.59 | 1.08 | 84.23 | 53.51 |
| | STD (±) | 4.74 | 2.28 | 2.51 | 0.10 | 1.20 | 0.53 | 2.79 | 0.29 | 0.44 | 0.10 | 0.42 | 0.18 | 4.33 | 9.25 | 9.28 | 0.34 | 7.09 | 9.06 |
| Gujarat (17) | Range | 42.88–50.36 | 13.04–16.24 | 6.13–10.57 | 0.10–0.24 | 2.51–4.29 | 1.65–6.38 | 0.18–1.31 | 0.66–1.83 | 0.99–2.20 | 0.11–0.36 | 2.71–3.77 | 0.38–0.76 | 7.38–16.10 | 61.78–84.19 | 53.70–80.76 | 0.87–1.65 | 63.94–82.35 | 39.99–58.96 |
| | Avg., | 47.35 | 14.43 | 8.91 | 0.15 | 3.39 | 3.05 | 0.54 | 1.29 | 1.44 | 0.17 | 3.29 | 0.62 | 10.39 | 75.02 | 68.39 | 1.31 | 74.02 | 47.15 |
| | STD (±) | 2.49 | 0.85 | 1.09 | 0.030 | 0.48 | 1.05 | 0.36 | 0.37 | 0.29 | 0.07 | 0.29 | 0.09 | 2.05 | 5.42 | 6.70 | 0.17 | 4.32 | 4.10 |
| Deccan Trap Terrain (DTT) | Range | 28.32–51.21 | 13.04–21.65 | 3.13–14.67 | 0.07–0.44 | 0.79–5.72 | 0.26–6.38 | 0.12–13.22 | 0.55–1.83 | 0.63–2.98 | 0.06–0.54 | 1.87–3.77 | 0.14–0.88 | 7.27–29.27 | 48.67–94.06 | 45.86–91.36 | 0.42–2.13 | 61.96–93.91 | 34.01–79.08 |
| | Avg., | 44.55 | 15.79 | 9.93 | 0.17 | 2.75 | 1.96 | 0.84 | 1.08 | 1.48 | 0.21 | 2.88 | 0.64 | 11.27 | 80.10 | 74.49 | 1.19 | 79.12 | 50.33 |
| | STD (±) | 4.63 | 2.16 | 2.19 | 0.08 | 1.11 | 1.28 | 2.08 | 0.38 | 0.38 | 0.10 | 0.53 | 0.14 | 3.55 | 7.33 | 7.99 | 0.25 | 5.70 | 5.12 |
| **West Coast of India River Average Clay (WCIRAC)** | **Range** | **28.32–52.33** | **11.37–32.01** | **3.13–17.71** | **0.65–5.72** | **0.11–6.38** | **0.06–25.28** | **0.51–2.88** | **0.01–2.98** | **0.04–0.58** | **0.06–0.83** | **1.05–3.77** | **0.14–1.13** | **7.26–37.05** | **26.95–96.60** | **20.82–94.35** | **0.42–3.76** | **38.75–97.07** | **21.72–79.08** |
| | **Avg.,** | **41.41** | **18.69** | **11.32** | **0.14** | **1.27** | **1.32** | **1.15** | **1.32** | **0.13** | **0.29** | **2.34** | **0.63** | **15.21** | **83.63** | **78.98** | **1.06** | **83.94** | **54.12** |
| | **STD (±)** | **3.26** | **4.06** | **2.60** | **0.98** | **0.86** | **3.43** | **0.42** | **0.34** | **0.09** | **0.14** | **0.31** | **0.14** | **5.98** | **9.01** | **12.87** | **0.47** | **10.40** | **9.51** |

**Table 1.** *Cont.*

| **Silt fraction** | | | | | | | | | | | | | | | | | | |
|---|---|---|---|---|---|---|---|---|---|---|---|---|---|---|---|---|---|---|
| **State (No. of Rivers)** | | **$SiO_2$** | **$Al_2O_3$** | **$Fe_2O_3$** | **MnO** | **MgO** | **CaO** | **$Na_2O$** | **$K_2O$** | **$TiO_2$** | **$P_2O_5$** | **$SiO_2/Al_2O_3$** | **$Fe_2O_3/Al_2O_3$** | **$Al_2O_3/TiO_2$** | **CIA** | **PIA** | **ICV** | **$MIA_{(O)}$** | **$MIA_{(R)}$** |
| Kerala (21) | Range | 34.08–48.17 | 15.44–26.06 | 9.55–16.03 | 0.06–0.22 | 0.60–3.53 | 0.30–2.59 | 0.17–1.89 | 0.72–2.66 | 0.74–1.57 | 0.15–0.80 | 1.38–2.21 | 0.37–0.71 | 11.29–34.19 | 76.13–94.19 | 67.23–91.28 | 0.57–1.14 | 75.61–93.55 | 50.39–67.10 |
| | Avg., | 38.75 | 22.71 | 12.09 | 0.13 | 1.71 | 0.94 | 0.49 | 1.54 | 1.24 | 0.41 | 1.71 | 0.53 | 18.31 | 88.36 | 82.33 | 0.81 | 88.09 | 59.34 |
| | STD (±) | 3.96 | 2.25 | 1.94 | 0.04 | 0.75 | 0.52 | 0.36 | 0.55 | 0.22 | 0.14 | 0.35 | 0.10 | 4.64 | 4.25 | 5.95 | 0.16 | 4.20 | 4.94 |
| Karnataka (20) | Range | 39.34–65.74 | 15.21–21.44 | 6.69–13.39 | 0.02–0.13 | 0.34–2.21 | 0.07–1.18 | 0.05–0.99 | 0.44–1.80 | 0.94–1.98 | 0.07–0.35 | 1.99–4.32 | 0.32–0.71 | 10.31–19.97 | 81.23–96.24 | 72.89–94.17 | 0.50–1.02 | 81.34–96.47 | 52.86–71.74 |
| | Avg., | 49.33 | 19.22 | 10.08 | 0.07 | 1.03 | 0.51 | 0.31 | 1.07 | 1.35 | 0.22 | 2.60 | 0.53 | 14.81 | 90.94 | 85.88 | 0.76 | 90.88 | 61.67 |
| | STD (±) | 5.38 | 1.64 | 1.85 | 0.03 | 0.48 | 0.29 | 0.24 | 0.37 | 0.33 | 0.08 | 0.48 | 0.10 | 2.71 | 3.49 | 4.90 | 0.14 | 3.48 | 5.17 |
| Goa (11) | Range | 43.19–56.47 | 14.81–20.41 | 6.03–14.47 | 0.05–0.55 | 1.23–3.50 | 0.42–2.35 | 0.20–0.72 | 1.08–1.51 | 1.16–2.10 | 0.21–0.49 | 2.46–3.15 | 0.31–0.86 | 8.57–14.90 | 80.13–90.81 | 74.00–84.87 | 0.60–1.32 | 78.79–91.41 | 47.05–67.95 |
| | Avg., | 49.38 | 17.65 | 9.66 | 0.17 | 2.23 | 1.06 | 0.42 | 1.30 | 1.59 | 0.32 | 2.81 | 0.56 | 11.46 | 86.43 | 80.05 | 0.95 | 84.54 | 56.52 |
| | STD (±) | 4.23 | 1.72 | 2.64 | 0.18 | 0.75 | 0.54 | 0.14 | 0.13 | 0.36 | 0.08 | 0.23 | 0.19 | 2.12 | 3.12 | 3.49 | 0.22 | 3.84 | 6.65 |
| Archean–Proterozoic Terrain (APT) | Range | 34.08–65.74 | 14.81–26.06 | 6.03–16.03 | 0.02–0.55 | 0.34–3.53 | 0.07–2.59 | 0.05–1.89 | 0.44–2.66 | 0.74–2.10 | 0.07–0.80 | 1.38–4.32 | 0.31–0.86 | 8.57–30.65 | 76.13–96.24 | 67.23–94.17 | 0.50–1.32 | 75.61–96.47 | 47.05–71.74 |
| | Avg., | 45.07 | 20.30 | 10.80 | 0.12 | 1.56 | 0.80 | 0.41 | 1.31 | 1.36 | 0.32 | 2.29 | 0.54 | 15.76 | 88.57 | 82.75 | 0.84 | 87.83 | 59.17 |
| | STD (±) | 6.93 | 2.82 | 2.30 | 0.10 | 0.80 | 0.50 | 0.29 | 0.47 | 0.32 | 0.14 | 0.61 | 0.12 | 4.53 | 3.62 | 14.34 | 0.17 | 3.84 | 4.9 |
| Maharashtra (21) | Range | 46.24–57.94 | 14.98–22.11 | 0.81–9.37 | 0.05–0.37 | 0.93–5.76 | 0.47–10.91 | 0.10–1.67 | 0.38–1.82 | 1.07–8.36 | 0.08–0.60 | 2.41–3.72 | 0.04–0.56 | 1.96–15.77 | 55.08–92.99 | 52.15–91.00 | 0.39–1.45 | 56.03–89.80 | 44.10–85.37 |
| | Avg., | 53.34 | 18.06 | 3.12 | 0.20 | 2.55 | 2.93 | 0.64 | 0.78 | 3.43 | 0.25 | 2.99 | 0.18 | 6.12 | 81.02 | 77.46 | 0.78 | 75.96 | 65.72 |
| | STD (±) | 3.46 | 2.11 | 2.45 | 0.08 | 1.20 | 2.25 | 0.40 | 0.32 | 1.49 | 0.11 | 0.38 | 0.15 | 2.67 | 8.77 | 8.73 | 0.27 | 9.41 | 10.54 |
| Gujarat (17) | Range | 50.55–63.44 | 12.26–16.32 | 0.30–7.08 | 0.09–0.24 | 2.30–3.72 | 3.03–10.88 | 0.77–1.91 | 0.79–1.58 | 1.59–3.42 | 0.13–0.33 | 3.17–4.75 | 0.02–0.50 | 4.19–8.81 | 46.56–77.56 | 41.06–73.78 | 0.97–1.87 | 48.67–75.85 | 37.37–57.14 |
| | Avg., | 55.71 | 14.17 | 3.68 | 0.15 | 2.93 | 6.16 | 1.31 | 1.25 | 2.36 | 0.17 | 3.97 | 0.26 | 6.27 | 62.20 | 56.72 | 1.28 | 60.58 | 48.93 |
| | STD (±) | 3.36 | 1.46 | 1.62 | 0.04 | 0.41 | 1.86 | 0.32 | 0.26 | 0.53 | 0.05 | 0.50 | 0.12 | 1.35 | 7.54 | 8.09 | 0.27 | 6.24 | 6.17 |
| Deccan Trap Terrain (DTT) | Range | 46.63–63.44 | 12.26–22.11 | 0.30–9.37 | 0.05–0.37 | 0.93–5.76 | 0.47–10.91 | 0.10–1.91 | 0.38–1.82 | 1.07–8.36 | 0.08–0.60 | 2.41–4.75 | 0.02–0.56 | 1.96–15.77 | 46.56–92.99 | 41.06–91.00 | 0.39–1.87 | 48.67–89.80 | 37.37–85.37 |
| | Avg., | 54.40 | 16.32 | 3.37 | 0.17 | 2.72 | 4.37 | 0.94 | 0.99 | 2.95 | 0.22 | 3.43 | 0.22 | 6.19 | 71.61 | 67.09 | 1.03 | 68.27 | 57.32 |
| | STD (±) | 3.57 | 2.67 | 2.11 | 0.07 | 0.94 | 2.63 | 0.50 | 0.38 | 1.27 | 0.09 | 0.66 | 0.14 | 2.16 | 8.15 | 8.41 | 0.27 | 7.82 | 8.35 |

**Table 1.** *Cont.*

| **Silt fraction** | | | | | | | | | | | | | | | | | | |
|---|---|---|---|---|---|---|---|---|---|---|---|---|---|---|---|---|---|---|
| **State (No. of Rivers)** | | **$SiO_2$** | **$Al_2O_3$** | **$Fe_2O_3$** | **MnO** | **MgO** | **CaO** | **$Na_2O$** | **$K_2O$** | **$TiO_2$** | **$P_2O_5$** | **$SiO_2/Al_2O_3$** | **$Fe_2O_3/Al_2O_3$** | **$Al_2O_3/TiO_2$** | **CIA** | **PIA** | **ICV** | **$MIA_{(O)}$** | **$MIA_{(R)}$** |
| **West Coast of India River Average Silt (WCIRAS)** | **Range** | **34.08–65.74** | **12.26–26.06** | **0.30–16.03** | **0.34–5.76** | **0.07–10.91** | **0.05–1.91** | **0.38–2.66** | **0.74–8.36** | **0.02–0.55** | **0.07–0.80** | **1.61–4.75** | **0.02–0.86** | **1.96–30.65** | **46.56–96.24** | **41.06–94.17** | **0.39–1.87** | **48.67–96.47** | **37.37–85.37** |
| | **Avg.,** | **49.30** | **18.62** | **7.66** | **2.14** | **2.58** | **0.67** | **1.17** | **2.03** | **0.14** | **0.27** | **2.81** | **0.41** | **1.96–30.65** | **81.79** | **76.86** | **0.89** | **80.24** | **59.03** |
| | **STD (±)** | **4.07** | **3.38** | **4.30** | **0.87** | **1.56** | **0.39** | **0.46** | **1.16** | **0.08** | **0.13** | **0.38** | **0.13** | **1.96–30.65** | **5.43** | **12.14** | **0.28** | **12.47** | **8.96** |
| Reference Sediments | UCC | 66.20 | 15.30 | 5.57 | 0.09 | 2.47 | 3.57 | 3.25 | 2.78 | 0.63 | 0.15 | 4.33 | 0.36 | 24.29 | 61.44 | - | - | 75.67 | 47.24 |
| | PAAS | 62.80 | 18.90 | 7.22 | 0.11 | 2.20 | 1.30 | 1.20 | 3.70 | 1.00 | 0.16 | 3.32 | 0.38 | 18.90 | 75.29 | - | - | 63.36 | 55.92 |

CIA: Chemical Index of Alteration [1]; PIA: Plagioclase Index of Alteration [6]; ICV: Index of Chemical Variability [16,76]; $MIA_{(O)}$: Mafic Index of Alteration (Oxic) and $MIA_{®}$: Mafic Index of Alteration (Redox) [60]; APT: Archean–Proterozoic Terrain (this study); DTT: Deccan Trap Terrain (this study); WCIRAC: West Coast of India River Average Clay (this study); WCIRAS: West Coast of India River Average Silt (this study); UCC: Upper Continental Crust [77]; PAAS: Post-Archean average Australian Shale [78].

**Table 2.** Trace element content (μg/g) of the clay fraction (<4 μm) of sediments in the rivers of the west coast of India.

| **State (No. of Rivers)** | | **Sc** | **V** | **Cr** | **Co** | **Ni** | **Cu** | **Zn** | **Ga** | **Rb** | **Sr** | **Nb** | **Cs** | **Ba** | **Hf** | **Th** | **U** | **Zr** | **Ta** | **Pb** | **Y** | **La** | **Ce** | **Yb** |
|---|---|---|---|---|---|---|---|---|---|---|---|---|---|---|---|---|---|---|---|---|---|---|---|---|
| Kerala (21) | Range | 20.63–32.93 | 111.22–247.00 | 108.93–286.56 | 18.62–41.83 | 42.60–101.54 | 29.20–111.95 | 29.81–155.05 | 24.97–37.80 | 36.92–91.31 | 45.69–160.74 | 10.99–21.14 | 2.39–6.01 | 169.20–805.44 | 3.64–6.87 | 7.09–24.33 | 1.54–5.11 | 106.61–220.88 | 0.73–1.28 | 12.15–55.83 | 16.55–32.17 | 29.48–95.76 | 63.29–179.62 | 1.86–3.33 |
| | Avg., | 26.54 | 175.49 | 158.78 | 29.48 | 63.45 | 73.45 | 58.06 | 33.53 | 61.77 | 79.31 | 14.93 | 3.57 | 381.11 | 4.77 | 11.92 | 2.57 | 147.03 | 0.97 | 31.71 | 25.82 | 55.64 | 109.03 | 2.72 |
| | STD ± | 3.29 | 39.86 | 52.25 | 7.77 | 16.01 | 19.72 | 30.32 | 3.59 | 15.08 | 29.62 | 2.81 | 0.83 | 199.44 | 0.85 | 3.97 | 1.00 | 27.29 | 0.14 | 11.62 | 3.76 | 19.96 | 36.47 | 0.38 |
| Karnataka (20) | Range | 14.30–36.60 | 136.10–347.61 | 82.77–897.42 | 11.39–55.12 | 46.31–129.46 | 76.34–231.77 | 53.65–195.43 | 24.54–39.11 | 31.90–88.76 | 29.47–71.71 | 11.33–26.53 | 3.22–6.99 | 104.12–288.19 | 4.02–10.58 | 7.93–25.70 | 1.62–6.16 | 136.56–393.66 | 1.04–2.38 | 17.31–51.19 | 8.57–27.41 | 8.03–42.58 | 29.50–86.72 | 1.23–2.96 |
| | Avg., | 22.49 | 228.55 | 203.82 | 24.74 | 72.18 | 133.00 | 85.45 | 32.48 | 61.71 | 49.21 | 16.63 | 4.98 | 177.67 | 5.63 | 13.92 | 3.92 | 199.00 | 1.55 | 31.86 | 16.31 | 24.51 | 66.32 | 1.88 |
| | SD (±) | 7.09 | 64.94 | 168.25 | 11.36 | 18.10 | 48.96 | 33.00 | 4.01 | 17.04 | 10.62 | 3.60 | 1.29 | 49.70 | 1.67 | 4.88 | 1.13 | 66.10 | 0.37 | 9.97 | 4.83 | 9.14 | 15.29 | 0.48 |
| Goa (11) | Range | 16.04–29.54 | 178.55–273.34 | 146.39–237.87 | 17.48–39.65 | 57.23–74.55 | 91.65–194.89 | 63.40–128.70 | 23.87–31.19 | 53.52–87.73 | 53.38–80.88 | 12.60–20.29 | 4.42–7.33 | 140.51–255.50 | 4.93–7.86 | 9.14–15.50 | 3.51–7.61 | 175.51–282.74 | 1.07–1.85 | 21.79–88.87 | 16.05–28.52 | 17.45–37.34 | 52.80–87.53 | 1.89–2.74 |
| | Avg., | 24.12 | 222.57 | 187.98 | 30.54 | 63.89 | 121.41 | 84.62 | 27.00 | 74.51 | 70.70 | 15.60 | 5.93 | 185.07 | 6.14 | 12.54 | 4.94 | 220.42 | 1.43 | 34.10 | 22.73 | 28.77 | 71.29 | 2.33 |
| | SD (±) | 3.63 | 31.30 | 23.42 | 7.85 | 5.55 | 33.43 | 18.87 | 2.27 | 9.91 | 10.21 | 2.86 | 0.91 | 36.73 | 0.99 | 1.89 | 1.18 | 37.97 | 0.24 | 18.69 | 4.87 | 6.24 | 10.34 | 0.33 |
| Archean–Proterozoic Terrain (APT) | Range | 14.31–36.60 | 111.22–347.61 | 82.77–897.42 | 11.395–55.12 | 42.60–129.46 | 29.20–231.77 | 29.81–195.43 | 23.87–39.11 | 31.90–91.31 | 29.47–160.74 | 10.99–26.53 | 2.39–7.33 | 104.12–805.44 | 3.64–10.58 | 7.09–25.70 | 1.54–7.61 | 106.61–393.66 | 0.73–2.38 | 12.15–88.87 | 8.57–32.17 | 8.03–95.76 | 29.50–179.62 | 1.23–3.33 |
| | Avg., | 24.47 | 205.86 | 182.28 | 27.88 | 66.90 | 106.50 | 74.21 | 31.75 | 64.44 | 65.91 | 15.73 | 4.61 | 261.40 | 5.39 | 12.82 | 3.59 | 182.54 | 1.29 | 32.27 | 21.51 | 37.98 | 84.62 | 2.32 |
| | SD (±) | 5.37 | 55.03 | 110.18 | 9.50 | 15.70 | 45.14 | 31.88 | 4.29 | 15.63 | 24.39 | 3.18 | 1.39 | 163.37 | 1.35 | 4.07 | 1.42 | 56.01 | 0.38 | 12.63 | 6.12 | 20.32 | 32.32 | 0.56 |

**Table 2.** *Cont.*

| State (No. of Rivers) | | Sc | V | Cr | Co | Ni | Cu | Zn | Ga | Rb | Sr | Nb | Cs | Ba | Hf | Th | U | Zr | Ta | Pb | Y | La | Ce | Yb |
|---|---|---|---|---|---|---|---|---|---|---|---|---|---|---|---|---|---|---|---|---|---|---|---|---|
| Maharashtra (21) | Range | 26.37–58.58 | 194.68–465.37 | 86.18–267.99 | 27.03–70.83 | 53.67–104.41 | 133.71–275.27 | 64.06–192.93 | 23.34–45.45 | 26.92–92.18 | 42.26–217.87 | 9.00–18.21 | 1.67–7.82 | 128.83–362.78 | 4.31–9.14 | 5.40–18.30 | 1.00–5.90 | 158.73–321.44 | 0.90–1.71 | 8.60–39.25 | 20.64–54.54 | 20.08–46.22 | 45.04–127.80 | 2.05–3.92 |
| | Avg., | 40.15 | 343.61 | 159.77 | 48.83 | 67.89 | 204.18 | 102.43 | 30.10 | 49.72 | 75.98 | 12.77 | 4.01 | 193.90 | 6.80 | 8.65 | 2.69 | 248.78 | 1.25 | 23.46 | 34.76 | 28.20 | 68.63 | 2.80 |
| | SD (±) | 8.21 | 75.77 | 46.99 | 12.27 | 12.02 | 47.94 | 32.05 | 4.77 | 19.26 | 39.00 | 2.94 | 1.82 | 59.51 | 1.23 | 3.33 | 1.38 | 45.46 | 0.25 | 8.44 | 8.95 | 6.90 | 19.88 | 0.47 |
| Gujarat (17) | Range | 27.04–43.05 | 164.99–424.36 | 105.93–968.39 | 28.29–91.34 | 42.41–536.77 | 110.88–391.21 | 52.21–697.89 | 23.00–30.96 | 41.53–101.17 | 83.44–374.88 | 11.19–15.15 | 3.44–8.56 | 163.61–382.99 | 4.95–7.04 | 6.81–14.28 | 1.14–2.44 | 182.27–270.61 | 0.966–1.57 | 11.17–77.11 | 26.25–32.43 | 20.98–35.59 | 47.11–71.30 | 2.01–2.38 |
| | Avg., | 36.24 | 264.24 | 173.00 | 40.26 | 75.47 | 165.34 | 117.30 | 25.96 | 65.38 | 129.26 | 13.05 | 5.02 | 225.60 | 5.90 | 8.73 | 1.58 | 221.23 | 1.23 | 21.67 | 29.64 | 26.78 | 57.51 | 2.24 |
| | SD (±) | 3.93 | 73.68 | 205.49 | 13.68 | 118.93 | 66.20 | 151.43 | 1.94 | 15.48 | 65.98 | 1.09 | 1.20 | 56.85 | 0.58 | 1.77 | 0.33 | 22.51 | 0.16 | 15.57 | 2.19 | 3.70 | 5.57 | 0.14 |
| Deccan Trap Terrain (DTT) | Range | 26.37–58.58 | 164.99–465.37 | 86.18–968.39 | 27.03–91.34 | 42.41–536.77 | 110.88–391.21 | 52.21–697.89 | 23.007–45.45 | 26.92–101.17 | 42.26–374.88 | 9.00–18.21 | 1.67–8.56 | 128.83–382.99 | 4.32–9.14 | 5.40–18.30 | 1.00–5.90 | 158.73–321.44 | 0.90–1.71 | 8.60–77.11 | 20.65–54.54 | 20.08–46.22 | 45.04–127.80 | 2.01–3.92 |
| | Avg., | 38.40 | 308.10 | 165.69 | 45.00 | 71.28 | 186.81 | 109.08 | 28.25 | 56.73 | 99.82 | 12.90 | 4.46 | 208.08 | 6.40 | 8.69 | 2.20 | 236.46 | 1.24 | 22.66 | 32.47 | 27.56 | 63.66 | 2.55 |
| | SD (±) | 6.85 | 83.97 | 139.63 | 13.45 | 78.80 | 59.34 | 102.61 | 4.27 | 19.14 | 58.53 | 2.28 | 1.63 | 59.73 | 1.08 | 2.71 | 1.18 | 39.10 | 0.21 | 12.01 | 7.21 | 5.67 | 16.08 | 0.46 |
| **West Coast of India River Average Clay (WCIRAC)** | **Range** | **14.30–58.58** | **111.22–465.37** | **82.77–968.39** | **11.39–91.34** | **42.41–536.77** | **29.20–391.21** | **29.81–697.89** | **23.00–45.45** | **26.92–101.17** | **29.47–374.88** | **9.00–26.53** | **1.67–8.56** | **104.12–805.44** | **3.64–10.58** | **5.40–25.70** | **1.00–7.61** | **106.61–393.66** | **0.73–2.38** | **8.60–88.87** | **8.57–54.54** | **8.03–95.76** | **29.50–179.62** | **1.23–3.92** |
| | **Avg.,** | **30.35** | **249.03** | **175.27** | **35.11** | **68.75** | **140.41** | **88.94** | **30.27** | **61.18** | **80.23** | **14.53** | **4.55** | **238.88** | **5.81** | **11.08** | **3.00** | **205.31** | **1.27** | **28.21** | **26.14** | **33.58** | **75.77** | **2.41** |
| | **SD (±)** | **9.16** | **85.12** | **123.01** | **14.12** | **52.22** | **64.98** | **72.52** | **4.60** | **17.52** | **45.26** | **3.15** | **1.49** | **132.21** | **1.33** | **4.10** | **1.49** | **56.13** | **0.32** | **13.19** | **8.53** | **16.63** | **28.54** | **0.53** |
| Reference Sediments | PAAS | 15.89 | 150.00 | 110.00 | 23.00 | 55.00 | 50.00 | 85.00 | 20.00 | 160.00 | 200.00 | 19.00 | 15.00 | 650.00 | 5.00 | 14.60 | 3.10 | 210.00 | 1.50 | 20.00 | 27.31 | 44.56 | 88.25 | 2.04 |
| | UCC | 14.00 | 97.00 | 92.30 | 17.30 | 47.30 | 27.70 | 67.00 | 17.50 | 82.00 | 320.00 | 11.80 | 4.10 | 624.00 | 5.26 | 10.10 | 2.63 | 193.00 | 0.88 | 17.00 | 21.00 | 31.40 | 63.40 | 3.01 |

| State (No. of Rivers) | | ∑TE | Th/Sc | Zr/Sc | Cr/V | Y/Ni | Co/Th | La/Sc | Zr/Co | La/Th | Th/Yb | Th/U | Rb/Sr | $K_2O$/Rb | Cr/Th | Cr/Ni | V/Th |
|---|---|---|---|---|---|---|---|---|---|---|---|---|---|---|---|---|---|
| Kerala (21) | Range | 991.58–1802.55 | 0.23–0.94 | 3.85–9.73 | 0.69–1.38 | 0.21–0.66 | 1.05–5.89 | 0.95–3.91 | 2.68–9.09 | 3.02–10.48 | 2.21–8.02 | 2.44–12.31 | 0.36–1.58 | 0.06–0.01 | 5.74–36.89 | 1.98–3.11 | 6.53–31.27 |
| | Avg., | 1358.44 | 0.46 | 5.62 | 0.91 | 0.43 | 2.76 | 2.14 | 5.36 | 4.81 | 4.45 | 5.24 | 0.87 | 0.02 | 14.95 | 2.49 | 16.30 |
| | STD ± | 212.30 | 0.17 | 1.30 | 0.18 | 0.12 | 1.29 | 0.83 | 1.80 | 1.70 | 1.51 | 2.61 | 0.35 | 0.01 | 7.90 | 0.33 | 6.83 |
| Karnataka (20) | Range | 1097.93–2027.12 | 0.22–1.47 | 4.23–1.28 | 0.42–3.35 | 0.09–0.35 | 0.44–4.20 | 0.28–2.38 | 3.57–23.38 | 0.75–2.51 | 3.56–20.75 | 1.93–7.17 | 0.72–2.03 | 0.01–0.02 | 3.22–110.23 | 1.78–6.93 | 5.74–33.78 |
| | Avg., | 1368.79 | 0.69 | 9.33 | 0.91 | 0.23 | 1.97 | 1.23 | 9.45 | 1.77 | 8.06 | 3.69 | 1.28 | 0.02 | 17.98 | 2.63 | 18.57 |
| | STD ± | 218.06 | 0.35 | 3.22 | 0.62 | 0.07 | 1.02 | 0.63 | 5.10 | 0.37 | 4.18 | 1.18 | 0.37 | 0.00 | 22.36 | 1.07 | 8.42 |
| Goa (11) | Range | 1269.83–1611.23 | 0.34–0.84 | 6.54–17.62 | 0.71–1.07 | 0.22–0.45 | 1.14–4.03 | 0.74–1.64 | 4.42–15.09 | 1.28–2.89 | 4.40–7.20 | 2.03–3.11 | 0.89–1.26 | 0.01–0.27 | 9.58–23.10 | 2.55–4.01 | 13.41–29.90 |
| | Avg., | 1393.51 | 0.54 | 9.56 | 0.86 | 0.36 | 2.53 | 1.20 | 8.03 | 2.32 | 5.45 | 2.60 | 1.06 | 0.02 | 15.43 | 2.95 | 18.20 |
| | SD (±) | 92.54 | 0.15 | 3.35 | 0.14 | 0.09 | 0.90 | 0.22 | 3.71 | 0.48 | 0.99 | 0.37 | 0.13 | 0.00 | 3.64 | 0.41 | 4.53 |
| Archean–Proterozoic Terrain (APT) | Range | 991.58–2027.12 | 0.22–1.47 | 3.85–17.62 | 0.42–3.35 | 0.09–0.66 | 0.44–5.89 | 0.28–3.91 | 2.68–23.38 | 0.75–10.48 | 2.21–20.75 | 1.93–12.31 | 0.36–2.03 | 0.01–0.2 | 3.22–110.23 | 1.78–6.93 | 5.74–33.78 |
| | Avg., | 1369.84 | 0.57 | 7.88 | 0.90 | 0.34 | 2.41 | 1.59 | 7.50 | 3.12 | 6.05 | 4.08 | 1.07 | 0.02 | 16.22 | 2.64 | 17.58 |
| | SD (±) | 192.99 | 0.27 | 3.20 | 0.40 | 0.13 | 1.15 | 0.80 | 4.14 | 1.81 | 3.21 | 2.08 | 0.37 | 0.00 | 14.68 | 0.73 | 7.06 |

**Table 2.** *Cont.*

| State (No. of Rivers) | | ∑TE | Th/Sc | Zr/Sc | Cr/V | Y/Ni | Co/Th | La/Sc | Zr/Co | La/Th | Th/Yb | Th/U | Rb/Sr | $K_2O$/Rb | Cr/Th | Cr/Ni | V/Th |
|---|---|---|---|---|---|---|---|---|---|---|---|---|---|---|---|---|---|
| Maharashtra (21) | Range | 1360.43–1980.54 | 0.11–0.67 | 4.30–10.75 | 0.23–0.73 | 0.29–0.77 | 1.88–10.90 | 0.45–1.70 | 3.20–11.73 | 2.01–4.67 | 1.65–7.34 | 1.88–5.39 | 0.28–2.02 | 0.01–0.02 | 9.13–47.41 | 1.39–3.61 | 15.62–72.53 |
| | Avg., | 1624.96 | 0.24 | 6.37 | 0.49 | 0.52 | 6.41 | 0.75 | 5.47 | 3.48 | 3.23 | 3.61 | 0.77 | 0.02 | 20.82 | 2.35 | 44.28 |
| | SD (±) | 164.49 | 0.15 | 1.52 | 0.16 | 0.13 | 2.81 | 0.31 | 2.13 | 0.87 | 1.57 | 1.05 | 0.48 | 0.00 | 10.62 | 0.51 | 16.84 |
| Gujarat (17) | Range | 1248.28–3733.64 | 0.16–0.52 | 5.30–6.74 | 0.28–3.06 | 0.05–0.72 | 1.98–12.38 | 0.52–1.31 | 2.06–7.23 | 2.49–3.37 | 2.99–6.81 | 4.33–6.28 | 0.19–0.76 | 0.01–0.02 | 10.31–131.34 | 1.80–3.17 | 11.55–55.57 |
| | Avg., | 1596.46 | 0.25 | 6.12 | 0.65 | 0.60 | 4.85 | 0.76 | 5.82 | 3.10 | 3.93 | 5.55 | 0.55 | 0.02 | 21.33 | 2.59 | 32.20 |
| | SD (±) | 565.62 | 0.08 | 0.42 | 0.63 | 0.16 | 2.17 | 0.19 | 1.10 | 0.23 | 0.92 | 0.49 | 0.14 | 0.00 | 28.54 | 0.29 | 13.04 |
| Deccan Trap Terrain (DTT) | Range | 1248.28–3733.65 | 0.11–0.67 | 4.30–10.75 | 0.23–3.06 | 0.06–0.77 | 1.88–12.38 | 0.45–1.70 | 2.06–11.73 | 2.01–4.67 | 1.65–7.35 | 1.88–6.28 | 0.19–2.02 | 0.01–0.02 | 9.13–131.34 | 1.39–3.61 | 11.55–72.53 |
| | Avg., | 1612.21 | 0.24 | 6.26 | 0.56 | 0.56 | 5.72 | 0.75 | 5.63 | 3.31 | 3.55 | 4.48 | 0.67 | 0.02 | 21.05 | 2.46 | 38.87 |
| | SD (±) | 391.38 | 0.13 | 1.16 | 0.44 | 0.15 | 2.63 | 0.26 | 1.73 | 0.69 | 1.35 | 1.29 | 0.38 | 0.00 | 20.33 | 0.44 | 16.24 |
| **West Coast of India River Average Clay (WCIRAC)** | **Range** | **991.58–3734.37** | **0.11–1.47** | **3.85–17.62** | **0.23–3.35** | **0.06–0.77** | **0.44–12.38** | **0.28–3.92** | **2.06–23.38** | **0.75–10.48** | **1.65–20.75** | **1.88–12.31** | **0.19–2.03** | **0.01–0.06** | **3.22–131.34** | **1.39–6.93** | **5.74–72.53** |
| | **Avg.,** | **1473.05** | **0.43** | **7.20** | **0.75** | **0.43** | **3.81** | **1.24** | **6.71** | **3.20** | **4.99** | **4.25** | **0.90** | **0.02** | **18.26** | **2.56** | **26.57** |
| | **SD (±)** | **315.46** | **0.27** | **2.66** | **0.45** | **0.17** | **2.52** | **0.76** | **3.45** | **1.44** | **2.87** | **1.79** | **0.42** | **0.01** | **17.35** | **0.63** | **15.81** |
| Reference Sediments | UCC | 1650.87 | 0.72 | 13.79 | 0.95 | 0.44 | 1.71 | 2.24 | 11.16 | 3.11 | 3.35 | 3.84 | 0.26 | - | 9.14 | 1.95 | 9.60 |
| | PAAS | 1807.09 | 0.92 | 13.22 | 0.73 | 0.50 | 1.58 | 2.80 | 9.13 | 3.05 | 7.16 | 4.71 | 0.80 | - | 7.53 | 2.00 | 10.27 |

APT: Archean–Proterozoic Terrain (this study); DTT: Deccan Trap Terrain (this study); WCIRAC: West Coast of India River Average Clay (this study); UCC: Upper Continental Crust [77]; PAAS: Post-Archean average Australian Shale [78].

**Table 3.** Trace element content (μg/g) of the silt fraction (>4 to 63 μm) of sediments in the rivers of the west coast of India.

| State (No. of Rivers) | | Sc | V | Cr | Co | Ni | Cu | Zn | Ga | Rb | Sr | Nb | Cs | Ba | Hf | Th | U | Zr | Ta | Pb | Y | La | Ce | Yb |
|---|---|---|---|---|---|---|---|---|---|---|---|---|---|---|---|---|---|---|---|---|---|---|---|---|
| Kerala (21) | Range | 14.85–29.27 | 97.66–254.56 | 118.32–350.87 | 15.53–43.83 | 35.91–90.85 | 31.87–94.86 | 57.81–262.67 | 18.21–47.22 | 26.99–90.74 | 61.44–337.38 | 11.15–34.86 | 1.09–2.93 | 186.31–1503.00 | 5.49–65.31 | 6.93–116.47 | 1.26–14.63 | 188.07–2435.71 | 0.60–2.58 | 19.12–87.62 | 19.01–38.58 | 44.16–232.43 | 88.86–521.22 | 2.07–4.32 |
| | Avg., | 24.27 | 181.09 | 174.38 | 29.60 | 56.46 | 68.22 | 148.77 | 33.53 | 59.27 | 155.88 | 20.47 | 2.20 | 642.24 | 18.71 | 30.73 | 3.92 | 646.91 | 1.28 | 41.00 | 30.51 | 105.36 | 201.27 | 3.10 |
| | STD ± | 3.97 | 45.16 | 76.90 | 7.46 | 15.72 | 17.49 | 67.62 | 6.19 | 20.96 | 79.16 | 6.36 | 0.49 | 401.36 | 15.03 | 27.44 | 3.27 | 538.36 | 0.52 | 18.69 | 5.38 | 56.70 | 111.54 | 0.54 |
| Karnataka (20) | Range | 11.30–39.13 | 104.96–536.01 | 80.64–2350.39 | 10.73–35.55 | 35.12–146.15 | 50.12–185.46 | 44.01–98.21 | 11.63–39.13 | 15.11–79.79 | 36.62–101.55 | 10.20–23.31 | 1.66–4.70 | 98.82–290.56 | 5.39–27.48 | 6.27–28.43 | 1.95–7.14 | 19.57–1237.72 | 1.15–2.31 | 12.94–42.77 | 13.63–33.74 | 15.87–72.91 | 32.63–132.22 | 1.50–3.90 |
| | Avg., | 22.53 | 228.92 | 296.12 | 21.22 | 63.73 | 106.65 | 67.10 | 29.13 | 40.54 | 61.83 | 16.91 | 2.97 | 194.49 | 10.92 | 14.31 | 4.14 | 426.76 | 1.72 | 25.19 | 21.57 | 32.06 | 68.19 | 2.40 |
| | SD (±) | 8.35 | 101.91 | 489.51 | 6.12 | 23.30 | 37.28 | 15.70 | 6.65 | 17.40 | 18.35 | 3.21 | 0.99 | 49.97 | 4.85 | 5.98 | 1.43 | 234.76 | 0.30 | 7.82 | 5.28 | 13.16 | 23.49 | 0.60 |

**Table 3.** *Cont.*

| State (No. of Rivers) | | Sc | V | Cr | Co | Ni | Cu | Zn | Ga | Rb | Sr | Nb | Cs | Ba | Hf | Th | U | Zr | Ta | Pb | Y | La | Ce | Yb |
|---|---|---|---|---|---|---|---|---|---|---|---|---|---|---|---|---|---|---|---|---|---|---|---|---|
| Goa (11) | Range | 18.96–28.72 | 183.73–348.37 | 185.49–245.62 | 16.63–39.02 | 44.34–68.93 | 85.38–166.15 | 51.77–73.84 | 16.93–26.49 | 28.96–58.61 | 52.11–107.48 | 13.64–25.62 | 2.45–5.29 | 102.86–274.01 | 6.26–13.27 | 4.34–16.79 | 4.01–7.93 | 229.78–502.26 | 1.35–4.11 | 19.44–57.53 | 18.00–31.95 | 16.75–39.64 | 31.78–89.49 | 2.11–3.34 |
| | Avg., | 22.99 | 242.94 | 211.09 | 28.10 | 58.58 | 108.90 | 63.52 | 22.55 | 47.64 | 84.84 | 17.56 | 3.85 | 203.64 | 8.72 | 10.84 | 5.30 | 326.41 | 2.06 | 29.87 | 27.51 | 28.41 | 61.81 | 2.77 |
| | SD (±) | 2.90 | 49.26 | 18.60 | 7.03 | 6.88 | 28.24 | 7.53 | 2.67 | 9.23 | 17.14 | 3.83 | 0.98 | 50.62 | 2.26 | 3.27 | 1.27 | 88.03 | 0.81 | 11.12 | 4.80 | 6.40 | 16.24 | 0.34 |
| Archean–Proterozoic Terrain (APT) | Range | 11.31–39.13 | 97.66–536.01 | 80.64–2350.39 | 10.73–43.83 | 35.12–146.15 | 31.87–185.46 | 44.01–262.67 | 11.63–47.22 | 15.11–90.74 | 36.62–337.38 | 10.20–34.86 | 1.09–5.29 | 98.82–1503.01 | 5.39–65.31 | 4.34–116.47 | 1.26–14.63 | 188.07–2435.71 | 0.60–4.11 | 12.94–87.62 | 13.63–38.58 | 15.87–232.43 | 31.78–521.22 | 1.50–4.32 |
| | Avg., | 23.33 | 212.57 | 228.97 | 26.06 | 59.70 | 91.61 | 99.33 | 29.51 | 49.61 | 104.68 | 18.48 | 2.84 | 377.25 | 13.60 | 20.21 | 4.30 | 494.44 | 1.62 | 32.56 | 26.44 | 60.89 | 120.58 | 2.76 |
| | SD (±) | 5.87 | 76.53 | 307.77 | 7.79 | 17.88 | 34.24 | 59.89 | 7.07 | 19.32 | 67.27 | 5.03 | 1.02 | 336.33 | 10.82 | 19.72 | 2.36 | 391.37 | 0.60 | 15.37 | 6.53 | 51.97 | 98.18 | 0.61 |
| Maharashtra (21) | Range | 18.19–54.44 | 179.81–1308.25 | 124.63–576.09 | 25.65–82.14 | 42.06–103.18 | 84.52–424.44 | 46.005–156.51 | 19.14–39.99 | 12.76–60.43 | 50.55–380.44 | 11.85–68.14 | 0.53–5.17 | 83.55–340.66 | 5.15–21.47 | 2.63–15.64 | 0.83–5.56 | 195.08–1119.75 | 0.90–7.48 | 7.03–38.44 | 21.64–40.05 | 12.69–40.81 | 29.29–98.56 | 2.26–3.65 |
| | Avg., | 37.24 | 599.33 | 219.29 | 54.57 | 65.73 | 229.67 | 88.68 | 27.21 | 28.02 | 114.67 | 23.68 | 1.96 | 176.60 | 9.63 | 7.46 | 2.47 | 397.79 | 2.38 | 18.59 | 31.77 | 25.04 | 56.91 | 2.98 |
| | SD (±) | 10.18 | 276.65 | 125.91 | 13.82 | 11.95 | 91.62 | 30.58 | 6.01 | 13.30 | 68.84 | 12.21 | 1.22 | 70.63 | 3.97 | 3.61 | 1.42 | 222.87 | 1.41 | 8.29 | 4.98 | 6.93 | 17.66 | 0.46 |
| Gujarat (17) | Range | 15.15–28.24 | 165.01–403.65 | 77.84–732.65 | 21.72–66.59 | 31.26–440.13 | 81.24–264.51 | 37.10–387.41 | 15.97–21.98 | 30.36–67.08 | 127.08–340.74 | 13.12–23.77 | 1.27–4.38 | 166.05–323.90 | 4.84–9.07 | 6.66–24.50 | 1.28–3.24 | 179.65–353.63 | 0.853–2.12 | 10.54–51.99 | 26.21–38.23 | 22.81–53.57 | 47.95–103.57 | 2.29–3.51 |
| | Avg., | 20.39 | 280.24 | 153.23 | 34.95 | 62.75 | 130.62 | 72.73 | 18.32 | 45.90 | 189.43 | 18.45 | 2.60 | 238.46 | 6.71 | 11.42 | 1.97 | 250.86 | 1.56 | 17.29 | 31.15 | 32.94 | 67.29 | 2.82 |
| | SD (±) | 3.54 | 73.03 | 153.31 | 9.93 | 97.39 | 40.97 | 82.15 | 2.03 | 11.31 | 52.79 | 3.09 | 0.83 | 39.80 | 1.12 | 4.36 | 0.55 | 45.84 | 0.33 | 9.77 | 3.19 | 7.96 | 14.94 | 0.30 |
| Deccan Trap Terrain (DTT) | Range | 15.15–54.44 | 165.01–1308.25 | 77.84–732.65 | 21.72–82.14 | 31.26–440.13 | 81.24–424.44 | 37.10–387.41 | 15.974–39.99 | 12.76–67.08 | 50.56–380.44 | 11.85–68.14 | 0.53–5.17 | 83.55–340.66 | 4.84–21.47 | 2.63–24.50 | 0.83–5.56 | 179.65–1119.75 | 0.85–7.48 | 7.03–51.99 | 21.64–40.05 | 12.69–53.57 | 29.29–103.57 | 2.26–3.65 |
| | Avg., | 29.70 | 456.58 | 189.74 | 45.79 | 64.39 | 185.36 | 81.55 | 23.23 | 36.02 | 148.11 | 21.34 | 2.25 | 204.28 | 8.32 | 9.23 | 2.25 | 332.06 | 2.02 | 18.01 | 31.49 | 28.57 | 61.55 | 2.91 |
| | SD (±) | 11.55 | 263.68 | 140.86 | 15.61 | 64.66 | 88.06 | 59.06 | 6.43 | 15.24 | 72.01 | 9.57 | 1.10 | 65.98 | 3.35 | 4.39 | 1.13 | 182.32 | 1.14 | 8.88 | 4.23 | 8.32 | 17.10 | 0.40 |
| **West Coast of India River Average Silt (WCIRAS)** | **Range** | **11.31–54.44** | **97.66–1308.25** | **77.85–2350.39** | **10.73–82.14** | **31.26–440.13** | **31.87–424.44** | **37.10–387.41** | **11.63–47.22** | **12.76–90.74** | **36.62–380.44** | **10.21–68.14** | **0.53–5.29** | **83.55–1503.01** | **4.85–65.31** | **2.63–116.47** | **0.931–14.63** | **179.65–1435.70** | **0.60–7.48** | **7.03–87.63** | **13.63–40.05** | **12.69–232.43** | **29.29–521.22** | **1.50–4.32** |
| | **Avg.,** | **26.02** | **315.60** | **212.40** | **34.39** | **61.68** | **131.19** | **91.82** | **26.86** | **43.87** | **123.02** | **19.69** | **2.59** | **304.22** | **11.37** | **15.58** | **3.43** | **425.88** | **1.78** | **26.42** | **28.57** | **47.25** | **95.66** | **2.82** |
| | **SD (±)** | **9.23** | **216.68** | **250.82** | **15.23** | **43.89** | **77.87** | **59.86** | **7.46** | **18.87** | **72.21** | **7.39** | **1.09** | **272.05** | **8.87** | **16.14** | **2.18** | **328.78** | **0.89** | **14.85** | **6.18** | **42.83** | **80.65** | **0.53** |
| Reference Sediments | PAAS | 15.89 | 150.00 | 110.00 | 23.00 | 55.00 | 50.00 | 85.00 | 20.00 | 160.00 | 200.00 | 19.00 | 15.00 | 650.00 | 5.00 | 14.60 | 3.10 | 210.00 | 1.50 | 20.00 | 27.31 | 44.56 | 88.25 | 2.04 |
| | UCC | 14.00 | 97.00 | 92.30 | 17.30 | 47.30 | 27.70 | 67.00 | 17.50 | 82.00 | 320.00 | 11.80 | 4.10 | 624.00 | 5.26 | 10.10 | 2.63 | 193.00 | 0.88 | 17.00 | 21.00 | 31.40 | 63.40 | 3.01 |

| State (No. of Rivers) | | ∑TE | Th/Sc | Zr/Sc | Cr/V | Y/Ni | Co/Th | La/Sc | Zr/Co | La/Th | Th/Yb | Th/U | Rb/Sr | $K_2O$/Rb | Cr/Th | Cr/Ni | V/Th |
|---|---|---|---|---|---|---|---|---|---|---|---|---|---|---|---|---|---|
| Kerala (21) | Range | 1395.11–3848.58 | 0.23–5.31 | 8.22–111.19 | 0.71–1.48 | 0.27–0.93 | 0.20–6.29 | 1.51–10.61 | 5.99–103.99 | 1.99–6.75 | 1.81–31.85 | 2.761–18.26 | 0.18–1.35 | 0.02–0.03 | 1.01–46.17 | 2.03–4.89 | 1.08–36.29 |
| | Avg., | 2338.94 | 1.27 | 26.65 | 0.96 | 0.54 | 0.96 | 4.34 | 21.85 | 3.43 | 9.91 | 7.83 | 0.38 | 0.03 | 5.67 | 3.09 | 5.89 |
| | STD ± | 601.68 | 1.31 | 26.08 | 0.23 | 0.18 | 1.66 | 2.67 | 27.47 | 1.56 | 7.53 | 4.79 | 0.31 | 0.00 | 11.99 | 0.69 | 9.80 |
| Karnataka (20) | Range | 1148.90–3826.03 | 0.24–1.64 | 5.67–71.39 | 0.34–6.73 | 0.183–0.63 | 0.43–4.67 | 0.43–4.20 | 5.47–79.21 | 1.15–3.18 | 2.61–16.46 | 1.90–7.52 | 0.32–1.32 | 0.02–0.04 | 3.26–236.69 | 1.68–16.08 | 5.94–39.05 |
| | Avg., | 1635.17 | 0.73 | 21.90 | 1.20 | 0.36 | 1.81 | 1.64 | 22.34 | 2.32 | 6.51 | 3.60 | 0.67 | 0.03 | 25.73 | 3.77 | 18.94 |
| | STD ± | 600.64 | 0.41 | 15.32 | 1.34 | 0.11 | 1.07 | 0.90 | 16.14 | 0.54 | 3.77 | 1.46 | 0.27 | 0.00 | 50.13 | 3.01 | 11.37 |

**Table 3.** *Cont.*

| State (No. of Rivers) | | ∑TE | Th/Sc | Zr/Sc | Cr/V | Y/Ni | Co/Th | La/Sc | Zr/Co | La/Th | Th/Yb | Th/U | Rb/Sr | $K_2O$/Rb | Cr/Th | Cr/Ni | V/Th |
|---|---|---|---|---|---|---|---|---|---|---|---|---|---|---|---|---|---|
| Goa (11) | Range | 1319.37–1753.87 | 0.20–0.67 | 9.67–21.27 | 0.59–1.11 | 0.29–0.59 | 1.26–8.08 | 0.79–1.78 | 6.92–23.74 | 1.94–3.86 | 1.85–5.21 | 1.043–3.16 | 0.39–0.71 | 0.02–0.03 | 12.99–53.11 | 3.04–4.92 | 15.71–62.36 |
| | Avg., | 1499.40 | 0.48 | 14.45 | 0.90 | 0.48 | 3.04 | 1.24 | 12.71 | 2.74 | 3.90 | 2.06 | 0.57 | 0.03 | 22.02 | 3.66 | 25.56 |
| | SD (±) | 144.14 | 0.15 | 4.45 | 0.16 | 0.10 | 1.93 | 0.26 | 5.91 | 0.60 | 1.03 | 0.55 | 0.09 | 0.00 | 10.98 | 0.64 | 14.06 |
| Archean–Proterozoic Terrain (APT) | Range | 1148.90–3848.58 | 0.20–5.32 | 5.67–111.19 | 0.340–6.734 | 0.18–0.93 | 0.20–8.08 | 0.43–10.61 | 5.47–103.99 | 1.15–6.76 | 1.81–31.86 | 1.04–18.26 | 0.18–1.35 | 0.02–0.04 | 1.02–236.69 | 1.68–16.08 | 1.08–62.36 |
| | Avg., | 1890.66 | 0.93 | 22.86 | 1.03 | 0.47 | 2.10 | 2.73 | 21.72 | 3.24 | 7.17 | 5.22 | 0.57 | 0.03 | 19.27 | 3.46 | 17.32 |
| | SD (±) | 649.46 | 0.94 | 19.63 | 0.85 | 0.17 | 1.57 | 2.32 | 20.60 | 1.44 | 5.70 | 4.15 | 0.27 | 0.00 | 32.53 | 1.94 | 12.43 |
| Maharashtra (21) | Range | 1483.29–3738.62 | 0.06–0.66 | 5.90–28.97 | 0.13–1.23 | 0.25–0.58 | 2.28–24.94 | 0.31–1.72 | 3.26–18.51 | 2.36–5.67 | 1.01–4.97 | 1.62–6.19 | 0.06–0.95 | 0.02–0.04 | 10.22–96.15 | 2.04–9.17 | 15.98–253.89 |
| | Avg., | 2104.98 | 0.23 | 11.32 | 0.46 | 0.49 | 9.62 | 0.75 | 7.82 | 3.73 | 2.53 | 3.40 | 0.31 | 0.03 | 35.78 | 3.30 | 105.72 |
| | SD (±) | 483.88 | 0.16 | 6.69 | 0.35 | 0.08 | 5.87 | 0.38 | 4.78 | 0.95 | 1.20 | 1.33 | 0.24 | 0.00 | 23.82 | 1.68 | 75.20 |
| Gujarat (17) | Range | 1081.08–2897.20 | 0.30–1.44 | 7.65–20.75 | 0.30–2.77 | 0.06–1.12 | 0.88–6.92 | 1.01–3.16 | 3.03–12.90 | 2.18–3.46 | 2.77–7.64 | 4.91–7.71 | 0.13–0.45 | 0.02–0.03 | 4.54–76.12 | 1.66–5.74 | 6.73–48.79 |
| | Avg., | 1557.88 | 0.59 | 12.69 | 0.56 | 0.77 | 3.45 | 1.68 | 7.64 | 2.99 | 3.99 | 5.72 | 0.26 | 0.03 | 14.75 | 2.91 | 27.16 |
| | SD (±) | 381.93 | 0.29 | 3.43 | 0.58 | 0.22 | 1.45 | 0.58 | 2.33 | 0.33 | 1.21 | 0.71 | 0.08 | 0.00 | 16.13 | 0.86 | 10.03 |
| Deccan Trap Terrain (DTT) | Range | 1081.08–3738.62 | 0.06–1.44 | 5.90–28.97 | 0.13–2.77 | 0.06–1.12 | 0.88–24.94 | 0.31–3.16 | 3.03–18.51 | 2.18–5.67 | 1.01–7.64 | 1.62–7.70 | 0.06–0.95 | 0.02–0.04 | 4.54–96.15 | 1.66–9.17 | 6.73–253.89 |
| | Avg., | 1860.22 | 0.39 | 11.93 | 0.51 | 0.62 | 6.86 | 1.17 | 7.74 | 3.40 | 3.18 | 4.44 | 0.29 | 0.03 | 26.37 | 3.13 | 70.57 |
| | SD (±) | 515.40 | 0.29 | 5.45 | 0.46 | 0.21 | 5.40 | 0.67 | 3.83 | 0.82 | 1.40 | 1.59 | 0.19 | 0.00 | 23.06 | 1.37 | 68.32 |
| **West Coast of India River Average Silt (WCIRAS)** | **Range** | **1082.66–3848.58** | **0.06–5.32** | **5.67–111.19** | **0.13–6.73** | **0.06–1.12** | **0.20–24.94** | **0.31–10.61** | **3.03–103.99** | **1.15–6.76** | **1.01–31.86** | **1.04–18.26** | **0.06–1.35** | **0.02–0.04** | **1.01–236.69** | **1.66–16.08** | **1.08–253.89** |
| | **Avg.,** | **1878.63** | **0.70** | **18.25** | **0.81** | **0.53** | **4.11** | **2.07** | **15.82** | **3.31** | **5.49** | **4.89** | **0.45** | **0.03** | **22.27** | **3.32** | **39.80** |
| | **SD (±)** | **593.28** | **0.78** | **16.21** | **0.75** | **0.20** | **4.38** | **1.97** | **17.25** | **1.21** | **4.83** | **3.33** | **0.28** | **0.01** | **28.98** | **1.72** | **52.24** |
| Reference Sediments | UCC | 1650.87 | 0.72 | 13.79 | 0.95 | 0.44 | 1.71 | 2.24 | 11.16 | 3.11 | 3.35 | 3.84 | 0.26 | - | 9.14 | 1.95 | 9.60 |
| | PAAS | 1807.09 | 0.92 | 13.22 | 0.73 | 0.50 | 1.58 | 2.80 | 9.13 | 3.05 | 7.16 | 4.71 | 0.80 | - | 7.53 | 2.00 | 10.27 |

APT: Archean-Proterozoic Terrain (this study); DTT: Deccan Trap Terrain (this study); WCIRAS: West Coast of India River Average Silt (this study); UCC: Upper Continental Crust [77]; PAAS: Post-Archean average Australian Shale [78].

**Table 4.** Correlation matrix (APT—Archean–Proterozoic Terrain; DTT—Deccan Trap Terrain). The red colored values belong to APT and the black colored values belong to DTT.

| | $SiO_2$ | $Al_2O_3$ | $Fe_2O_3$ | MnO | MgO | CaO | $Na_2O$ | $K_2O$ | $TiO_2$ | $P_2O_5$ | ∑REE | Y | La | Ce | Yb | Zr | Hf | U | Th | Sc | V | Cr | Co | Ni | Cu | Zn | Ga | Rb | Sr | Nb | Cs | Ba | Ta | Pb |
|---|---|---|---|---|---|---|---|---|---|---|---|---|---|---|---|---|---|---|---|---|---|---|---|---|---|---|---|---|---|---|---|---|---|---|
| $SiO_2$ | 1 | −0.27 | −0.57 | −0.07 | 0.18 | 0.43 | −0.58 | 0.08 | 0.06 | −0.38 | −0.50 | −0.15 | −0.41 | −0.50 | −0.45 | 0.03 | 0.01 | −0.61 | −0.28 | 0.01 | −0.20 | 0.01 | −0.15 | −0.01 | −0.37 | 0.01 | −0.37 | 0.04 | 0.26 | −0.11 | −0.04 | 0.14 | −0.26 | −0.20 |
| $Al_2O_3$ | −0.39 | 1 | −0.02 | −0.21 | −0.53 | −0.60 | −0.18 | −0.28 | 0.45 | 0.50 | 0.09 | −0.19 | −0.03 | 0.28 | 0.24 | 0.54 | 0.59 | 0.67 | 0.28 | −0.01 | 0.34 | −0.16 | −0.21 | −0.09 | 0.22 | −0.11 | 0.68 | −0.04 | −0.31 | 0.54 | 0.11 | −0.31 | 0.60 | 0.20 |
| $Fe_2O_3$ | −0.31 | −0.04 | 1 | 0.24 | −0.18 | −0.39 | 0.15 | 0.02 | −0.39 | 0.14 | 0.64 | 0.22 | 0.51 | 0.64 | 0.36 | −0.18 | −0.17 | 0.50 | 0.34 | 0.06 | 0.15 | 0.16 | 0.40 | 0.13 | 0.30 | 0.10 | 0.26 | 0.03 | −0.38 | −0.12 | 0.06 | 0.13 | 0.03 | 0.23 |
| MnO | −0.19 | −0.12 | 0.32 | 1 | −0.10 | −0.05 | −0.12 | −0.29 | −0.08 | 0.31 | 0.28 | 0.68 | 0.17 | 0.03 | 0.57 | −0.01 | −0.01 | −0.29 | −0.33 | 0.42 | 0.20 | 0.21 | 0.66 | 0.21 | 0.40 | 0.23 | −0.12 | −0.46 | −0.20 | −0.47 | −0.44 | 0.38 | −0.28 | 0.15 |
| MgO | −0.21 | −0.28 | 0.02 | 0.36 | 1 | 0.65 | −0.14 | 0.52 | −0.27 | −0.33 | −0.24 | −0.11 | −0.02 | −0.35 | −0.43 | −0.44 | −0.44 | −0.38 | −0.18 | −0.27 | −0.61 | −0.08 | −0.28 | −0.11 | −0.33 | −0.03 | −0.66 | 0.19 | 0.44 | −0.28 | 0.05 | −0.06 | −0.30 | −0.21 |
| CaO | −0.29 | −0.45 | −0.06 | 0.13 | 0.50 | 1 | −0.18 | 0.58 | −0.23 | −0.34 | −0.30 | −0.17 | −0.07 | −0.38 | −0.52 | −0.40 | −0.45 | −0.56 | −0.10 | −0.23 | −0.57 | −0.12 | −0.33 | −0.14 | −0.41 | −0.12 | −0.63 | 0.31 | 0.77 | −0.16 | 0.18 | 0.34 | −0.17 | −0.27 |
| $Na_2O$ | −0.20 | −0.50 | −0.28 | −0.15 | 0.17 | 0.71 | 1 | −0.06 | −0.11 | −0.10 | 0.13 | 0.10 | 0.14 | 0.09 | 0.23 | −0.12 | −0.14 | 0.12 | 0.00 | 0.08 | 0.08 | −0.06 | 0.02 | −0.05 | 0.12 | −0.09 | 0.10 | −0.05 | −0.12 | −0.06 | −0.05 | −0.17 | −0.09 | −0.11 |
| $K_2O$ | −0.10 | −0.63 | −0.24 | 0.11 | 0.53 | 0.62 | 0.75 | 1 | −0.35 | −0.12 | 0.12 | −0.40 | 0.33 | 0.19 | −0.52 | −0.45 | −0.47 | 0.09 | 0.50 | −0.58 | −0.74 | −0.25 | −0.47 | −0.25 | −0.36 | −0.17 | −0.28 | 0.83 | 0.47 | 0.31 | 0.72 | 0.14 | 0.26 | −0.01 |
| $TiO_2$ | 0.37 | −0.05 | −0.05 | −0.25 | 0.00 | −0.14 | −0.08 | −0.02 | 1 | 0.33 | −0.30 | −0.06 | −0.42 | −0.20 | 0.15 | 0.70 | 0.70 | 0.06 | −0.18 | 0.22 | 0.61 | −0.11 | −0.13 | −0.05 | 0.07 | −0.08 | 0.50 | −0.36 | −0.43 | 0.44 | −0.24 | −0.19 | 0.38 | −0.05 |
| $P_2O_5$ | −0.67 | 0.34 | 0.15 | 0.23 | 0.17 | 0.11 | −0.05 | −0.04 | −0.16 | 1 | 0.24 | 0.17 | 0.18 | 0.25 | 0.40 | 0.20 | 0.25 | 0.36 | 0.23 | −0.03 | 0.18 | 0.18 | 0.21 | 0.24 | 0.61 | 0.30 | 0.28 | −0.08 | −0.34 | 0.27 | 0.01 | 0.13 | 0.41 | 0.58 |
| ∑REE | −0.64 | 0.43 | −0.02 | 0.23 | 0.06 | 0.15 | −0.02 | −0.02 | −0.15 | 0.79 | 1 | 0.35 | 0.92 | 0.91 | 0.46 | −0.33 | −0.32 | 0.51 | 0.57 | −0.06 | −0.01 | −0.05 | 0.21 | −0.09 | 0.11 | −0.09 | 0.23 | 0.16 | −0.26 | 0.09 | 0.10 | −0.02 | 0.25 | 0.12 |
| Y | −0.71 | 0.31 | 0.26 | 0.41 | 0.21 | 0.22 | −0.01 | 0.00 | −0.28 | 0.58 | 0.70 | 1 | 0.14 | −0.02 | 0.84 | 0.18 | 0.18 | −0.33 | −0.50 | 0.71 | 0.30 | 0.07 | 0.66 | 0.06 | 0.41 | 0.12 | −0.08 | −0.65 | −0.23 | −0.62 | −0.68 | −0.02 | −0.46 | −0.19 |
| La | −0.62 | 0.46 | −0.08 | 0.19 | 0.03 | 0.13 | −0.01 | −0.02 | −0.12 | 0.76 | 0.99 | 0.66 | 1 | 0.84 | 0.19 | −0.60 | −0.58 | 0.43 | 0.69 | −0.31 | −0.30 | −0.02 | 0.02 | −0.09 | −0.06 | −0.09 | 0.01 | 0.39 | −0.08 | 0.13 | 0.27 | 0.08 | 0.27 | 0.15 |
| Ce | −0.58 | 0.41 | −0.01 | 0.21 | 0.01 | 0.10 | −0.07 | −0.03 | −0.15 | 0.77 | 0.98 | 0.62 | 0.95 | 1 | 0.21 | −0.26 | −0.26 | 0.75 | 0.79 | −0.27 | 0.03 | −0.06 | 0.04 | −0.09 | 0.04 | −0.12 | 0.43 | 0.37 | −0.28 | 0.40 | 0.36 | −0.02 | 0.50 | 0.25 |
| Yb | −0.71 | 0.39 | 0.25 | 0.32 | 0.08 | 0.16 | 0.01 | −0.08 | −0.20 | 0.47 | 0.59 | 0.94 | 0.55 | 0.50 | 1 | 0.39 | 0.42 | 0.10 | −0.26 | 0.65 | 0.50 | 0.01 | 0.57 | 0.03 | 0.53 | 0.04 | 0.30 | −0.63 | −0.48 | −0.29 | −0.57 | −0.16 | −0.11 | −0.06 |
| Zr | 0.40 | −0.29 | 0.05 | −0.15 | 0.05 | −0.10 | −0.07 | 0.09 | 0.53 | −0.39 | −0.52 | −0.28 | −0.52 | −0.52 | −0.16 | 1 | 0.99 | 0.07 | −0.37 | 0.53 | 0.68 | −0.24 | 0.07 | −0.14 | 0.25 | −0.16 | 0.59 | −0.45 | −0.39 | 0.22 | −0.26 | −0.23 | 0.21 | −0.20 |
| Hf | 0.31 | −0.23 | 0.02 | −0.15 | 0.07 | −0.05 | −0.03 | 0.09 | 0.56 | −0.33 | −0.44 | −0.21 | −0.44 | −0.45 | −0.07 | 0.98 | 1 | 0.09 | −0.36 | 0.50 | 0.65 | −0.23 | 0.06 | −0.14 | 0.26 | −0.15 | 0.56 | −0.50 | −0.42 | 0.20 | −0.29 | −0.27 | 0.21 | −0.17 |
| U | 0.41 | −0.48 | 0.00 | −0.13 | 0.15 | −0.09 | 0.01 | 0.31 | 0.15 | −0.43 | −0.46 | −0.26 | −0.43 | −0.43 | −0.34 | 0.53 | 0.44 | 1 | 0.70 | −0.34 | 0.13 | −0.08 | −0.19 | −0.04 | 0.19 | −0.07 | 0.65 | 0.34 | −0.32 | 0.61 | 0.44 | −0.23 | 0.65 | 0.36 |
| Th | 0.20 | 0.03 | −0.13 | −0.07 | −0.23 | −0.21 | −0.17 | 0.00 | 0.27 | −0.04 | 0.18 | −0.16 | 0.25 | 0.25 | −0.23 | −0.01 | −0.05 | 0.31 | 1 | −0.67 | −0.28 | −0.09 | −0.35 | −0.11 | −0.15 | −0.13 | 0.25 | 0.77 | −0.05 | 0.70 | 0.74 | 0.13 | 0.72 | 0.36 |
| Sc | −0.33 | 0.15 | 0.27 | 0.18 | −0.01 | 0.11 | 0.06 | −0.15 | 0.14 | 0.06 | 0.15 | 0.46 | 0.11 | 0.07 | 0.62 | 0.01 | 0.11 | −0.45 | −0.38 | 1 | 0.60 | −0.06 | 0.44 | −0.05 | 0.30 | −0.06 | 0.29 | −0.74 | −0.26 | −0.51 | −0.69 | −0.06 | −0.44 | −0.40 |
| V | 0.23 | −0.33 | 0.50 | −0.04 | −0.21 | −0.06 | −0.03 | −0.10 | 0.40 | −0.32 | −0.43 | −0.16 | −0.50 | −0.40 | −0.01 | 0.55 | 0.54 | 0.05 | −0.19 | 0.48 | 1 | 0.11 | 0.41 | 0.12 | 0.35 | 0.04 | 0.66 | −0.63 | −0.60 | 0.07 | −0.45 | 0.03 | 0.09 | −0.01 |
| Cr | 0.21 | −0.13 | 0.10 | −0.08 | −0.13 | 0.04 | −0.02 | −0.18 | 0.09 | −0.22 | −0.25 | −0.08 | −0.32 | −0.21 | −0.01 | 0.03 | 0.09 | −0.16 | −0.27 | 0.37 | 0.34 | 1 | 0.67 | 0.98 | 0.56 | 0.94 | −0.17 | −0.16 | −0.13 | −0.19 | −0.13 | 0.17 | −0.22 | 0.73 |
| Co | −0.46 | −0.14 | 0.60 | 0.50 | 0.28 | 0.30 | 0.05 | 0.17 | −0.22 | 0.28 | 0.24 | 0.56 | 0.16 | 0.21 | 0.52 | −0.10 | −0.07 | −0.19 | −0.28 | 0.48 | 0.39 | −0.01 | 1 | 0.66 | 0.66 | 0.65 | −0.03 | −0.51 | −0.32 | −0.45 | −0.46 | 0.18 | −0.38 | 0.41 |
| Ni | 0.08 | −0.14 | 0.27 | −0.09 | −0.20 | 0.02 | −0.01 | −0.21 | 0.05 | −0.21 | −0.33 | −0.15 | −0.40 | −0.31 | −0.05 | 0.05 | 0.10 | −0.22 | −0.32 | 0.40 | 0.55 | 0.78 | 0.23 | 1 | 0.63 | 0.96 | −0.12 | −0.16 | −0.13 | −0.14 | −0.11 | 0.11 | −0.17 | 0.75 |
| Cu | 0.32 | −0.38 | 0.42 | −0.05 | −0.12 | −0.09 | −0.11 | −0.12 | 0.05 | −0.34 | −0.53 | −0.24 | −0.57 | −0.50 | −0.18 | 0.30 | 0.21 | 0.11 | −0.19 | 0.22 | 0.69 | 0.22 | 0.29 | 0.37 | 1 | 0.68 | 0.23 | −0.34 | −0.38 | −0.12 | −0.19 | 0.08 | −0.01 | 0.61 |
| Zn | 0.40 | −0.29 | −0.07 | −0.12 | −0.10 | −0.11 | 0.12 | 0.12 | −0.05 | −0.28 | −0.39 | −0.34 | −0.35 | −0.38 | −0.40 | −0.03 | −0.15 | 0.36 | 0.08 | −0.35 | −0.03 | 0.01 | −0.24 | −0.05 | 0.31 | 1 | −0.18 | −0.14 | −0.10 | −0.17 | −0.10 | 0.09 | −0.20 | 0.78 |
| Ga | −0.04 | 0.56 | −0.23 | −0.28 | −0.75 | −0.38 | −0.20 | −0.51 | 0.07 | 0.23 | 0.39 | 0.03 | 0.41 | 0.43 | 0.12 | −0.28 | −0.24 | −0.47 | 0.33 | 0.11 | −0.05 | 0.10 | −0.24 | 0.11 | −0.17 | −0.12 | 1 | −0.06 | −0.51 | 0.52 | 0.13 | −0.16 | 0.52 | 0.05 |
| Rb | −0.10 | −0.05 | 0.04 | 0.28 | 0.33 | −0.05 | −0.19 | 0.37 | −0.04 | 0.07 | 0.17 | 0.24 | 0.17 | 0.19 | 0.10 | 0.02 | −0.06 | 0.41 | 0.36 | −0.25 | −0.27 | −0.36 | 0.11 | −0.41 | −0.13 | 0.07 | −0.27 | 1 | 0.34 | 0.59 | 0.95 | 0.19 | 0.50 | 0.18 |
| Sr | −0.45 | 0.07 | −0.03 | 0.28 | 0.51 | 0.40 | 0.11 | 0.25 | 0.01 | 0.68 | 0.71 | 0.50 | 0.68 | 0.67 | 0.35 | −0.23 | −0.16 | −0.22 | −0.15 | 0.02 | −0.36 | −0.21 | 0.23 | −0.27 | −0.44 | −0.30 | −0.11 | 0.12 | 1 | −0.15 | 0.25 | 0.14 | −0.15 | −0.18 |
| Nb | 0.31 | −0.06 | −0.19 | −0.30 | −0.35 | −0.17 | −0.07 | −0.04 | 0.64 | −0.06 | 0.10 | −0.27 | 0.14 | 0.15 | −0.25 | 0.24 | 0.25 | 0.19 | 0.72 | −0.19 | 0.13 | −0.06 | −0.34 | −0.04 | −0.15 | −0.11 | 0.44 | 0.04 | −0.04 | 1 | 0.69 | −0.03 | 0.91 | 0.25 |
| Cs | 0.28 | −0.48 | 0.25 | 0.07 | 0.20 | −0.04 | −0.07 | 0.32 | 0.25 | −0.39 | −0.46 | −0.18 | −0.46 | −0.43 | −0.23 | 0.45 | 0.36 | 0.75 | 0.28 | −0.20 | 0.28 | −0.05 | 0.08 | 0.06 | 0.28 | 0.29 | −0.46 | 0.61 | 0.61 | 0.22 | 1 | 0.21 | 0.62 | 0.25 |
| Ba | −0.54 | 0.40 | 0.03 | 0.21 | 0.04 | 0.08 | −0.09 | −0.03 | −0.03 | 0.80 | 0.91 | 0.56 | 0.90 | 0.89 | 0.47 | −0.41 | −0.34 | −0.52 | 0.07 | 0.13 | −0.32 | −0.27 | 0.23 | −0.31 | −0.44 | −0.37 | 0.37 | 0.15 | 0.15 | 0.11 | −0.45 | 1 | 0.01 | 0.22 |
| Ta | 0.64 | −0.40 | −0.08 | −0.26 | −0.24 | −0.22 | −0.12 | 0.05 | 0.48 | −0.44 | −0.43 | −0.53 | −0.39 | −0.36 | −0.54 | 0.47 | 0.40 | 0.61 | 0.65 | −0.38 | 0.29 | 0.01 | −0.31 | 0.06 | 0.20 | 0.23 | 0.06 | 0.15 | 0.15 | 0.75 | 0.61 | −0.39 | 1 | 0.25 |
| Pb | −0.04 | 0.24 | 0.14 | 0.02 | −0.16 | −0.10 | −0.16 | −0.08 | −0.11 | 0.16 | 0.18 | 0.12 | 0.19 | 0.21 | 0.04 | −0.20 | −0.30 | 0.13 | 0.23 | −0.27 | −0.19 | −0.21 | 0.00 | −0.22 | 0.00 | 0.43 | 0.18 | 0.35 | 0.35 | −0.03 | 0.13 | 0.15 | −0.04 | 1 |

## 4. Results

### *4.1. Clay Minerals in the Sediments*

Two contrasting clay mineral assemblages are found in the sediments. Kaolinite is the most dominant mineral (av. 78%), followed by minor illite (6%) and gibbsite (6%) and traces of goethite (3%) in the sediments from Kerala, Karnataka and Goa (A-P terrain; Figure 2). Quartz content ranges up to 7%. Contrastingly, the river sediments from Maharashtra and Gujarat (DT terrain) showed predominant smectite (av. 58%), followed by illite, (17%) kaolinite and chlorite (25%), and traces of feldspar (Figure 2). Indeed, the continental shelf sediments of Goa, Karnataka and Kerala also showed similar clay mineral assemblages, but with decreasing proportions of gibbsite as one moves from Kerala to Goa [56,61]. Very high proportions of smectite with minor kaolinite and illite were reported in the sediments from the Narmada and Tapi Rivers [46] and shelf sediments off Maharashtra and Gujarat.

### *4.2. Distribution of Major Elements*

The Post-Archean average Australian Shale (PAAS)-normalised distribution of major elements (Figure 3) showed depleted $SiO_2$, MgO, CaO, $Na_2O$ and $K_2O$ and enriched $Al_2O_3$, $Fe_2O_3$, MnO, $TiO_2$ and $P_2O_5$ in both fractions. However, the relative enrichment/depletion of these oxides varies differently in river sediments of different states and terrains. The sediments weathered from the A-P terrain are more enriched with $Al_2O_3$, $Fe_2O_3$ and $P_2O_5$, while those weathered from the DT terrain are enriched with MgO, CaO and $TiO_2$ (Table 1). The mean $Al_2O_3$ content of the sediments decreased gradually from Kerala (23.5%) to Gujarat (14.43%). The mean $Fe_2O_3$ content, however, increased for the clays from Kerala (11.8%) to Goa (13.2%), with low mean values for Maharashtra (10.75%) and Gujarat (8.9%). The mean $SiO_2/Al_2O_3$ ratios (Table 1) for the clays of Kerala (1.45), Karnataka (2.22), Goa (2.24), Maharashtra (2.64) and Gujarat (3.29) are much lower than those from the Upper Continental Crust (UCC: 4.33) and PAAS (3.32). The mean $SiO_2/Al_2O_3$ ratio for the silt fraction of sediments was $2.99 \pm 0.61$ for A-P terrain and $3.43 \pm 0.66$ for DT terrain (Table 1). The mean $Fe_2O_3/Al_2O_3$ ratio gradually increased in the clay fraction of sediments from Kerala (0.5) to Karnataka (0.64) and then to Goa (0.74) of the A-P terrain, but remained at 0.64 for Maharashtra and Gujarat. Similarly, the mean $Fe_2O_3/Al_2O_3$ ratio for the silt fraction of sediments was higher for the A-P terrain (0.54) than for the DT terrain (0.22). The mean $Al_2O_3/TiO_2$ ratio decreased gradually from 21.22 to 10.39 in the clay fraction, and from 18.3 to 6.12 in the silt fraction of sediments from Kerala in the south to Gujarat in the north (Table 1).

### *4.3. Weathering Indices*

To better understand the degree of chemical weathering and extent of lateritisation, various weathering indices are determined, using the oxides of major elements.

**(a) The chemical index of alteration (CIA)** is determined by the equation of Nesbitt and Young [1].

$$CIA = [Al_2O_3/(Al_2O_3 + CaO^* + Na_2O + K_2O)] \times 100 \quad (1)$$

CaO* is related to CaO in the silicate fraction of the sediment [6].

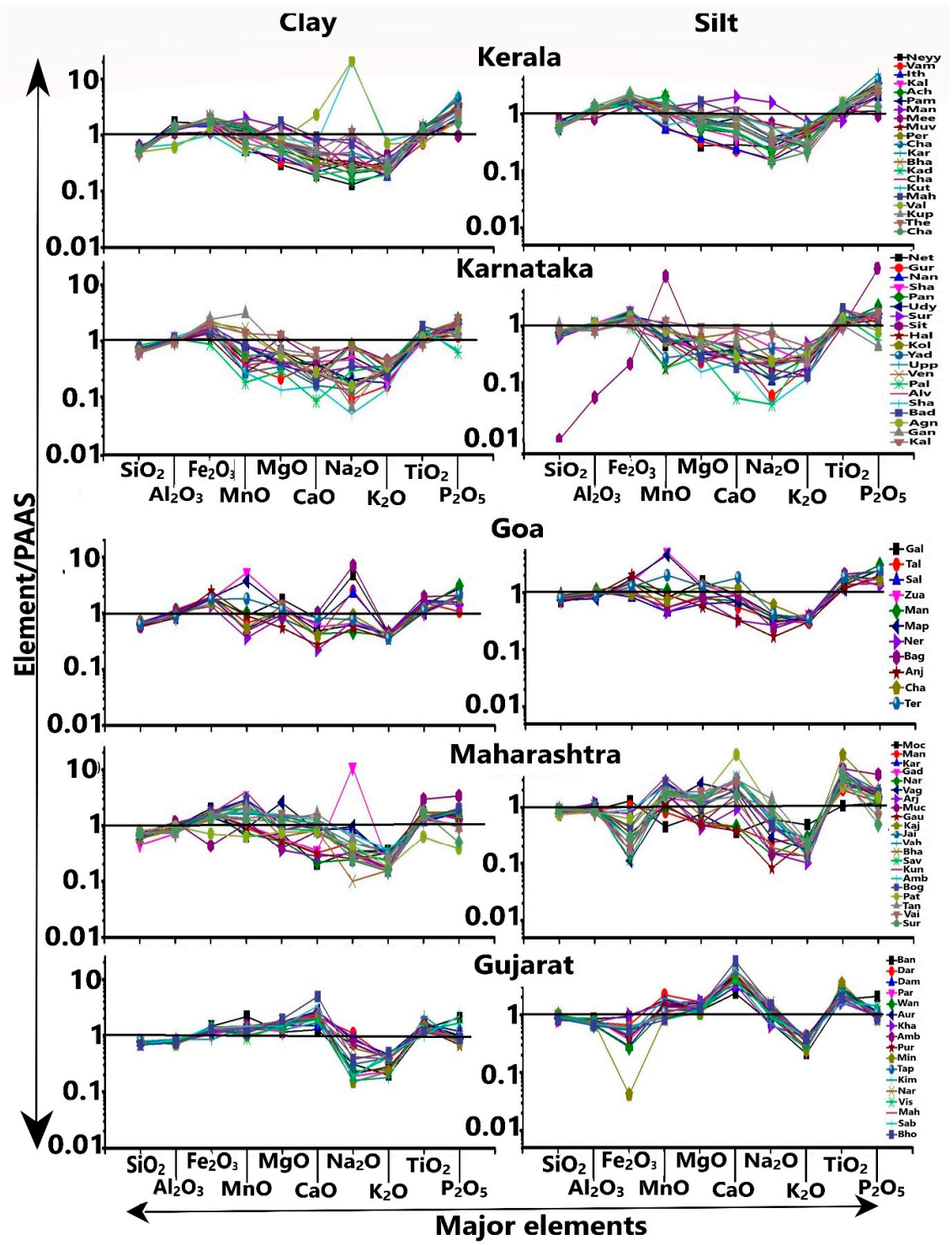


**Figure 3.** Post-Archean average Australian Shale (PAAS)-normalised distribution of major element oxides in the clay and silt fractions of sediments in the rivers from each state.

The CIA values ranged from 27 to 97 for clay fractions and from 47 to 96 for silt fractions of sediments (Table 1), with low CIA values in both fractions corresponding to the sediments of Gujarat. The mean CIA values for the clay and silt fractions of the sediments are 86 and 88 from the A-P terrain and 80 and 72 for DT terrain, respectively. The plot of CIA values in the A-CN-K diagram (Figure 4A) showed that the clay fractions of sediments from Kerala, Karnataka and Maharashtra plot closely to the $Al_2O_3$ pole, indicating strong (intense) chemical weathering, while those from Goa and Gujarat plot

in the intermediate to strong weathering region (Figure 4A). On the other hand, the silt fractions of sediments from Kerala and Karnataka exhibit strong weathering, while those of Goa and Maharashtra exhibit intermediate to strong weathering and those from Gujarat exhibit weak to intermediate weathering (Figure 4A). High CIA values in the clay fraction indicate strong weathering, and this fraction is not influenced by sorting processes [20,21]. Relatively low CIA values in the silt fractions of Goa, Maharashtra and Gujarat suggest that this fraction may have been influenced by hydraulic sorting processes and/or source rock characteristics. Since the sediments from DT terrain are mafic component-dominated and mafic rocks are more vulnerable to weathering, it is possible that the low CIA values in the silts of Maharashtra and Gujarat are influenced by physical weathering of source rocks.

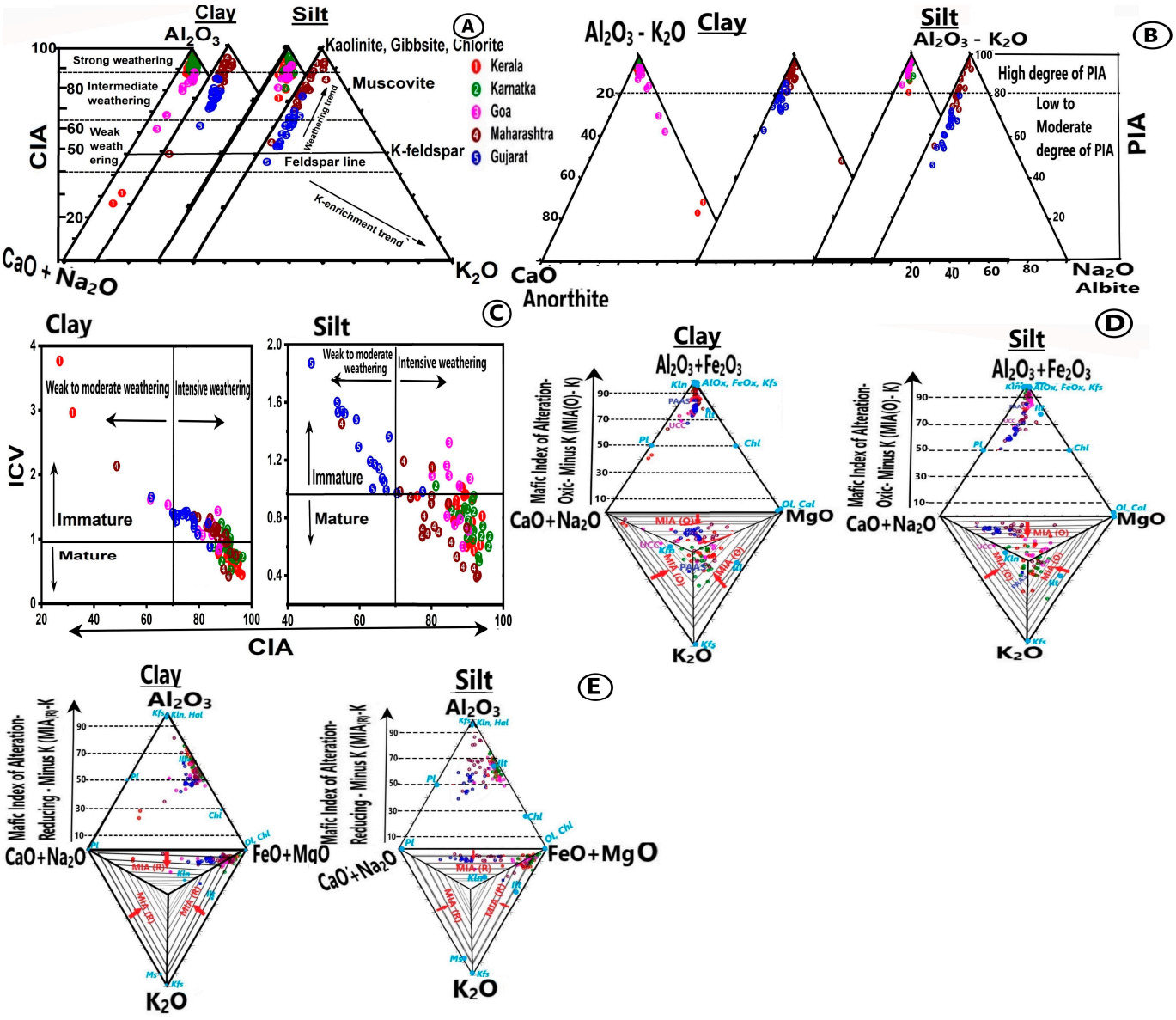


**Figure 4.** Ternary diagrams showing (**A**) the plots of $Al_2O_3$–(CaO + $Na_2O$)–$K_2O$ along with chemical index of alteration (CIA) (adopted from Nesbit and Young [1]) and (**B**) ($Al_2O_3$–$K_2O$)-CaO-$Na_2O$ along with plagioclase index of alteration (PIA) (adopted from Fedo [6]). (**C**) Plot of chemical index of alteration (CIA) vs index of chemical variability (ICV) (adopted from Cox [16]), (**D**) Tetrahedral plot of AF–CN–K–M (($Al_2O_3$ + $Fe_2O_3$)–(CaO + $Na_2O$)–($K_2O$)–(MgO)) (modified adopted from Babechuk and Fedo, [60]), (**E**) Tetrahedral plot of A–CN–K–FM (($Al_2O_3$)–(CaO + $Na_2O$)–($K_2O$)–(FeO + MgO)) (modified adopted from Babechuk and Fedo, [60]).

**(b) The plagioclase index of alteration (PIA)** is used to quantify the degree of weathering of plagioclase feldspar. It is determined by the equation of Fedo et al. [6].

$$PIA = (Al_2O_3\text{-}K_2O)/(Al_2O_3 + CaO^* + Na_2O\text{-}K_2O) \times 100 \quad (2)$$

CaO* is related to CaO in the silicate fraction of the sediment [6].

The PIA values are in the range 21 to 94 for the clay fractions and 41 to 94 for the silt fractions of sediments (Table 1). The average PIA values for the clay and silt fractions of sediments are 86 and 88 for A-P terrain and 80 and 71 for DT terrain, respectively. The plot of major element oxides in the ternary diagram ($(Al_2O_3–K_2O)$-CaO–$Na_2O$) indicates that the sediments from Kerala, Karnataka, Goa and Maharashtra exhibit a high degree of plagioclase weathering, while those from Gujarat exhibit a low to moderate degree of plagioclase weathering (Figure 4B).

**(c) The index of chemical variability (ICV)** is used as a proxy indicator to assess the role of mineralogical maturity of the sediments. It is determined by the equation of Cox et al. [16].

$$ICV = (Fe_2O_3 + K_2O + Na_2O + CaO + MgO + MnO + TiO_2)/Al_2O_3. \quad (3)$$

Typical rock-forming minerals such as feldspars, amphiboles and pyroxenes have ICV value > 1, whereas the alteration products like kaolinite, illite and muscovite have ICV value < 1 [16,76]. High ICV values imply compositionally immature sediments due to high content of non-clay silicate minerals. Sediments that contain high quartz content and/or Fe and Ti oxides also exhibit ICV values > 1. Low ICV values correspond to mature sediments deposited in areas of sediment recycling and intense chemical weathering. The mean ICV values of the clays from Kerala, Karnataka and Goa are 0.97, 0.87 and 1.21, respectively, with an overall mean of 1.02 for the A-P terrain. The mean ICV values of the clays from Maharashtra and Gujarat are 1.08 and 1.31, respectively, with an overall mean of 1.20 for the DT terrain. Similarly, the mean ICV values are <1 for the silts from Kerala, Karnataka, Goa and Maharashtra and 1.28 (range: 0.97–1.87) for Gujarat. The ore particulates (Fe-oxides) in the sediments of Goa and Fe- and Ti- minerals in the sediments from DT terrain (see chemistry below) may have influenced ICV values to be >1. The plot of ICV vs. CIA (Figure 4C) indicates that the clays from Kerala, Karnataka and Maharashtra are intensely weathered and compositionally mature, whereas the clays from Goa and Gujarat are intensely weathered, with a few showing compositional immaturity (Figure 4C). On the other hand, most of the silt fractions of sediments from Kerala, Karnataka and Maharashtra are intensely weathered and mature. A few silt samples from Goa are immature but intensely weathered. Almost all silt samples from Gujarat are compositionally immature and weakly weathered (Figure 4C).

(d) Babechuk et al. [58] proposed the **Mafic Index of Alteration (MIA)** to quantify the total loss of mobile elements relative to that of immobile elements. Subsequently, Babechuk and Fedo [60] proposed $MIA_{(O)}$ and $MIA_{(R)}$, respectively, for oxidative and reductive weathering, to separate the effects of feldspars (both plagioclase and K-feldspar) and mafic mineral weathering and the addition of labile elements during diagenesis/metasomatism. Following the equations of Babechuk and Fedo [60],

$$MIA_{(O)} = [(Al_2O_3 + Fe_2O_{3(T)})/(Al_2O_3 + Fe_2O_{3(T)} + MgO + CaO + Na_2O + K_2O)] \times 100 \quad (4)$$

$$MIA_{(R)} = [(Al_2O_3)/(Al_2O_3 + FeO_{(T)} + MgO + CaO + Na_2O + K_2O)] \times 100$$

are calculated. The $MIA_{(O)}$ values (Table 1) are close to that of CIA. The mean $MIA_{(O)}$ values range from 82 to 91 for the clay and from 84 to 91 for silt fractions of sediments from the

A-P terrain. It ranges from 74 to 84 for the clay and 62 to 75 for silt fractions of sediments from the DT terrain. Indeed, the $MIA_{(O)}$ values are lower for the sediments from DT terrain than those from A-P terrain. The $MIA_{(R)}$ values are much lower than $MIA_{(O)}$ in both size fractions (Table 1). The mean $MIA_{(R)}$ values are 55 and 50 for the clay fractions and 50 and 57 for the silt fractions of sediments from A-P terrain and DT terrain, respectively.

Babechuk and Fedo [60] proposed the AF-CN-K-M tetrahedral plot (Figure 4D), useful for oxidative weathering, where Fe is retained alongside Al across all stages of incipient to advanced weathering. One ternary diagram (AF-CN-M) of the tetrahedron is integrated with the $MIA_{(o)}$–K weathering index (Figure 4D). The sediments from A-P terrain and the DT terrain of Maharashtra showed $MIA_{(o)}$ values > 80 in both size fractions and plot very close to the AF pole in the AF-CN-M diagram, indicating extreme leaching and net loss of Ca, Na, K and Mg, released from plagioclase and mafic minerals, and Fe is retained via oxyhydroxide development. This agrees with the results from X-ray diffraction studies, where Al is retained as gibbsite and Fe as goethite (Figure 2) in the sediments from A-P terrain. The sediments from Gujarat plot slightly away from the AF pole (with $MIA_{(o)}$ values 50 to 80 in both fractions), suggesting intermediate leaching of labile elements. However, in another ternary diagram (CN-K-M) of the tetrahedron, our samples plot in the central inner space designated for $MIA_{(o)}$ (Figure 4D), indicating strong leaching of labile elements and that subsequent diagenesis has not obscured the chemical weathering effects.

Babechuk and Fedo [60] also proposed the A-CN-K-FM tetrahedral plot (Figure 4E), useful to study reductive weathering, where Fe is lost and/or redistributed in the system. One ternary diagram (A-CN-FM) of the tetrahedron is integrated with the $MIA_{(R)}$-K weathering index (Figure 4E). Our samples plot slightly away from the FM pole and slightly towards the A pole in the A-CN-FM diagram, suggesting an advanced weathering stage where Fe and Mg were lost, since our sediment samples show high values of Fe and some Fe may have been retained as goethite. The average $MIA_{(R)}$ values for the clay ($55 \pm 7.1$) and silt ($59 \pm 4.9$) fractions from A-P terrain may indicate only loss of Mg during advanced weathering of sediments. In another ternary diagram (CN-K-FM) of the tetrahedron (Figure 4E), our samples plot close to the FM pole, but not in the inner space designated for $MIA_{(R)}$ reduction, implying subsequent that diagenesis has not obscured the chemical weathering effects. The silt samples from Gujarat plot mid-way between AN and FM (Figure 4E), suggesting that intermediate weathering has minimal effect on labile elements.

### *4.4. Distribution of Trace Elements*

The PAAS-normalised distribution of trace elements (Figure 5) showed strong depletion of alkaline earth elements (Rb, Sr, Cs, Ba) in the sediments from both terrains. The Th, U, La and Ce are enriched relative to PAAS in the sediments of Kerala and Karnataka, but depleted as one moves towards Goa, Maharashtra and Gujarat. The transition trace elements (TTEs: Sc, V, Cr, Co, Ni, Cu and Zn) are enriched relative to PAAS in the sediments of all rivers (Figure 5). The TTE content is higher in the silt fractions than in clay fractions of sediments. Moreover, the ΣTTE is higher in the sediments from DT terrain than in A-P terrain (Tables 2 and 3). The Ga content is enriched relative to that of PAAS, with higher values in the sediments from A-P terrain than in DT terrain (Tables 2 and 3). Among the high-field-strength elements (HFSE: Zr, Hf, Ta, Nb and Y), Nb is depleted relative to PAAS in the sediments of all rivers. The mean values of Zr, Hf, Ta and Y are lower in the clay fraction of sediments from A-P terrain than DT terrain (Table 2). In the silt fractions, the mean values of Zr, Hf and Ta are much higher, and Y is much lower, for the sediments from A-P terrain than those from DT terrain (Figure 5).

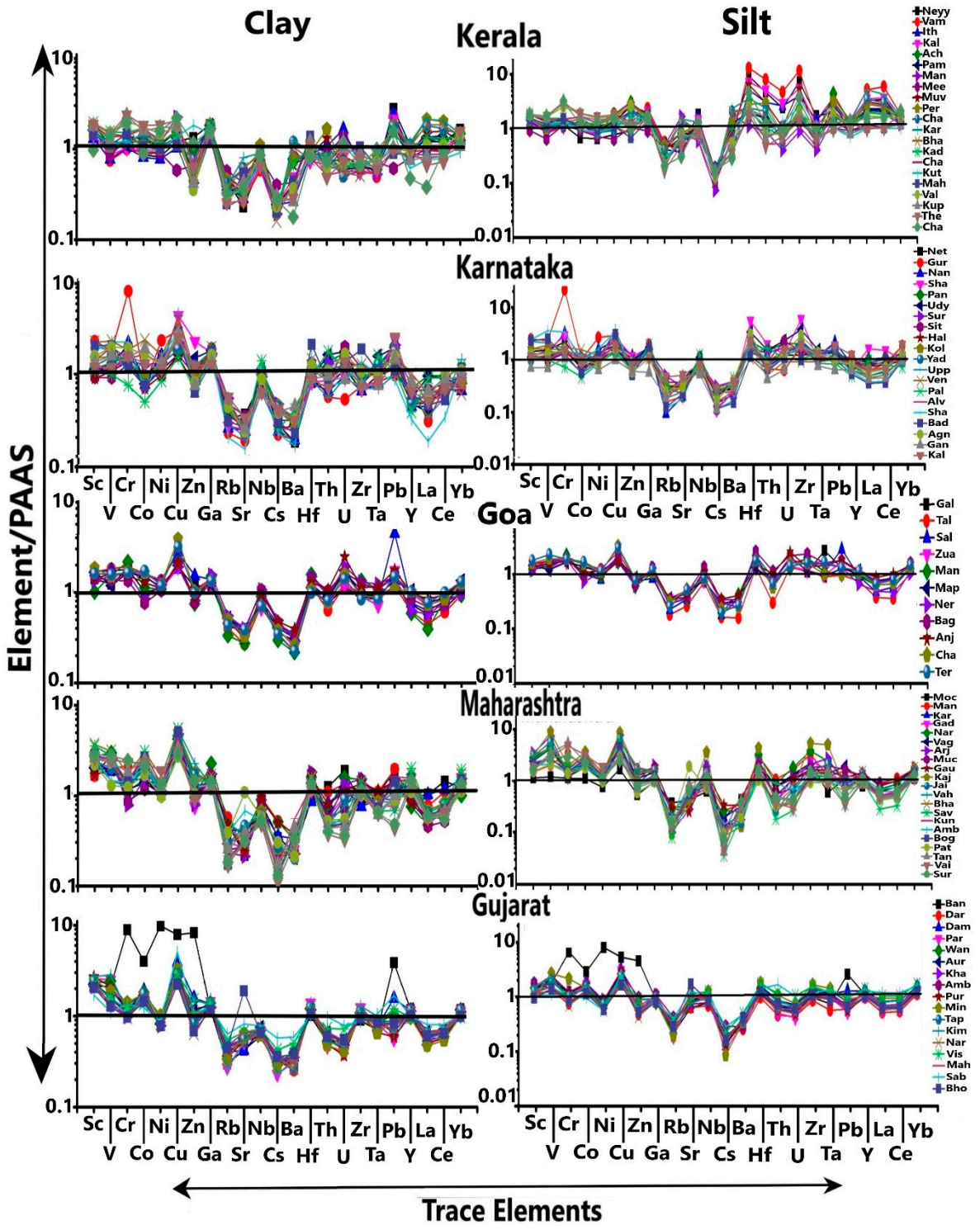


**Figure 5.** Post-Archean average Australian Shale (PAAS)-normalised distribution of trace elements in the clay and silt fractions of sediments in the rivers from each state.

**Total Trace element (ΣTE) content:** A total of 23 trace elements, excluding rare earth elements (REEs), are considered in this study. Sai Babu et al. [36] reported the REE distribution of these sediments. The distributions of trace elements, along with a few REEs (La, Ce, Yb, Y), are given in Tables 2 and 3 and considered here for discussion. The total trace element content (ΣTE) varied from 991.6 to 2027.1 µg/g in the clay fractions and from 1081.1 to 3848.6 µg/g in the silt fractions of sediments from different states (Figure 6A). Within the clay fractions, the ΣTE of Maharashtra was high compared to those of other

states (Table 2). The mean ΣTE of the clay fraction of sediments from all rivers (1468.4 µg/g) was lower than for their silt fraction (1827.2 µg/g), UCC (1650.57 µg/g; [77]) and PAAS (1807.09 µg/g; [78]). The silt fractions of sediments showed broad peaks of high ΣTE corresponding to the rivers of Kerala and Maharashtra (Figure 6A). The peaks of high ΣTE correspond to broad peaks of high ΣREE in the sediments of Kerala, but in other states, ΣTE distribution is significantly different from that of ΣREE (Figure 6A,B).

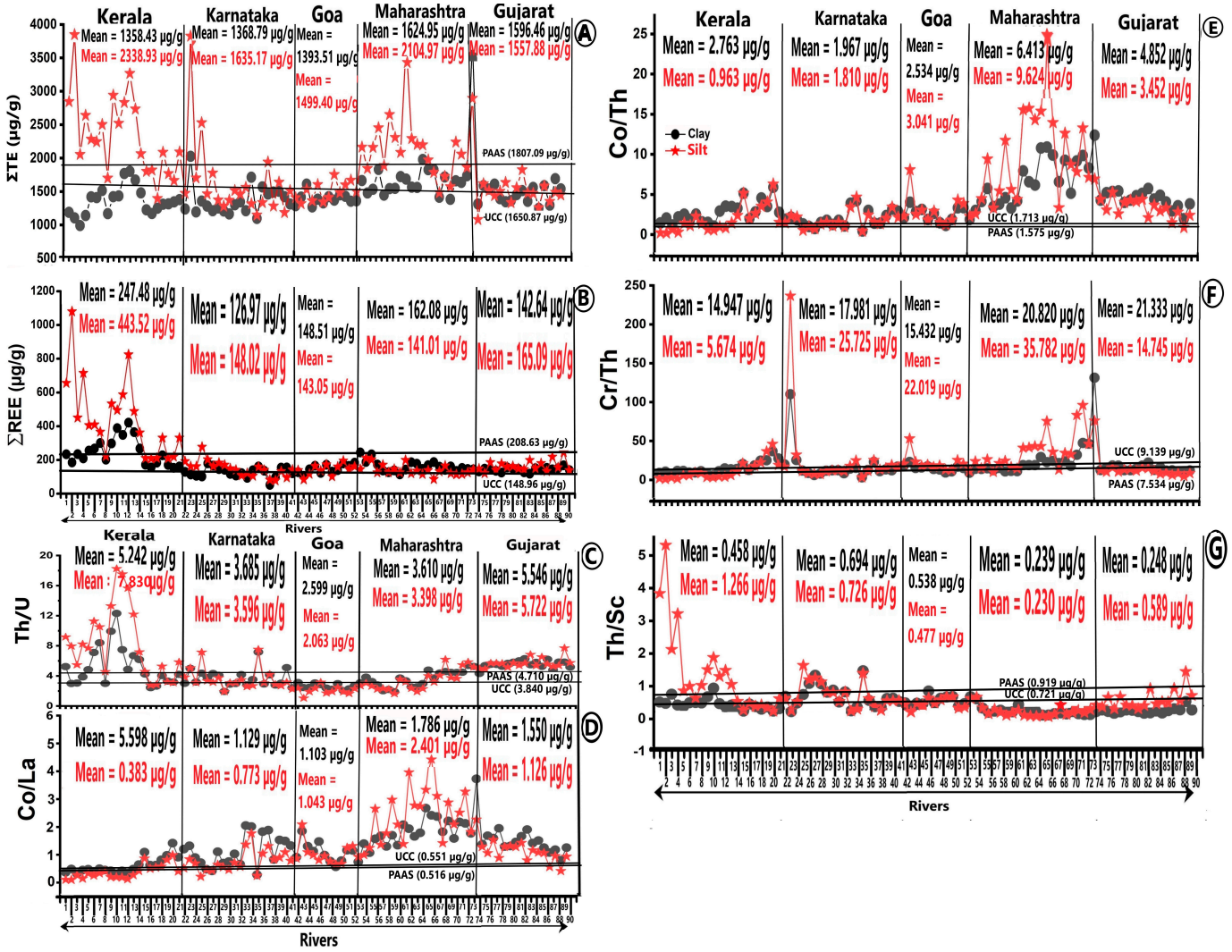


**Figure 6.** (**A**) The total trace element content (∑TE) and (**B**) total rare earth element content (∑REE), (**C**) Th/U, (**D**) Co/La, (**E**) Cr/Th, (**F**) Co/Th and (**G**) Th/Sc ratios in the clay and silt fractions of sediments in the rivers along the west coast of India.

**Th/U and Rb/Sr ratios**: The distribution of the Th/U ratio (Figure 7A) shows that this ratio is lower in the clay than silt fractions of sediments of all rivers. The peak high Th/U ratio in the sediments of Kerala broadly coincides with peak ΣTE (Figure 6C). The mean Th/U ratios for the clay and silt fractions of sediments from Karnataka and Maharashtra are close to that of UCC. The mean ratio is much lower for the sediments of Goa and higher for the sediments of Gujarat than for UCC. The Th contents and Th/U ratios plotted on the binary diagram of Gu et al. [79] indicate significant positive correlation between the two in the sediments from A-P terrain, weak correlation in the clay fractions and moderate positive correlation in silt fractions of sediments from DT terrain (Figure 7B).

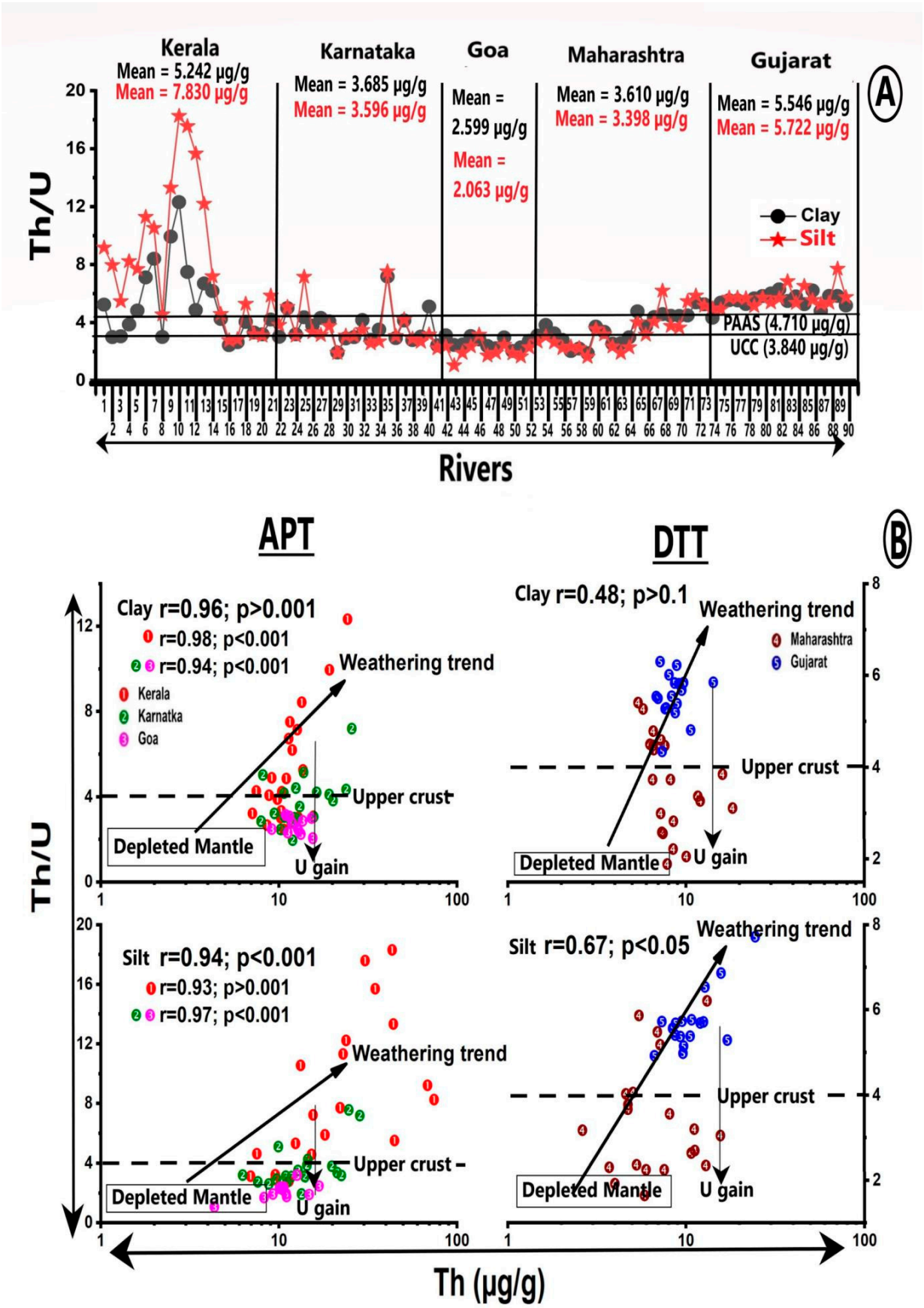


**Figure 7.** *Cont.*

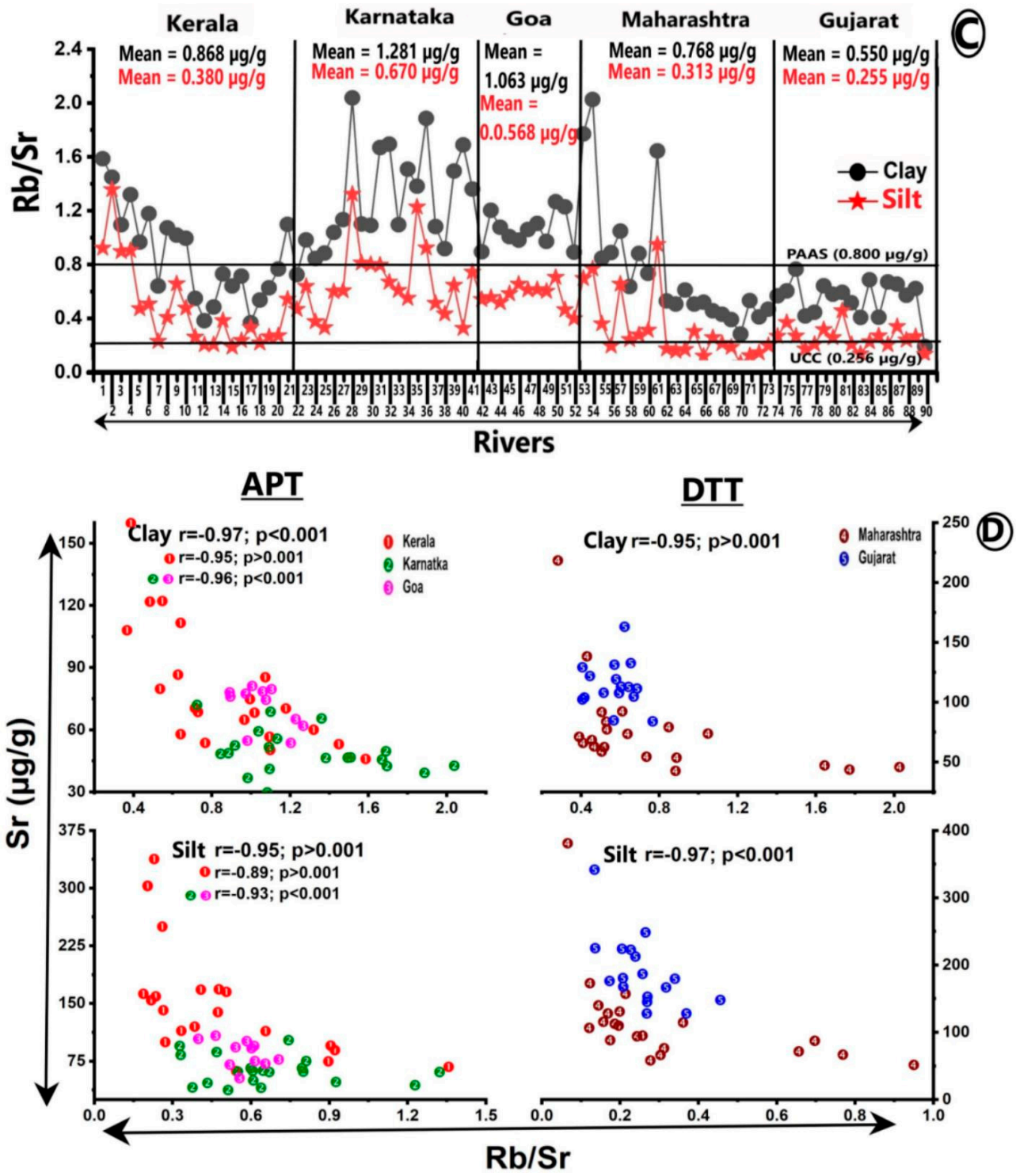


**Figure 7.** (**A**) Variations in the Th/U ratio, (**B**) binary plot of Th content versus Th/U ratio (fields and trends from Gu et al. [79]), (**C**) Variations in the Rb/Sr ratio and (**D**) binary plot of Rb/Sr versus Sr content, adopted from Xu et al. [80] in the clay and silt fractions of sediments in the rivers of western India.

The distribution of the Rb/Sr ratio shows much higher ratios in the clay than in their silt fractions of sediments (Figure 7C). The mean Rb/Sr ratios for the clay fractions of sediments from A-P terrain (1.07) and DT terrain (0.67) were much higher than in UCC (0.26; Table 2). The mean Rb/Sr ratio was highest for the sediments of Karnataka and Goa, followed by Kerala, Maharashtra and Gujarat (Figure 7C). The mean ratio was low for the silt fractions of sediments from DT terrain and close to that of UCC. The plot of Rb/Sr ratio against Sr content (Figure 7D) showed strong negative correlation between the two in the sediments from both terrains.

### *4.5. Relationships of Major and Trace Elements*

Table 4 is the correlation matrix of elements for the clay fraction of sediments, separately for A-P terrain and DT terrain. Figure 8 shows the important binary plots between the elements. Within the A-P terrain, $Al_2O_3$ showed negative correlation with CaO, $Na_2O$, MgO and $K_2O$ (Figure 8A). The $TiO_2$ showed strong positive correlation with Zr, Hf and Nb (Figure 8B), while $P_2O_5$ showed strong positive correlation with Sr, Ba and ∑REE (Figure 8C). Moderate to strong correlation exists among U, Th, Nb, Cs and Ta. The $Fe_2O_3$ and MnO showed strong correlation with V and Co (Figure 8D). On the other hand, the sediments from DT terrain showed negative correlation of $Al_2O_3$ with CaO, MgO and $Na_2O$ and strong positive correlation with $P_2O_5$ (Figure 8E). The $Al_2O_3$ also showed moderate to strong correlation with Zr, Hf, U, Ga Nb and Ta. The $Fe_2O_3$ showed positive correlation with ∑REE (Figure 8F), U and Co. $TiO_2$ showed strong correlation with Zr, Hf, V and Ga. Strong correlation exists among TTEs (Sc, Co, Cr, Ni, Cu and Zn; Figure 8G) elements and TTEs with Zr and Hf (Figure 8H).

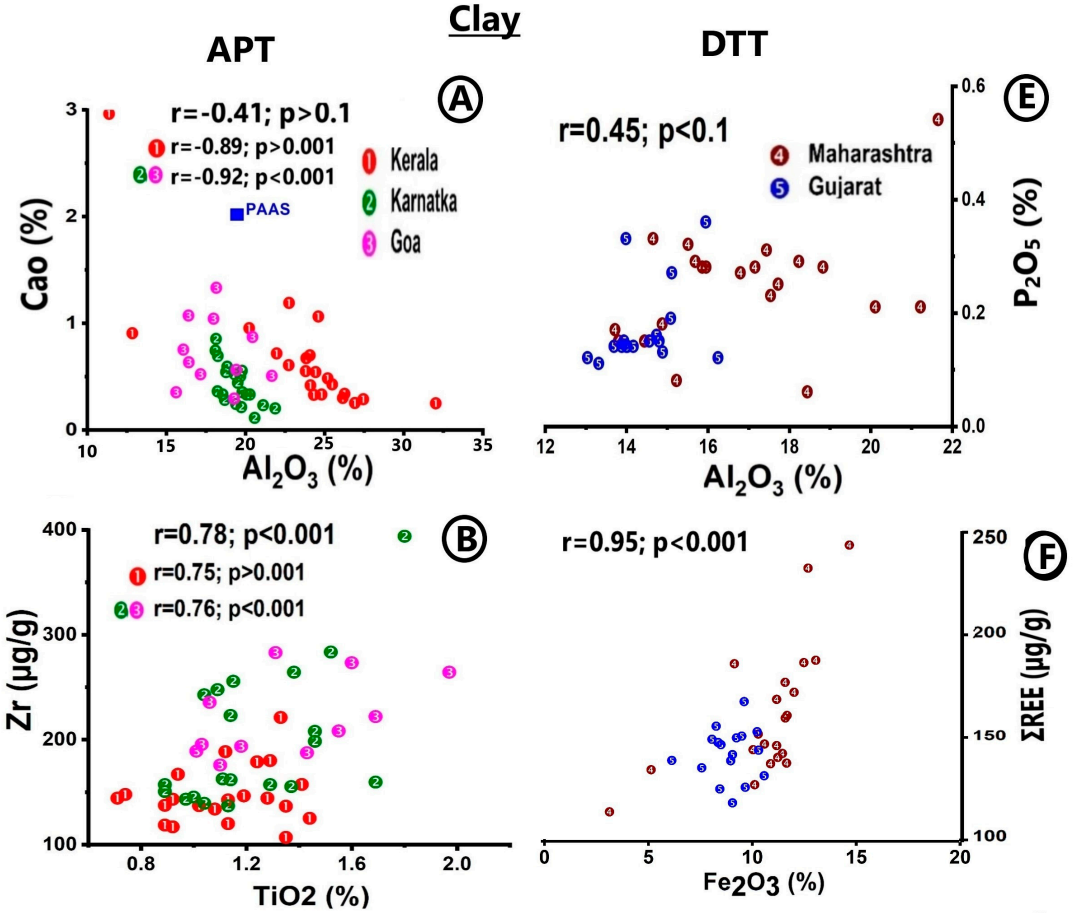


**Figure 8.** *Cont.*

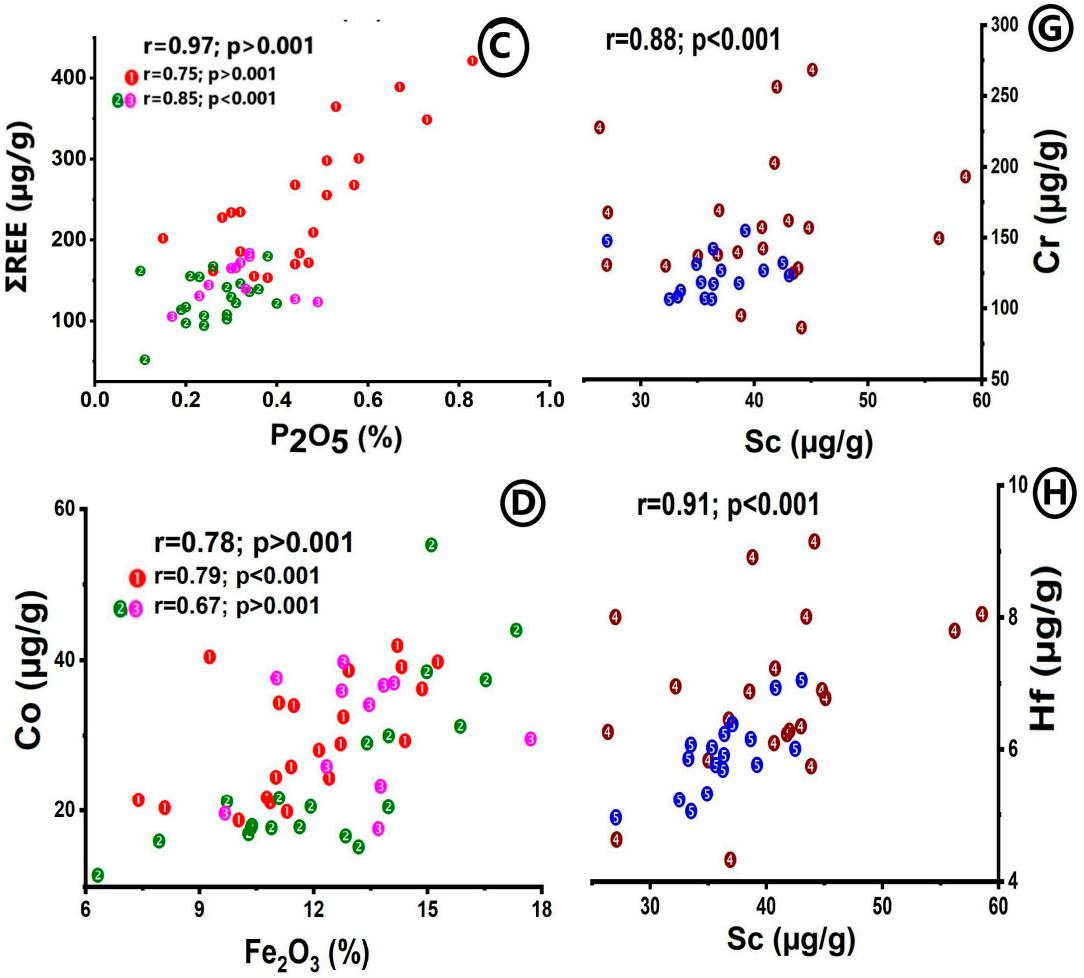


**Figure 8.** Selective correlation plots in the clay fraction of sediments: Correlation (**A**) between $Al_2O_3$ and CaO, (**B**) $TiO_2$ and Zr, (**C**) $P_2O_5$ and ∑REE and (**D**) $Fe_2O_3$ and Co from the sediment of A-P terrain. Correlation (**E**) between $Al_2O_3$ and $P_2O_5$, (**F**) $Fe_2O_3$ and ∑REE, (**G**) Sc and Cr and (**H**) Sc vs. Hf from the sediments of DT terrain.

## 5. Discussion

### *5.1. Mineralogy and Major Element Geochemistry—Stages of Weathering and Provenance*

The Western Ghats (WG) experience humid, tropical climatic conditions. Therefore, the rivers draining the WG obviously carry the weathering products of rocks subjected to chemical weathering, prevalent under tropical conditions. Kaolinite is a product of intense chemical weathering [25]. Occurrence of abundant kaolinite along with gibbsite in the sediments from A-P terrain (Figure 2) indicates that the hinterland rocks were subjected to intense chemical weathering and lateritisation, and/or sediments are weathered from laterites. Babechuk and Fedo [60] reported that the breaking down of 2:1 clay and formation of dominant 1:1 clay such as kaolinite, and Al- and Fe-(oxy)-(hydr)oxides such as gibbsite and goethite indicate that the sediments have undergone intense to extreme weathering conditions. The highest CIA values (Figure 4A) and kaolinite (Figure 2) in the clays from A-P terrain also suggest strongest chemical hydrolysis [20]. The relatively high gibbsite content in the offshore sediments of Kerala and its decreasing content towards Goa was attributed to decrease in lateritisation from Kerala to Goa [61].

Smectite is the dominant weathering product of Deccan Trap basalts under tropical conditions. Abundant smectite, together with minor illite, kaolinite and chlorite in the sediments from DT terrain (Figure 2), thus reflect dominant weathering products from basalts. The sediments with abundant smectite and minor kaolinite and chlorite indicate

the abundant occurrence of 2:1 clay (smectite) and an early stage of 1:1 clay (kaolinite) formation, suggesting an advanced to intense stage of chemical weathering, according to the classification of Babechuk and Fedo [81].

The depletion of Ca, Mg, Na and K relative to PAAS (Figure 3) indicates that they are leached and carried away as a solute during chemical weathering of source rocks. The extent of leaching of labile elements is much higher in the sediments from A-P terrain than in DT terrain. High CIA and PIA values for the clay fractions of sediments from Kerala, Karnataka and Maharashtra indicate strong weathering (Figure 4). Relatively low CIA values for the silts of Goa, Maharashtra and Gujarat (Figure 4A) indicate the influence of hydraulic sorting processes and provenance. The $MIA_{(O)}$ values are close to that of CIA (Table 1) and point out extreme leaching and net loss of labile elements, probably released from plagioclase and mafic minerals.

In general, the $SiO_2/Al_2O_3$ ratio is close to that of UCC or higher for the sediment weathered from intense chemical weathering of silicate rocks and much lower than in UCC for the sediment weathered from laterites. This ratio is <1.33 for laterites, 1.33–2.0 for lateritic soils and >2.0 for non-lateritic, chemically weathered tropical soils [71,82]. The $SiO_2/Al_2O_3$ ratio, however, can range from 1.33 to 2.2 in lateritic soils [81]. The mean $SiO_2/Al_2O_3$ ratio for the clay fractions of sediments from Kerala (1.45), Karnataka (2.22) and Goa (2.24) and the silt fraction of sediments from Kerala (1.71) suggests that they resemble lateritic soils. The mean $SiO_2/Al_2O_3$ ratio for the silts from Karnataka (2.6) and Goa (2.81) suggests dilution of lateritic soils by material weathered from the hinterland. The gradually decreasing $Al_2O_3$ content coinciding with increasing $Fe_2O_3$ content and mean $Fe_2O_3/Al_2O_3$ ratio in the clay fraction of sediments from Kerala to Goa (Table 1) suggest an increase in particulate iron, probably from Fe-Mn ore mines, located in north Karnataka and Goa [67,83–85]). As the rivers from northern Karnataka and Goa drain these open cast mines, weathered material from the ores, together with lateritic material, are transported as suspended and bed load and deposited in the lower reaches of rivers and estuaries. Several workers reported ore material-dominated sediments in the rivers and estuaries of northern Karnataka and Goa [52,55,57,86,87]. Hence, the sediments of Karnataka and Goa are lateritic soils admixed with ore material. Sai Babu et al. [36] reported MREE- and HREE-enriched REE patterns with positive Ce and Eu anomalies in both fractions of sediments from the rivers of northern Karnataka and Goa and suggested that the sediments consist of weathered material from source rocks, Fe-Mn ores and laterites. On the other hand, the mean $SiO_2/Al_2O_3$ ratios of the clay and silt fractions of sediments from Maharashtra (2.54 and 2.99, respectively) and Gujarat (3.29 and 3.97) suggest that the sediments are non-lateritic and chemically weathered soils. Moreover, the mean low $Al_2O_3/TiO_2$ ratios for the clay (11.7) and silt (6.2) fractions of sediments from DT terrain compared to UCC (24.29), and strong correlation of $TiO_2$ with Zr, Hf, Nb, V and Ga (Figure 8B; Table 4) suggest Ti association with heavy metal-enriched minerals, i.e., heavy minerals, such as rutile and ilmenite, abundantly reported from the Deccan Trap basalts.

### *5.2. Relationships Among Major Elements and Trace Elements*

Strong correlation among labile alkali and alkaline earth elements and their negative correlation with $Al_2O_3$, $Fe_2O_3$ and $TiO_2$ in the sediments from both terrains (Table 4; Figure 8A) may be related to chemical weathering of source rocks, wherein labile elements are transported as dissolved species, and immobile elements such as Al, Fe and Ti are enriched in solid detritus. The correlation of $TiO_2$ with Zr, Hf and Nb in the sediments from both terrains (Table 4; Figure 8B) implies association of these elements with heavy minerals. Strong correlation of $Fe_2O_3$ and MnO with Co (Figure 8D) suggests Co adsorbed onto Fe-Mn oxy-(hydr) oxides. The moderate to strong correlation of $P_2O_5$, $Fe_2O_3$ and

MnO with ΣREE in the clay fractions of sediments from A-P terrain (Figures 4 and 8C) suggests that REEs released during weathering are bound to secondary mineral phases such as Fe-Mn oxy-(hydr)oxides and phosphate. Strong positive correlation of ΣREE with $Fe_2O_3$ (Figure 8F) and moderate correlation with $Al_2O_3$ (Table 4) in the sediments from DT terrain suggest that the clay minerals and Fe-oxy-(hydr)oxides are important hosts for REEs. It appears that that the primary hosts for REEs are secondary weathering products such as Fe-oxy-hydroxides and phosphates in the A-P terrain and clay minerals and Fe oxy-(hydr)oxides in the DT terrain. Pourret et al. [88] and Du et al. [89] suggested that REEs are adsorbed onto Fe-Mn oxy- (hydr) oxides and phosphates abundantly. The correlation of Sr and Ba with $P_2O_5$ in both terrains indicates that they are associated with secondary mineral phases like phosphates. Strong correlation of $Al_2O_3$ with Ga in both terrains (Table 4) suggests its association with clay minerals. Higher Ga content in the A-P terrain than in the DT terrain may be due to preferential binding of Ga with kaolinite and gibbsite-rich sediments. Several workers reported association of high Ga content with laterites [71,90]. Positive correlation of $Al_2O_3$ with Zr, Hf, U, Ga, Nb and Ta (Table 4) implies that these elements are immobile during weathering and associated with the weathered detritus. Within the DT terrain, strong correlation exists among TTEs (Figure 8G), and TTEs (Sc, Co, Cr, Ni, Cu and Zn) are negatively correlated with Rb, Cs and Nb (Table 4) maybe because TTEs are retained and alkaline earth elements are removed during chemical weathering. High TTE and Yb contents and strong correlation of Yb with TTEs (Table 4) suggest that TTEs and heavy rare earth elements (HREEs) like Yb occur in higher proportions in basalts. Sai Babu et al. [36] reported PAAS-normalised MREE- and HREE-enriched and LREE-depleted patterns in the weathered products of basalts. Correlation of REEs with U, Th and Ta (Table 4) indicates that some REEs are associated with heavy metal-associated minerals (i.e., heavy minerals). Positive correlation of Zr and Hf with Sc, V and Ga and positive correlation of U and Th with Rb, Cs, Nb, Ta and Ga suggest a mixed source for these elements. It has been reported that the basalts are contaminated with crustal rocks away from the Deccan Plateau, and crustal rocks are exposed because of thin cover of Deccan basalts. Heavy monsoonal rains may have eroded these contaminated crustal rocks and released these metals to the sediments.

### *5.3. Factors Controlling ∑TE, Th/U and Rb/Sr Ratios*

∑TE: Trace elements are usually associated with fine-grained sediments and heavy minerals. The low ∑TE or ∑TE values close to that of UCC in the clay fractions and relatively high ∑TE in silt fractions of sediments (Figure 6A; Tables 2 and 3) imply that the trace elements released during chemical weathering are largely transported away from source rocks. The steep slopes of the western Ghats and chemical and physical weathering associated with heavy monsoonal rains (>250 mm/yr) in short duration (within 4 months during southwest monsoon—June to September) may have facilitated quick erosion of dissolved and particulate material as suspended load of the rivers, resulting in low ∑TE in the clay fraction of sediments.

The peaks of high ∑TE in the silt fraction of sediments from Kerala and Maharashtra correspond to two different geographic terrains (Figure 6A). The peak high ∑TE in the sediments of Kerala is associated with peaks of high Th/U ratio, peak high ∑REE (Figure 6A–C), low Co/La, Cr/Th and Co/Th ratios (Figure 6D–F), peak high Th/Sc (Figure 6G) and higher HFSE elements relative to PAAS (Figure 5). It implies that high ∑TE is associated with Th- and La-enriched minerals and minerals that contain both high REEs and heavy (HFSE) elements i.e., heavy minerals. Felsic granites are usually enriched with heavy metal-enriched minerals (i.e., heavy minerals) and high REEs [5]. Felsic granites are predominant in the Western Ghats (WG) of south Kerala and WG, with steep slopes occuring at close

proximity to the coast. Therefore, it is likely that the heavy monsoonal rains promoted both physical and chemical weathering and quick erosion of rocks from the WG, and transported and deposited weathered sediments in the lower reaches of rivers and adjacent coastal region. This results in high heavy metal- and high REE-enriched minerals in the silt fraction of sediments. Sai Babu et al. [36] reported PAAS-normalised LREE- and MREE-enriched and HREE-depleted patterns in both clay and silt fractions of sediments from Kerala and suggested their derivation from felsic granites and laterites from hinterland. In other words, the peak high ∑TE of the silts from south Kerala is related to the source rock geology, high relief of the Western Ghats (WG) and intense chemical and physical weathering of the rocks. Heavy mineral (such as monazite, ilmenite, zircon)-enriched sediments have been reported in the coastal region of south Kerala [91].

The broad peaks of high ∑TE in the silts of Maharashtra coincide with peaks of high Co/La and Co/Th ratios (Figure 6D,E) and, to some extent, peak high Cr/Th ratios (Figure 6F), a very low Th/Sc ratio (av. 0.2 compared to 0.9 of UCC; Figure 6G) and high transition trace elements (TTEs; Figure 5; Table 3) and Fe and Ti contents relative to PAAS (Figure 3; Table 1). This implies that high ∑TE is associated with TTE-dominated mafic minerals and Fe- and Ti-enriched minerals, such as magnetite, ilmenite and rutile. Since basalts contain high concentrations of TTEs and Ti- and Fe-rich minerals, the silts may have eroded from the Deccan Traps. Moreover, the Western Ghats in this region exhibit a steep gradient, known as the Great Escarpment of India. Therefore, the peaks of high ∑TE in the silt fraction are most probably related to physical or mechanical erosion and weathering of Deccan Trap material. The MREE- and HREE-enriched patterns in the clay and silt fractions of sediments from Maharashtra were attributed to their derivation from Deccan Trap basalts [36]. Therefore, peak high ∑TE in the silt fractions of sediments is related to source rock composition, topography of the WG and associated physical and chemical weathering. Unlike Kerala, the peak high ∑TE in the silts of Maharashtra corresponds to high content of TTEs and low ∑REE (Figure 6A,B), implying that basalts are enriched with TTEs, but not enriched with REEs. The peaks of high ∑TE in the silt fractions of sediments from two different geographic domains suggest that the processes for enrichment of trace elements are similar.

Th/U ratios: Trace element (Th, U, Rb and Sr) content and ratios of Th/U and Rb/Sr can be used to measure the intensity of weathering in the source region [92–96]. Th is immobile in the sedimentary environment. U is strongly mobile, and weathering and recycling result in oxidation of U to the soluble $U^{6+}$ state [5]. The higher Th (mean: 12.8 μg/g) and U (mean: 3.5 μg/g) contents in the clay fraction of sediments from A-P Terrain than in UCC (Th: 10.1 μg/g; U: 2.63 μg/g; Table 2) suggest that high Th and U contents may be from a granitic source. The higher mean Th/U ratio (4.1) of the A-P terrain than in UCC (3.8) probably suggests oxidation of U to the soluble $U^{6+}$ [5], and thus the intensity of chemical weathering affected this ratio. Significant positive correlation between Th content and Th/U ratio in both fractions of sediments from A-P terrain (Figure 7B) suggests that chemical weathering modified the Th/U ratio. Usually, the Th/U ratio increases with increasing degree of chemical weathering. However, in the sediments of Kerala, the peak high Th/U ratio (Figure 6C) coincides with peak high ΣTE (Figure 6A), suggesting that the lithology of the source rocks also affected this ratio. Felsic granites are major rock types in south and central Kerala and contain Th-enriched minerals [70]. The adsorption of Th by clay minerals produced under strong weathering results in high Th/U ratios [5]. Therefore, chemical weathering, the lithology of source rocks and adsorption of Th onto clays affected the Th/U ratio in the sediments of Kerala. The mean Th and U contents increases and Th/U ratios decreases as one moves from Kerala to Karnataka and then to Goa in both fractions of sediments (Tables 2 and 3). In other words, the sediments

from Karnataka and Goa gained U and, as a result, the Th/U ratios are lower than in UCC (Figure 7A), and do not fall on the weathering trend line shown in Figure 7B. Since the sediments from Karnataka and Goa contain particulates from Fe-Mn ores together with lateritic material, the U contents are influenced by ore material, favouring gaining U, leading to a decrease in the Th/U ratio of the sediments.

The mean low Th (8.6 μg/g) and U (2.19 μg/g) contents and mean high Th/U ratio (4.47) for the clay fractions of sediments from DT terrain compared to UCC (Tables 2 and 3) imply low Th and U contents in source rocks and strong oxidation of U due to weathering. Weak correlation of Th/U ratio with Th content (Figure 7B) in the clay fractions and moderate correlation in silt fractions of sediments negate that the intensity of weathering is a sole factor influencing the Th/U ratio. Moreover, nearly all sediments from Gujarat and a few sediments from Maharashtra fall on the weathering trend line (Figure 7B). A few sediment samples from Maharashtra gained U, resulting in low Th/U ratios, which plot below UCC (Figure 7A,B), suggesting that contaminated crust material could have affected this ratio. The strong positive correlation of U with $Al_2O_3$ and $Fe_2O_3$ (Table 4) indicate U associated with silicate, Fe-oxy-(hydr) oxides, and that weathering of contaminated crustal material with basalts at the transition zone of Goa and Maharashtra may have provided U to the sediments, causing a low Th/U ratio. A few sediments from Maharashtra fall within or close to the depleted mantle (Figure 7B), implying that they are weathered directly from basalts. In other words, the Th/U ratios of sediments from Maharashtra are affected by chemical weathering of basalts and contaminated crustal source material from hinterland. The Th/U ratios for the clay and silt fractions of sediments from Gujarat are higher than in UCC, and values plot on the weathering trend line (Figure 7C), suggesting oxidation of U may have enhanced the Th/U ratio. However, the sediments from Gujarat exhibit weak to intermediate weathering (Figure 4A,B) and are compositionally immature (Figure 4C), implying that high Th/U ratios are not due to chemical weathering but related to recycling of sediments.

Rb/Sr ratios: Rubidium (Rb) co-exists with K in silicate minerals such as K-feldspar, biotite and muscovite, whereas Sr prefers Ca-bearing minerals such as carbonates, plagioclase and pyroxenes [9]. Moreover, K-bearing minerals are more stable than Ca-bearing minerals, resulting in fractionation between Rb and Sr during weathering [97,98]. The much lower Rb and Sr contents compared to UCC and PAAS (Tables 2 and 3) in both terrains implies that some Rb and Sr is lost to solution during chemical weathering. Rubidium (Rb) is highly soluble and also adsorbs abundantly onto clay minerals [99]. Higher Rb/Sr ratios in the clay fractions than in the silt fractions of all sediments (Figure 7C) suggest that a high degree of chemical weathering and a very strong sorption capacity of Rb by clay minerals affected this ratio. Elevated concentrations of Rb have been reported in shale and mudstones [100]. Increasing Rb/Sr ratios indicate stronger chemical weathering [101]. Significant negative correlation between Rb/Sr ratio and Sr content of the sediments from both terrains (Figure 7D) suggests that the Rb/Sr ratios are strongly affected by chemical weathering. However, very high Rb/Sr ratios in both fractions of sediments from south Kerala (Figure 7C) could be due to Rb-enriched rocks in the hinterland and chemical weathering. Soman [70] reported khondalite–granulite–granite rocks intruded by large pegmatites in south and central Kerala and Archean schists and charnockites with mafic granulites in north Kerala. It is known that felsic granites and pegmatites contain Rb-enriched minerals (muscovite, albite, K-feldspar and lepidolite; [70]). Therefore, very high Rb/Sr ratios in south Kerala may have resulted from strong physical and chemical weathering of felsic granites and pegmatites. Relatively low Rb/Sr ratios in the north Kerala may be because of the increasing mafic component with high Sr in the hinterland rocks and more intense weathering.

Peninsular granites and gneisses are important source rocks in the hinterland of Karnataka and Goa. The Rb in metamorphic rocks is largely associated with K-bearing phyllosilicates, such as biotite and muscovite [98]. Rb also substitutes for $K^+$ in mica (muscovite) and to a lesser extent in K-feldspars. On the other hand, Sr is the most easily be removed from the parent rocks during chemical weathering and carried away as a solute. Therefore, the ion exchange and differential adsorption mechanisms tend to concentrate Rb during weathering, causing high Rb/Sr ratios in the clays of Karnataka and Goa. Therefore, high Rb/Sr ratios are related to the source rocks and intense chemical weathering.

High Rb/Sr ratios continued in the clay and silt fractions of sediments in a few rivers of southern Maharashtra (Figure 7C) appear anomalous because the surficial rocks are basalts. Since basalts contain high Sr, one would expect low Rb/Sr ratios, as seen in northern Maharashtra. As mentioned in the geology of the hinterland, the Proterozoic (peninsular granite and gneisses) rocks laterally change over to Deccan Traps at the border of Maharashtra and Goa (Figure 1). Since the Deccan Trap material is contaminated with crustal sediments at the transition zone of Maharashtra and Goa, high Rb/Sr ratios in the sediments of southern Maharashtra could be due to the weathering of subsurface rocks and their mixing with the products of Deccan Traps at the transition zone. Heavy monsoonal rains and steep slopes of Western Ghats may have favoured exposure of subsurface rocks and their erosion. Sai Babu et al. [36] reported a positive Ce anomaly in the sediments of southern Maharashtra and its absence in the sediments of northern Maharashtra, and attributed this to the mixing of weathered products from Deccan basalts with crustal rocks at the transition zone.

The Deccan Trap basalts (basic rocks) contain high Sr content. Mafic rocks weather 2 to 10 times faster than felsic rocks. Therefore, Sr is the most easily dissolved from basalts during chemical weathering. Strong negative correlation of Sr content with Rb/Sr ratio (Figure 7D) suggests that chemical weathering is the major process for modifying this ratio. Moreover, the silt fractions of sediments contain high Sr and low Rb/Sr ratios (Figure 7C), implying the influence of source rocks.

### *5.4. Dominance of Mafic/Felsic Source Components in the Sediments*

Binary plots and element to element ratios: The standard plots and element-to-element ratios provide valuable information on the dominance of mafic/felsic component in the sediments. The plot of $Al_2O_3$ and $TiO_2$ values on the binary diagram of Bhatia [44] shows that most of the clay and silt fractions from A-P terrain fall in the intermediate region between felsic and mafic provenance, with a few samples falling in the felsic provenance (Figure 9A). Within the DT terrain, the clays from Maharashtra fall in the intermediate provenance between mafic and felsic, while those from Gujarat fall in the mafic provenance (Figure 9A). The silt fractions of sediments from DT terrain fall in the intermediate provenance between mafic and felsic provenance. Similarly, the plot of $TiO_2$, MgO and $Fe_2O_3$ values in the $TiO_2$ versus $Fe_2O_3$ + MgO diagram of Bhatia [44] indicates that the sediments from both terrains plot more towards basalts, suggesting dominance of the mafic component in all samples (Figure 9B). The plot of $TiO_2$ and Zr values in the $TiO_2$-versus-Zr diagram of Hayashi et al. [17] indicates that the sediments from A-P terrain plot in the intermediate region between felsic and mafic, with clay fractions more towards the mafic region and silt samples more towards the felsic region (Figure 9C). The sediments from DT terrain plot in the intermediate zone between mafic and felsic (Figure 9C).

Felsic rocks are enriched with Th, whereas the basic igneous rocks are enriched with Sc, and the Th/Sc ratio can chemically differentiate the sediments. Taylor and McLennon [3] and Bhatia and Crook [102] reported Th/Sc ratios for the post-Archean (~1), granitic (>1) and Archean and basic rock (<1)-derived sediments. The much lower mean Th/Sc ratios

for the clay fractions of sediments (Tables 2 and 3) from A-P terrain (0.566) and DT terrain (0.243) than from PAAS (0.919) and UCC (0.721) suggest predominant Archean and basic rock-derived material. Accordingly, most of the clay fractions of sediments from both terrains fall in the mafic region, with a few samples falling in the intermediate provenance between mafic and felsic in the Th-versus-Sc plot (Figure 9D). However, the mean Th/Sc ratio of the silts from A-P terrain (0.93) is close to that of PAAS (0.919), but these silts extend from the mafic to the felsic region in the Th-vs-Sc plot (Figure 9D), with more samples from Kerala and Karnataka falling in the felsic region and samples from Goa falling in the intermediate zone between the mafic and felsic regions. The lower mean Th/Sc ratio of the silts from DT terrain (0.391) than from UCC suggests the dominance of mafic component. However, these samples extend from the mafic to the felsic region, with more samples from Maharashtra falling in the mafic region and more samples from Gujarat falling in the felsic region.

The ratios of Cr/Th, Co/Th, Sc/Th and La/Sc relative to UCC have been used to estimate the dominance of the mafic and felsic component in the sediments [103]. The much higher mean Cr/Th, Co/Th and Sc/Th ratios and much lower La/Sc ratio than in UCC for the clay fractions of sediments from A-P terrain (Table 2) imply dominance of the mafic component. However, in the silt fractions, the mean Cr/Th, Co/Th and La/Sc ratios are much higher, and Sc/Th is lower than in UCC (Table 3). Low Sc/Th ratios in the silts could be due to Th-enriched heavy minerals recycled into the sediments. In the case of DT terrain, the much higher Cr/Th, Co/Th and Sc/Th ratios and much lower La/Sc ratios in the clay fractions of sediments than in UCC (Table 2) imply dominance of mafic component. The mean Sc/Th ratio for the silts of Gujarat (0.59; Table 3) is much lower than in UCC (1.39), implying Th-enriched heavy minerals in this fraction.

Ratio–ratio plots of trace elements: The ratio–ratio plots of immobile trace elements are frequently used to understand the dominance of the source rock component and sedimentary processes. The ratio–ratio plot of trace elements in the Th/Sc-vs.-Zr/Sc diagram (Figure 9E) indicates that the clay samples from both terrains plot close to UCC and spread more towards andesite. High Zr concentrations in a few silt samples from Kerala and Karnataka (Table 3) indicate the presence of zircon, a heavy mineral. Moreover, these silt samples plot on the linear line in the Th/Sc vs. Zr/Sc (Figure 9E), representing zircon addition through the sediment recycling process or hydrodynamic transportation process. The Th/Yb and La/Th ratios are also helpful to determine the dominant source components. The mean Th/Yb ratio is much higher and the mean La/Th ratio is closer to that of UCC for both fractions of sediments from the A-P terrain. The mean Th/Yb and La/Th ratios of both fractions of sediments from DT terrain are close to that of UCC. The ratio–ratio plot of La/Th vs. Th/Yb (Figure 9F) shows intermediate source between mafic and felsic provenance for both clay and silt fractions. The data points from Kerala extend more towards a felsic source, pointing to dominance of the felsic component.

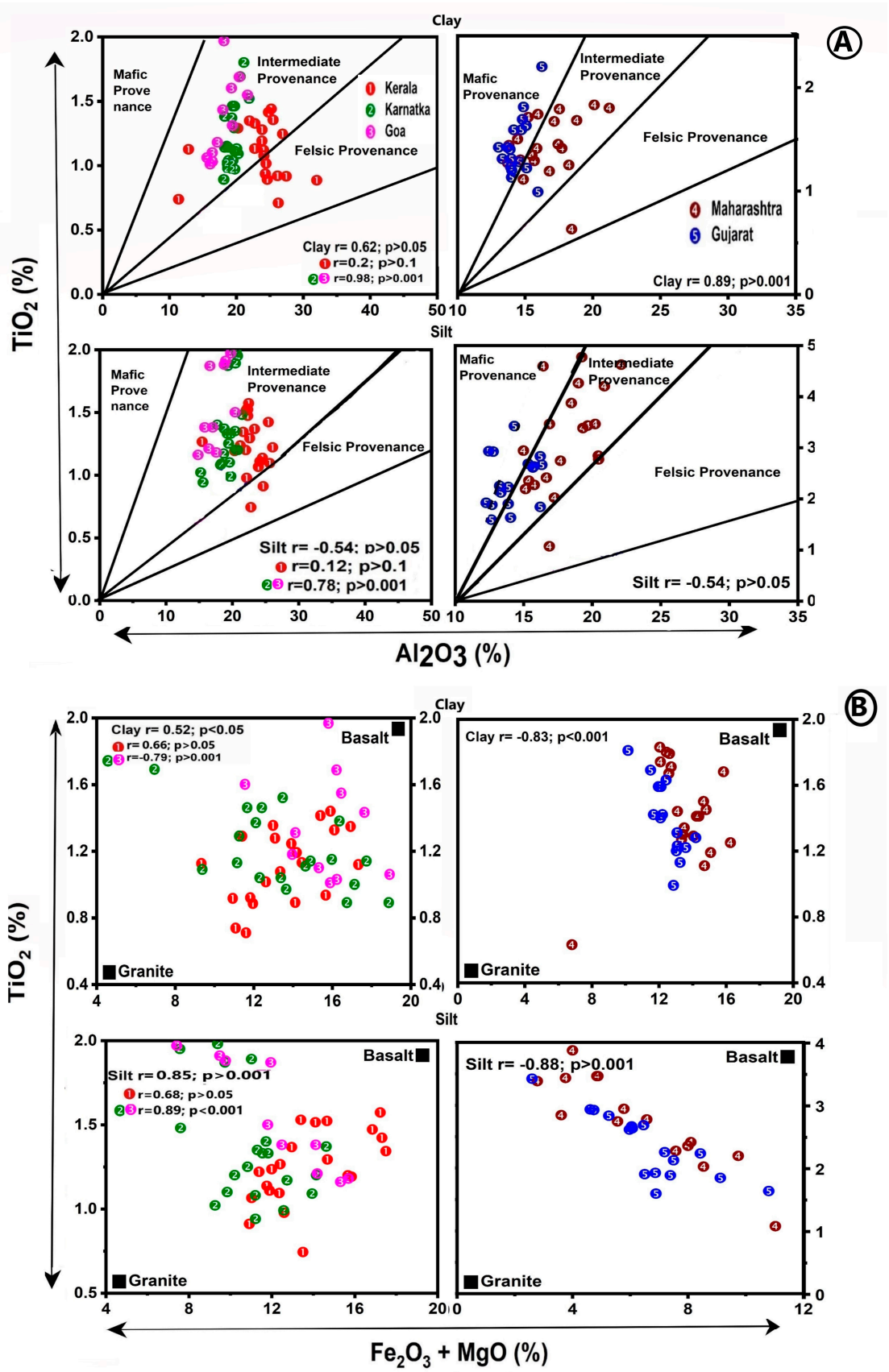


**Figure 9.** *Cont.*

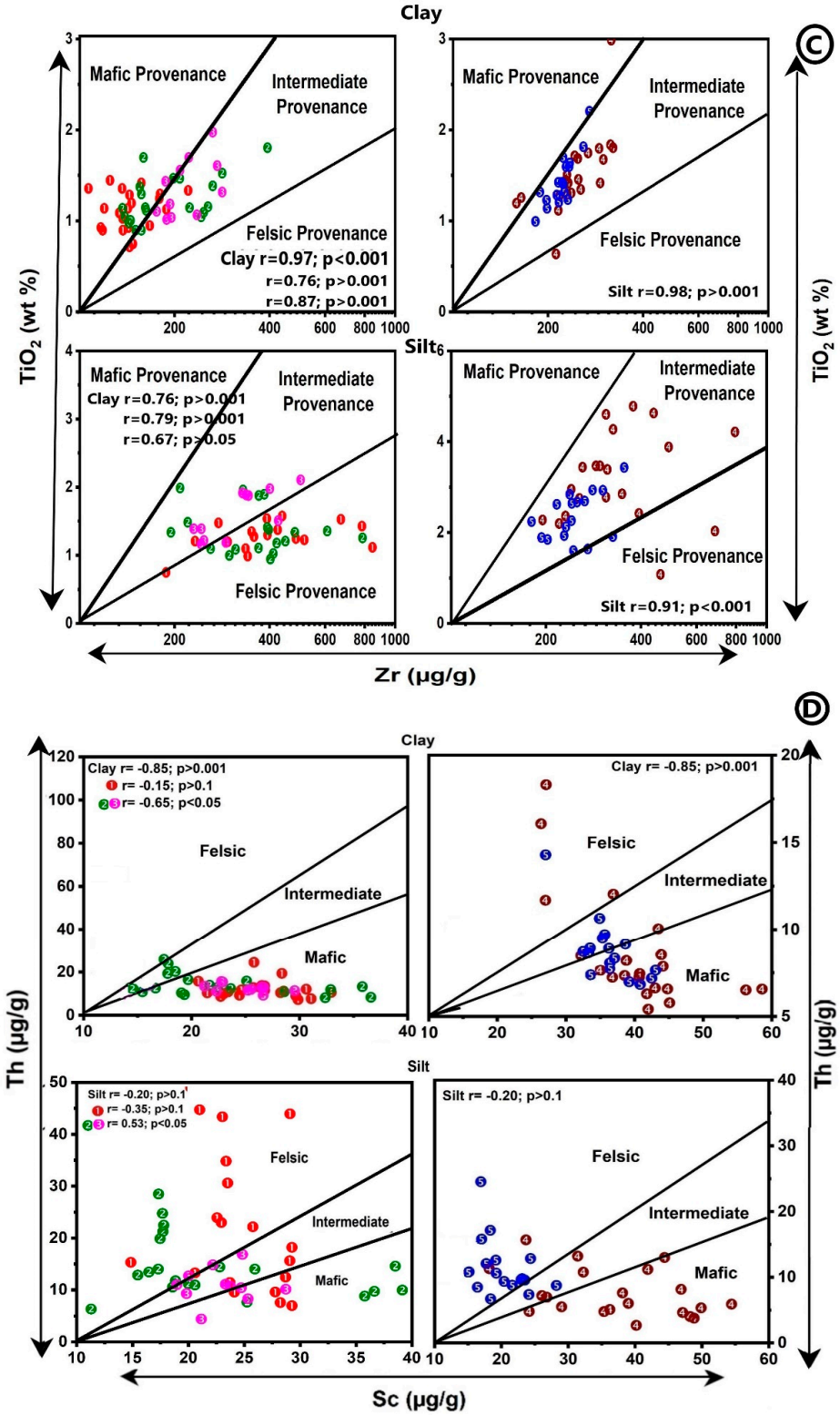


**Figure 9.** *Cont.*

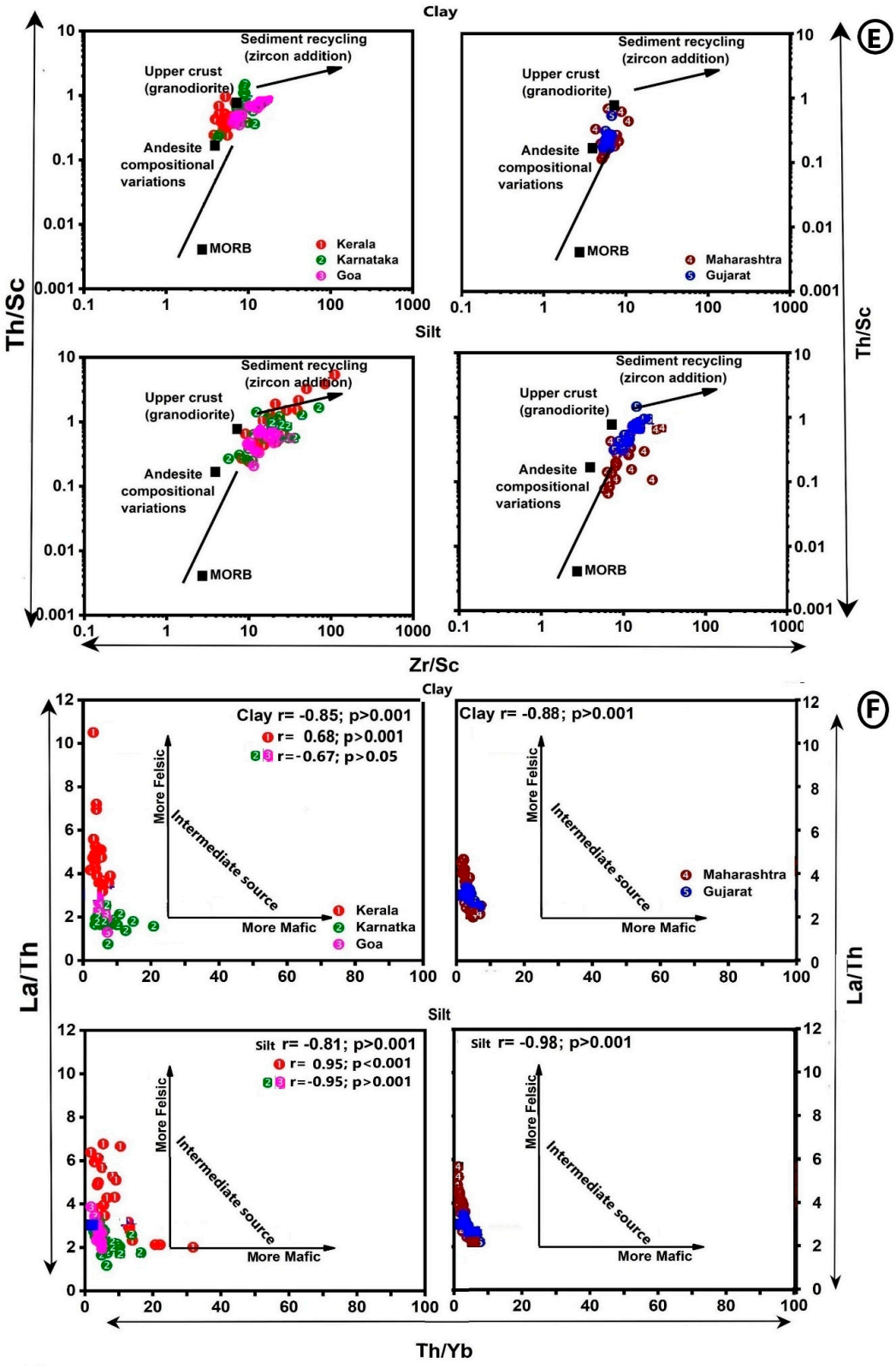


**Figure 9.** (**A**) Element-based provenance discrimination diagrams for the clay and silt fraction of river sediments. (**A**) $Al_2O_3$ vs. $TiO_2$; discrimination lines for the felsic, intermediate and mafic provenances are adopted from Bhatia [44] and Absar and Sreenivas [104]. (**B**) $Fe_2O_3$ + MgO vs. $TiO_2$ (adopted from Bhatia [44]); relationships of (**C**) Zr vs. $TiO_2$, discrimination lines are adopted from Absar and Sreenivas [104]) and (**D**) Th vs. Sc (adopted from Cullers, [105]); ratio-ratio plots of (**E**) Zr/Sc vs. Th/Sc (adopted from Condie, [106] and Roser, [107]) and (**F**) Th/Yb vs. La/Th (adopted from Mongelli et al. [108]).

Ternary diagrams: Ternary diagrams using trace metals are helpful to distinguish the dominant trend of the source components in the sediments. In the La-Th-Sc diagram ([102,109], the clay and silt fractions from A-P terrain extend from granite to basalt, while samples from Kerala are more towards granite and those from Karnataka plot more towards basalts (Figure 10A). The clay and silt samples from Goa plot in the granodiorite region (Figure 10A). The sediments from DT terrain fall within the region between granodiorite and basalts (Figure 10A).

Figure 10B shows the plot of V, Ni and Thx10 data in the ternary diagram [110]. Sediments from A-P terrain fall in the region between felsic and mafic rocks, with clay fractions plotting more towards mafic source. Some silt samples fall within felsic provenance region and others plot linearly between felsic and mafic provenance region. The clay fractions of sediments from DT terrain plot close to mafic rocks, while silt samples plot parallel to the V-Thx10 axis and more towards apex V.

Figure 10C shows the plot of Zr, Cr and Ga data in the ternary diagram [111]. All sediment samples plot parallel to the Cr-Zr axis. The major difference between clay and silt samples from A-P terrain is that silt fractions extend from acidic and metamorphic rocks (Zr apex) to the basic rocks, while clay fractions extend more towards Cr, from sedimentary rocks to basic rocks. Similarly, the clay and silt fractions of sediments from DT terrain extend from sedimentary to basic rocks region (Figure 10C). A few silts from DT terrain also fall in the region representing acidic and metamorphic rocks.

The provenance of river sediments from Figures 9 and 10 may be summarised as follows. The sediments from A-P terrain essentially represent an intermediate provenance between felsic and mafic sources. However, the clay fractions from A-P terrain trend more towards mafic composition (Figure 9B–D and Figure 10B,C). A few silt fractions exhibit distinct felsic provenance (Figures 9D and 10A–C). Since these silts contain heavy minerals, they may have been recycled or transported into the rivers. Similarly, the provenance of sediments from DT terrain is intermediate between felsic and mafic sources, with both fractions from Maharashtra and clays from Gujarat trending more towards a mafic (Figures 9D and 10B,C) source. The silts from Gujarat are dominated by a felsic source (Figure 9D). Sai Babu et al. [36] reported mafic component-dominated rare earth elements from the sediments of both terrains. Two implications can be drawn from the provenance of sediments. (a) One would expect the clays from the granitic terrain (A-P terrain) to be more felsic, but mafic component-dominated in their rivers, implying that the crystalline felsic components weathered from granitic terrain may have deposited more closely to the source and finer mafic component is transported farther from source [112]. The sediments from A-P terrain thus show size-sorting during transportation. (b) A curious point one should realize is that the clay fractions from both terrains are more mafic, despite the source rocks in the hinterland being distinctly different. The sediments from the inner continental shelf all along the west coast of India and the Arabian Sea are abundantly clayey [113]. Since the rivers from the west coast of India are transporting mafic component-dominated clays into the Arabian Sea, it would be a great challenge to identify the exact source of clays weathered from granitic rocks in the Arabian Sea sediments using trace element chemistry.

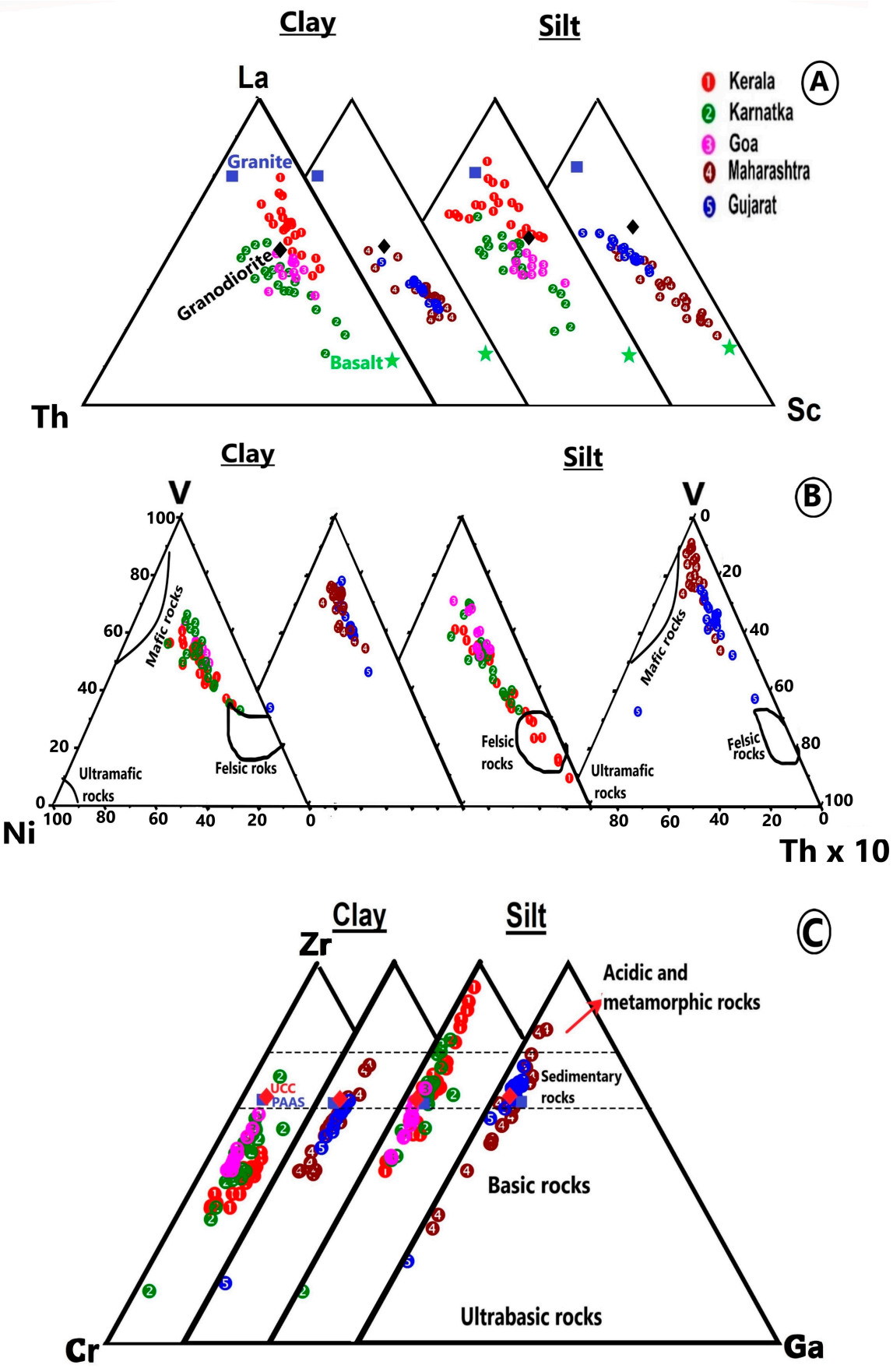


**Figure 10.** Ternary diagrams using trace elements to demarcate the provenance (**A**) La–Th–Sc (adopted from Bhatia and Crook [102]; Bracciali et al. [110]) and (**B**) V-Ni-Thx10 (adopted from Bracciali et al. [110] and (**C**) Zr–Cr–Ga (adopted from Balasubramaniam et al. [111]).

## 6. Summary and Conclusions

The clay mineralogy and major and trace element chemistry of the sediments deposited at the lower reaches of 90 medium and minor rivers along the west coast of India indicate the following:

(a) Distinct clay mineral assemblages, predominant kaolinite followed by illite, gibbsite and goethite in the sediments from A-P terrain, and predominant smectite followed by minor illite, kaolinite and chlorite in the sediments from DT terrain.
(b) Depletion of Si, Ca, Mg, Na and K and enrichment of Al, Fe, P and Ti relative to PAAS in the sediments from both terrains. $SiO_2/Al_2O_3$ ratios suggest that the sediments resemble lateritic soils from A-P terrain and non-lateritic and chemically weathered soils from DT terrain.
(c) Weathering indices suggest that clay fractions are intensely weathered and compositionally mature, while silt fractions from Goa, Maharashtra and Gujarat are size-sorted and recycled.
(d) Higher total trace element content (∑TE) in the silt fraction than clay fractions of all sediments and peaks of high ∑TE values correspond to the silts from Kerala and Maharashtra.
(e) The Th/U and Rb/Sr ratios are controlled by grain size, lithology of the source rocks and intensity of chemical weathering.
(f) Binary and ternary plots of trace elements suggest that the clay fractions from both terrains trend more towards a mafic source, while silt fractions exhibit intermediate provenance between felsic and mafic sources.
(g) It would be challenging to identify the source of sediments from the granitic terrain in the oceans by using trace element chemistry.

**Author Contributions:** Conceptualization, S.S.B. and V.P.R.; methodology, S.S.B., V.P.R. and M.R.M.; software, S.S.B. and M.R.M.; validation, S.S.B., V.P.R. and M.R.M.; formal analysis, S.S.B., V.P.R. and M.R.M.; investigation, S.S.B., V.P.R. and M.R.M.; resources, S.S.B., V.P.R. and M.R.M.; data curation, S.S.B., V.P.R. and M.R.M.; writing—original draft preparation, S.S.B., V.P.R. and M.R.M.; writing—review and editing, S.S.B., V.P.R. and M.R.M.; visualization, S.S.B., V.P.R. and M.R.M.; supervision, S.S.B., V.P.R. and M.R.M. All authors have read and agreed to the published version of the manuscript.

**Funding:** This work was carried out under the project "INSA-Senior Scientist funded by the Indian National Science Academy, New Delhi".

**Data Availability Statement:** The research data utilized in this study is given in the form of tables.

**Acknowledgments:** The authors thank the Vice-chancellor, VFSTR, Vignan's University and Director CSIR-NGRI for their encouragement. This work was carried out for the project awarded to VP Rao under the 'INSA-Senior Scientist' program by the Indian National Science Academy, New Delhi and, during the faculty position of Sk. Sai Babu at Vignan's University. We acknowledge these organisations for their financial support. We also acknowledge the help rendered by the Department of Physics, SRM University, Amaravati, A.P. India with regard to the X-ray diffraction studies on our samples.

**Conflicts of Interest:** The authors declare no conflict of interest.

## References

1. Nesbitt, H.W.; Young, G.M. Early Proterozoic climates and plate motions inferred from major element chemistry of lutites. *Nature* **1982**, *299*, 715–717. [CrossRef]
2. Nesbitt, H.W.; Young, G.M. Petrogenesis of sediments in the absence of chemical weathering: Effects of abrasion and sorting on bulk composition and mineralogy. *Sedimentology* **1996**, *43*, 341–358. [CrossRef]
3. Taylor, S.R.; McLennan, S.M. *The Continental Crust: Its Composition and Evolution*; Blackwell Scientific Publications: Palo Alto, CA, USA; Malden, MA, USA, 1985; p. 312.

4. McLennan, S.M. Rare earth elements in sedimentary rocks: Influence of provenance and sedimentary processes. *Rev. Mineral.* **1989**, *21*, 169–200.
5. McLennan, S.M.; Hemming, S.; McDaniel, D.K.; Hanson, G.N. Geochemical approaches to sedimentation, provenance and tectonics. In *Processes Controlling the Composition of Clastic Sediments*; Johnsson, J.M., Basu, A., Eds.; Geological Society of America: Boulder, CO, USA, 1993; Volume 284, pp. 1–21.
6. Fedo, C.M.; Wayne Nesbitt, H.; Young, G.M. Unraveling the effects of potassium metasomatism in sedimentary rocks and paleosols, with implications for paleoweathering conditions and provenance. *Geology* **1995**, *23*, 921–924. [CrossRef]
7. Selvaraj, K.; Chen, C.T.A. Moderate chemical weathering of subtropical Taiwan: Constraints from solid-phase geochemistry of sediments and sedimentary rocks. *J. Geol.* **2006**, *114*, 101–116. [CrossRef]
8. Borges, J.B.; Huh, Y.; Moon, S.; Noh, H. Provenance and weathering control on river bed sediments of the eastern Tibetan Plateau and the Russian Far East. *Chem. Geol.* **2008**, *254*, 52–72. [CrossRef]
9. Liu, S.; Zhang, J.; Li, Q.; Zhang, L.; Wang, W.; Yang, P. Geochemistry and U-Pb zircon ages of metamorphic volcanic rocks of the Paleoproterozoic Lüliang Complex and constraints on the evolution of the Trans-North China Orogen, North China Craton. *Precambr. Res.* **2012**, *222*, 173–190. [CrossRef]
10. Lupker, M.; France-Lanord, C.; Galy, V.; Lavé, J.; Kudrass, H. Increasing chemical weathering in the Himalayan system since the Last Glacial Maximum. *Earth Planet. Sci. Lett.* **2013**, *365*, 243–252. [CrossRef]
11. Garzanti, E.; Resentini, A. Provenance control on chemical indices of weathering (Taiwan river sands). *Sed. Geol.* **2016**, *336*, 81–95. [CrossRef]
12. Hossain, H.M.; Hasna Hossain, Q.; Kamei, A.; Araoka, D. Compositional variations, chemical weathering, and provenance of sands from the Cox's Bazar and Kuakata beach areas, Bangladesh. *Arabian J. Geosci.* **2018**, *11*, 1–17. [CrossRef]
13. Roser, B.P.; Korsch, R.J. Determination of tectonic setting of sandstone-mudstone suites using $SiO_2$ content and $K_2O/Na_2O$ ratio. *J. Geol.* **1986**, *94*, 635–650. [CrossRef]
14. Roser, B.P.; Korsch, R.J. Provenance signatures of sandstone-mudstone suites determined using discriminant function analysis of major-element data. *Chem. Geol.* **1988**, *67*, 119–139. [CrossRef]
15. Amajor, L.C. Major and trace element geochemistry of Albian and Turonian shales from the Southern Benue trough, Nigeria. *J. Afr. Earth Sci.* **1987**, *6*, 633–641. [CrossRef]
16. Cox, R.; Lowe, D.R.; Cullers, R.L. The influence of sediment recycling and basement composition on evolution of mudrock chemistry in the southwestern United States. *Geochim. Cosmochim. Acta* **1995**, *59*, 2919–2940. [CrossRef]
17. Hayashi, K.I.; Fujisawa, H.; Holland, H.D.; Ohmoto, H. Geochemistry of ~1.9 Ga sedimentary rocks from northeastern Labrador, Canada. *Geochim. Cosmochim. Acta* **1997**, *61*, 4115–4137. [CrossRef] [PubMed]
18. Price, J.R.; Velbel, M.A. Chemical weathering indices applied to weathering profiles developed on heterogeneous felsic metamorphic parent rocks. *Chem. Geol.* **2003**, *202*, 397–416. [CrossRef]
19. Roy, D.K.; Roser, B.P. Geochemical evolution of the Tertiary succession of the NW shelf, Bengal basin, Bangladesh: Implications for provenance, paleoweathering and Himalayan erosion. *J. Asian Earth Sci.* **2013**, *78*, 248–262. [CrossRef]
20. Guo, Y.; Yang, S.; Su, N.; Li, C.; Yin, P.; Wang, Z. Revisiting the effects of hydrodynamic sorting and sedimentary recycling on chemical weathering indices. *Geochim. Cosmochim. Acta* **2018**, *227*, 48–63. [CrossRef]
21. Dinis, P.; Sequeira, M.; Oliveira, T.; Alexandre, C.J.; Castilho, A.; Cabral, P.M. Post-wildfire denudation assessed from compositional features of river sediments (Central Portugal). *Appl. Clay Sci.* **2020**, *193*, 105675. [CrossRef]
22. Hossain, H.M. Major, trace, and REE geochemistry of the Meghna River sediments, Bangladesh: Constraints on weathering and provenance. *Geol. J.* **2020**, *55*, 3321–3343. [CrossRef]
23. Armstrong-Altrin, J.S.; Madhavaraju, J.; Vega-Bautista, F.; Ramos-Vázquez, M.A.; Pérez-Alvarado, B.Y.; Kasper-Zubillaga, J.J.; Bessa, A.Z.E. Mineralogy and geochemistry of Tecolutla and Coatzacoalcos beach sediments, SW Gulf of Mexico. *Appl. Geochem.* **2021**, *134*, 105103. [CrossRef]
24. Boruah, R.; Laskar, J.J. Geochemical characteristics of Neogene sandstones of the East and West Siang Districts of Arunachal Pradesh, NE India: Implications for source-area weathering, provenance, and tectonic setting. *Geochim. Cosmochim. Acta* **2022**, *41*, 100–120. [CrossRef]
25. Chamley, H. *Clay Mineralogy*; Springer: Berlin/Heidelberg, Germany, 1989; p. 623.
26. Sharma, A.; Rajamani, V. Weathering of charnockite and sediment production in the catchment area of the Cauvery River, southern India. *Sed. Geol.* **2001**, *143*, 169–184. [CrossRef]
27. Sensarma, S.; Rajamani, V.; Tripathi, J.K. Petrography and geochemical characteristics of the sediments of the small River Hemavati, Southern India: Implication for provenance and weathering processes. *Sed. Geol.* **2008**, *205*, 111–125. [CrossRef]
28. Bhuiyan, M.A.H.; Rahman, M.J.J.; Dampare, S.B.; Suzuki, S. Provenance, tectonics and source weathering of modern fluvial sediments of the Brahmaputra-Jamuna River, Bangladesh: Inference from geochemistry. *J. Geochem. Explor.* **2011**, *111*, 113–137. [CrossRef]

29. Maharana, C.; Srivastava, D.; Tripathi, J.K. Geochemistry of sediments of the Peninsular rivers of the Ganga basin and its implication to weathering, sedimentary processes and provenance. *Chem. Geol.* **2018**, *483*, 1–20. [CrossRef]
30. He, J.; Garzanti, E.; Dinis, P.; Yang, S.; Wang, H. Provenance versus weathering control on sediment composition in tropical monsoonal climate (South China)—1. Geochemistry and clay mineralogy. *Chem. Geol.* **2020**, *558*, 119860. [CrossRef]
31. Rahman, M.A.; Das, S.C.; Pownceby, M.I.; Alam, M.S.; Zaman, M.N. Geochemistry of Recent Brahmaputra River Sediments: Provenance, Tectonics, Source Area Weathering and Depositional Environment. *Minerals* **2020**, *10*, 813. [CrossRef]
32. Chougong, D.T.; Bessa, Z.E.; Ntyam, S.C.; Yongue, R.F.; Ngueutchoua, G.; Armstrong-Altrin, J.S. Mineralogy and geochemistry of Lobé River sediments, SW Cameroon: Implications for provenance and weathering. *J. Afr. Earth Sci.* **2021**, *183*, 104320. [CrossRef]
33. Babu, S.S.; Ramana, R.V.; Rao, V.P.; Rammohan, M.; Krishna, A.K.; Sawant, S.; Satyasree, N.; Krishna, A.K. Composition of the peninsular India rivers average clay (PIRAC): A reference sediment composition for the upper crust from peninsular India. *J. Earth Syst. Sci.* **2020**, *129*, 39. [CrossRef]
34. Babu, S.S.; Rao, V.P.; Satyasree, N.; Ramana, R.V.; Rammohan, M.; Sawant, S. Mineralogy and geochemistry of the sediments in rivers along the east coast of India: Inferences on weathering and provenance. *J. Earth Syst. Sci.* **2021**, *130*, 60. [CrossRef]
35. Babu, S.S.; Prajith, A.; Rao, V.P.; Rammohan, M.; Ramana, R.V.; Satyasree, N.S. Composition of river sediments from Kerala, southwest India: Inferences on lateritic weathering. *J. Earth Syst. Sci.* **2023**, *132*, 150. [CrossRef]
36. Babu, S.S.; Rao, V.P.; Rammohan, M. Controls on the distribution and fractionation of rare earth elements in recent sediments from the rivers along the west coast of India. *Environ. Earth Sci.* **2024**, *83*, 547. [CrossRef]
37. Saha, A.; Roy, D.K.; Khan, R.; Ornee, T.I.; Goswami, S.; Idris, A.M.; Biswas, P.K.; Tamim, U. Provenance, weathering, climate and tectonic setting of Padma River sediments, Bangladesh: A geo chemical approach. *Catena* **2023**, *233*, 107485. [CrossRef]
38. Sayem, A.S.M.; Rokonuzzaman, M.; Shahriar, M.S. Major and trace element geochemistry of the Atrai River sediments from the Bengal Basin (Bangladesh): Implication for provenance, chemical weathering, and tectonic setting in the southeastern Himalaya. *Arab. J. Geosci.* **2023**, *16*, 487. [CrossRef]
39. Guo, L.; Zhang, H.; Peng, X. Geochemistry and sedimentology of sediments in a short fluvial system, NW China: Implications to the provenance and tectonic setting. *J. Oceanol. Limnol.* **2023**, *41*, 1706–1728. [CrossRef]
40. Gurumurthy, G.P. Geochemical split among the suspended and mud sediments in the Nethravati River: Insights to compositional similarity of peninsular gneiss and the Deccan Basalt Derived sediments, and its implications on tracing the provenance in the Indian Ocean. *Geochem. Geophys. Geosyst.* **2024**, *25*, e2024GC011642. [CrossRef]
41. Maazallahi, M.; Khanehbad, M.; Moussavi-Harami, R.; Mahboubi, A.; Bajestani, M.S. Provenance analysis and maturity of the Rayen River sediments in Central Iran: Based on geochemical evidence. *Environ. Earth Sci.* **2023**, *82*, 89. [CrossRef]
42. Cullers, R.L. The controls on the major and trace element variation of shales, siltstones, and sandstones of Pennsylvanian-Permian age from uplifted continental blocks in Colorado to platform sediment in Kansas, USA. *Geochim. Cosmochim. Acta* **1994**, *58*, 4955–4972. [CrossRef]
43. Wronkiewicz, D.J.; Condie, K.C. Geochemistry and provenance of sediments from the Pongola Supergroup, South Africa: Evidence for a 3.0-Ga-old continental craton. *Geochim. Cosmochim. Acta* **1989**, *53*, 1537–1549. [CrossRef]
44. Bhatia, M.R. Plate tectonics and geochemical composition of sandstones. *J. Geol.* **1983**, *91*, 611–627. [CrossRef]
45. Kale, V. *The Western Ghat: The Great Escarpment of India*; Springer: Berlin/Heidelberg, Germany, 2009. [CrossRef]
46. Naidu, A.S.; Mowatt, T.C.; Somayajulu, B.L.K.; Rao, K.S. Characteristics of clay minerals in the bed loads of major rivers of India. In *Transport of Carbon and Minerals in Major World Rivers, Part 3*; Degens, E.T., Kempe, S., Herrera, R., Eds.; Mitteilungen aus dem Geologische-Palaontologischen Instituts der Universitat Hamburg: Hamburg, Germany, 1985; Volume 58, pp. 559–568.
47. Subramanian, V.; Van't Dack, L.; Van Grieken, R. Chemical composition of river sediments from the Indian subcontinent. *Chem. Geol.* **1985**, *48*, 271–279. [CrossRef]
48. Ramesh, R.; Subramanian, V.; Van Grieken, R.; Van't Dack, L. The elemental chemistry of sediments in the Krishna River basin, India. *Chem. Geol.* **1989**, *74*, 331–341. [CrossRef]
49. Singh, P.; Rajamani, V. REE geochemistry of recent clastic sediments from the Kaveri Flood plains, southern India: Implication to so urce area weathering and sedimentary processes. *Geochim. Cosmochim. Acta* **2001**, *65*, 3093–3108. [CrossRef]
50. Das, A.; Krishnaswami, S.; Sarin, M.M.; Pande, K. Chemical weathering in the Krishna Basin and Western Ghats of the Deccan Traps, India: Rate of basalt weathering and their controls. *Geochim. Cosmochim. Acta* **2005**, *69*, 2067–2084. [CrossRef]
51. Sharma, A.; Sensarma, S.; Kumar, K.; Khanna, P.P.; Saini, N.K. Mineralogy and geochemistry of the Mahi River sediments in tectonically active western India: Implications for Deccan large igneous province source, weathering and mobility of elements in a semi-arid climate. *Geochim. Cosmochim. Acta* **2013**, *104*, 63–83. [CrossRef]
52. Shynu, R.; Rao, V.P.; Kessarkar, P.M.; Rao, T.G. Rare earth elements in suspended and bottom sediments of the Mandovi estuary, central west coast of India: Influence of mining. *Estuar. Coast. Shelf Sci.* **2011**, *94*, 355–368. [CrossRef]
53. Shynu, R.; Rao, V.P.; Parthiban, G.; Balakrishnan, S.; Narvekar, T.; Kessarkar, P.M. REE in suspended particulate matter and sediment of the Zuari estuary and adjacent shelf, western India: Influence of mining and estuarine turbidity. *Mar. Geol.* **2013**, *346*, 326–342. [CrossRef]

54. Shynu, R.; Rao, V.P.; Kessarkar, P.M. Major and trace metals in suspended and bottom sediments of the Mandovi and Zuari estuaries: D istribution, source and pollution. *Environ. Sci. Pollut. Res.* **2017**, *24*, 27409–27429. [CrossRef]
55. Prajith, A.; Rao, V.P.; Kessarkar, P.M. Controls on the distri bution and fractionation of yttrium and rare earth elements in core sedimen ts from the Mandovi estuary, western India. *Cont. Shelf Res.* **2015**, *92*, 59–71. [CrossRef]
56. Kessarkar, P.M.; Rao, V.P.; Ahmad, S.M.; Babu, G.A. Clay minerals and Sr–Nd isotopes of sediments along the western margin of India and their implication for sediment provenance. *Mar. Geol.* **2003**, *202*, 55–69. [CrossRef]
57. Kessarkar, P.M.; Suja, S.; Sudheesh, V. Iron ore pollution in Mandovi and Zuari estuarine sediments and its fate after mining ban. *Environ. Monit. Assess.* **2015**, *187*, 572. [CrossRef] [PubMed]
58. Babechuk, M.G.; Widdowson, M.; Kamber, B.S. Quantifying chemical weathering intensity and trace element release from two contrast ing basalt profiles, Deccan traps, India. *Chem. Geol.* **2014**, *363*, 56–75. [CrossRef]
59. Babechuk, M.G.; Widdowson, M.; Murphy, M.; Kamber, B.S. A combined Y/Ho, high field strength element (HFSE) and isotope perspective on basalt weathering, Deccan traps, India. *Chem. Geol.* **2015**, *396*, 25–41. [CrossRef]
60. Babechuk, M.; Fedo, C. Analysis of chemical weathering trends across three compositional dimensions: Applications to modern and ancient mafic-rock weathering profiles. *Can. J. Earth Sci.* **2023**, *60*, 839–864. [CrossRef]
61. Rao, V.P.; Rao, B.R. Provenance and distribution of clay minerals in the continental shelf and slope sediments of the west coast of India. *Cont. Shelf Res.* **1995**, *15*, 1757–1771.
62. Rao, K.L. *India's Water Wealth*; Orient Longman Ltd.: New Delhi, India, 1975; p. 255.
63. Krishnan, M.S. *Geology of India and Burma*; Madras, Higgin Bothoms: Chennai, India, 1968; p. 536.
64. Widdowson, M.; Cox, K.G. Uplift and erosion history of the Deccan traps, India: Evidence from laterites and drainage patterns of the western ghats and Konkan Coast. *Earth Planet. Sci. Lett.* **1996**, *137*, 57–69. [CrossRef]
65. Lightfoot, P.C.; Hawkesworth, C.J.; Devey, C.W.; Rogers, N.W.; van Calsteren, P.W.C. Source and di¡erentia tion of Deccan Trap lavas: Imp lications of geochemical and mineral chemical variations. *J. Petrol.* **1990**, *31*, 1165–1200. [CrossRef]
66. Radhakrishna, B.P. Archaean granite-greenstone terrain of south Indian shield. In *Precambrian of South India*; Naqvi, S.M., Rogers, J.J.W., Eds.; Memoir; Geological Society India: Bangalore, India, 1983; Volume 4, pp. 1–46.
67. Gokul, A.R.; Srinivasan, M.D.; Gopalakrishnan, K.; Viswanathan, L.S. Stratig raphy and structure of Goa. In *Seminar Volume on Earth Resources for Goa's Development*; Geological Survey of India: Kolkata, India, 1985; pp. 1–13.
68. Mascarenhas, A.; Kalavampara, G. *Natural Resources of Goa: A Geological Perspective*; Geological Society of Goa: Kolkata, India, 2009; p. 213. ISBN 978-81-908737-0-3.
69. Jean, A.; Beauvais, A.; Chordon, D.; Arnaud, N.; Jayananda, M.; Mathe, P.E. Weathering history and landscape evolution of western ghats (India) from 40Ar/39Ar dating of supergene K–Mn oxides. *J. Geol. Soc.* **2020**, *177*, 523–536. [CrossRef]
70. Soman, K. *Geology of Kerala*, 2nd ed.; Geological Society of India: Bangalore, India, 2002; p. 335.
71. Narayanaswamy, S. Geochemistry and Genesis of Laterite in Parts of Cannanore District, North Kerala. Ph.D. Thesis, Cochin University of Science and Technology, Kochi, India, 1992; p. 116.
72. Kaotekwar, A.B.; Rajkumar, R.; Satyanarayana, M.; Keshav Krishna, A.; Charan, S.N. Structures, Petrography and Geochemistr y of Deccan Basalts at Anantagiri Hills, Andhra Pradesh. *J. Geol. Soc. India* **2014**, *84*, 675–685. [CrossRef]
73. Sreenath, A.V.; Abhilash, S.; Vijaykumar, P. West coast of India's rainfall is becoming more convective. *J. Clim. Atmos. Sci.* **2022**, *5*, 36. [CrossRef]
74. Folk, R.L. *Petrology of the Sedimentary Rocks*; Hemphills: Austin, TX, USA, 1968; p. 170.
75. Bock, B.; McLennan, S.M.; Hanson, G.N. Geochemistry and provenance of the Middle Ordovician Austin Glen Member (Normanskill Formation) and the Taconian Orogeny in New England. *Sedimentology* **1998**, *45*, 635–655. [CrossRef]
76. Cullers, R. The geochemistry of shales, siltstones and sandstones of Pennsylvanian–Permian age, Colorado, USA: Implications for provenance and metamorphic studies. *Lithos* **2000**, *51*, 181–203. [CrossRef]
77. Rudnick, R.L.; Gao, S.; Holland, H.D.; Turekian, K.K. Composition of the continental crust. *Crust* **2003**, *3*, 1–64.
78. Pourmand, A.; Dauphas, N.; Ireland, T.J. A novel extraction chromatography and MC–ICP–MS technique for rapid analysis of REE, sc and Y: Revising CI-chondrite and post-archean Australian Shale (PAAS) abundances. *Chem. Geol.* **2012**, *291*, 38–54. [CrossRef]
79. Gu, X.X.; Liu, J.M.; Zheng, M.H.; Tang, J.X.; Qt, L. Provenance and tectonic setting of the Proterozoic turbidites in Hunan, South China: Geochemical Evidence. *J. Sedim. Res.* **2002**, *72*, 393–407. [CrossRef]
80. Xu, H.; Liu, B.; Wu, F. Spatial and temporal variations of Rb/Sr ratios of the bulk surface sediments in Lake Qinghai. *Geochem. Trans.* **2010**, *11*, 3. [CrossRef] [PubMed]
81. Babechuk, M.G.; O'Sullivan, E.M.; McKenna, C.A.; Rosca, C.; Nägler, T.F.; Schoenberg, R.; Kamber, B.S. Ultra-trace Element Characterization of the Central Ottawa River Basin using a Rapid, Flexible, and Low-volume ICP-MS Method. *Aquat. Geochem.* **2020**, *26*, 327–374. [CrossRef]
82. Martin, F.J.; Doyne, H.C. Laterite and lateritic soils in Sierra Leone. *J. Agric. Sci.* **1927**, *17*, 530–547. [CrossRef]

83. Dhoundial, D.P.; Paul, D.K.; Sarkar, A.; Trivedi, J.R.; Gopalan, K.; Potts, P.J. Geochronology and geochemistry of the precambrian granitic r ocks of Goa, SW India. *J. Precambrian Res.* **1987**, *36*, 287–302. [CrossRef]
84. Naqvi, S.M. *Geology and Evolution of the Indian Plate (from Hadean to Holocene 4 Ga to 4 Ka)*; Capital Publishing Company: New Delhi, India, 2005; p. 450.
85. Desai, A.G.; Arolkar, D.B.; French, D.; Viegas, A.; Vishwanath, T.A. Petrogenesis of the Bondla layered mafic-ultramafic complex Usgaon, Goa. *J. Geol. Soc. India* **2009**, *73*, 697–714. [CrossRef]
86. Rao, V.P.; Shynu, R.; Singh, S.K.; Naqvi, S.W.; Kessarkar, P.M. Mineralogy and Sr-Nd isotopes of SPM and sediment from the Mandovi and Zuari estuaries: Influence of weathering and anthropogenic contribution. *Estuar. Coast. Shelf Sci.* **2014**, *156*, 103–115. [CrossRef]
87. Suja, S.; Lina, F.; Rao, V.P. Distribution and fractionation of rare earth elements and Yttrium in suspended and bottom sediments of the Kali estuary, western India. *Environ. Earth Sci.* **2017**, *76*, 174. [CrossRef]
88. Pourret, O.; Davranche, M. Rare earth element sorption onto hydrous manganese oxide: A modeling study. *J. Colloid Interface Sci.* **2013**, *395*, 18–23. [CrossRef] [PubMed]
89. Du, D.D.; Chen, L.Q.; Bai, Y.H.; Hu, H.P. Variations in rare earth elements with environmental factors in lake surface sediments from 17 lakes in western China. *J. Mt. Sci.* **2021**, *18*, 7. [CrossRef]
90. Abedini, A.; Calagari, A.A.; Mikaeili, K. Geochemical characteristics of laterites: The Ailibaltalu Deposit, Iran. *Bull. Miner. Res. Explor.* **2014**, *148*, 69–84. [CrossRef]
91. Mallik, T.K.; Vasudevan, V.; Verghese, P.A.; Machado, T. The black sand placer deposits of Kerala, Southwest India. *Mar. Geol.* **1987**, *77*, 129–150. [CrossRef]
92. McLennan, S.M.; Taylor, S.R.; McCulloch, M.T.; Maynard, J.B. Geochemistry and Nd–Sr isotopic composition of deepsea turbidites: Crustal evolution and plate tectonic associations. *Geochim. Cosmochim. Acta* **1990**, *54*, 2014–2050. [CrossRef]
93. Armstrong-Altrin, J.S.; Nagarajan, R.; Madhavaraju, J.; RosalezHoz, L.; Yong, I.L.L.; Balaram, V.; Cruz-Martınez, A.; AvilaRamırez, G. Geochemistry of the Jurassic and Upper Cretaceous shales from the Molango Region, Hidalgo, eastern Mexico: Implications for source-area weathering, provenance, and tectonic setting. *C. R. Geosci.* **2013**, *345*, 185–202. [CrossRef]
94. Sahoo, P.K.; Guimar, J.T.F.; Souza-Filho, P.W.M.; da Silva, M.S.; Nascimento, W., Jr.; Powell, M.A.; Reis, L.S.; Pessenda, L.C.R.; Rodrigues, T.M.; da Silva, D.F.; et al. Geochemical characterization of the largest upland lake of the Brazilian Amazonia: Impact of provenance and processes. *J. S. Am. Earth Sci.* **2017**, *80*, 541–558. [CrossRef]
95. Viers, J.; Dupré, B.; Raun, J.J.; Deberdt, S.; Angeletti, B.; Ngoupa, J.N.; Michard, A. Major and trace element abundances, and strontium isotopes in the Nyong basin rivers (Cameroon): Constraints on chemical weathering processes and elements transport mechanisms in humid tropical environments. *Chem. Geol.* **2000**, *169*, 211–241. [CrossRef]
96. Nagarajan, R.; Madhavaraju, J.; Nagendra, R.; Amstrong-Altrin, J.S.; Moutte, J. Geochemistry of Neoproterozoic shales of the Rabanpalli Formation, Bhima Basin, Northern Karnataka, southern India: Implications for provenance and paleoredox conditions. *Rev. Mex. Cienc. Geol.* **2007**, *24*, 150–160.
97. Jin, W.; Cao, J.; Wu, J.; Wang, S. A Rb/Sr record of catchment weathering response to Holocene climate change in Inner Mongolia. *Earth Surf. Process. Landf.* **2006**, *31*, 285–291. [CrossRef]
98. Liu, L.; Yu, K.; Li, A.; Zhang, C.; Wang, L.; Liu, X.; Lan, J. Weathering Intensity Response to Climate Change on Decadal Scales: A Record of Rb/Sr Ratios from Chaonaqiu Lake Sediments, Western Chinese Loess Plateau. *Water* **2007**, *15*, 1890. [CrossRef]
99. Blum, J.D.; Erel, Y. Rb-Sr isotope systematics of a granitic soil chronosequence: The importance of biotite weathering. *Geochim. Cosmochim. Acta* **1997**, *61*, 3193–3204. [CrossRef]
100. Wampler, J.W.; Krogstad, E.J.; Elliott, W.C.; Kahn, B.; Kaplan, D.J. Long-term selective retention of natural Cs and Rb by highly weathered coastal plain soils. *Environ. Sci. Technol.* **2012**, *46*, 3837–3843. [CrossRef]
101. Yang, S.Y.; Jung, H.S.; Li, C.X. Two unique weathering regimes in the Changjiang and Huanghe drainage basins: Geochemical evidence from river sediments. *Sediment. Geol.* **2004**, *164*, 19–34. [CrossRef]
102. Bhatia, M.R.; Crook, K.A.W. Trace element characteristics of graywackes and tectonic setting discrimination of sedimentary basin. *Contrib. Mineral. Petrol.* **1986**, *92*, 181–193. [CrossRef]
103. McLennan, S.M.; Taylor, S.R. Th and U in sedimentary rocks: Crustal evolution and sedimentary recycling. *Nature* **1980**, *285*, 621–624. [CrossRef]
104. Absar, N.; Sreenivas, B. Petrology and geochemistry of greywackes of the 1.6 Ga Middle Aravalli Supergroup, northwest India: Evidence for active margin processes. *Int. Geol. Rev.* **2015**, *57*, 134–158. [CrossRef]
105. Cullers, R.L. Implications of elemental concentrations for provenance, redox conditions, and metamorphic studies of shales and limestones near Pueblo, CO, USA. *Chem. Geol.* **2002**, *191*, 305–327. [CrossRef]
106. Condie, K.C. Chemical composition and evolution of the upper continental crust: Contrasting results from surface samples and shales. *Chem. Geol.* **1993**, *104*, 1–37. [CrossRef]
107. Roser, B.P. Whole-Rock Geochemical Studies of Clastic Sedimentary Suites. *Mem. Geol. Soc. Jpn.* **2000**, 57.

108. Mongelli, G.; Critelli, S.; Perri, F.; Maurizio, S.; Perrone, V. Sedimentary recycling, provenance and paleoweathering from chemistry and mineralogy of Mesozoic continental redbed mudrocks, Peloritani mountains, southern Italy. *Geochem. J.* **2006**, *40*, 197–209. [CrossRef]
109. Jahn, B.; Condie, K.C. Evolution of the Kaapvaal Craton as viewed from geochemical and Sm-Nd isotopic analyses of intracratonic pelites. *Geochim. Cosmochim. Acta* **1995**, *59*, 2239–2258. [CrossRef]
110. Bracciali, L.; Marroni, M.; Pandol, B.L.; Rocchi, S.; Arribas, J.; Critelli, S.; Johnsson, M.J. Geochemistry and petrography of Western Tethys Cretaceous sedimentary covers (Corsica and Northern Apennines): From source areas to configuration of margins. *Geol. Soc. Am. Spec. Pap.* **2007**, *420*, 73–93.
111. Balasubramaniam, K.S.; Surendra, M.; Kumar, T.V. Genesis of certain bauxite profiles from India. *Chem. Geol.* **1987**, *60*, 227–235. [CrossRef]
112. Garçon, M.; Chauvel, C. Where is basalt in river sediments, and why does it matter? *Earth Planet. Sci. Lett.* **2014**, *407*, 61–69. [CrossRef]
113. Rao, V.P.; Wagle, B.G. Geomorphology and surBcial geology of the western continental shelf and slope of India: A review. *Curr. Sci.* **1997**, *73*, 330–350.